

MOLECULAR DYNAMIC SIMULATION OF
AMINE-BASED ABSORPTION PROCESS
FOR CO₂ CAPTURE



EMYRA EZZATY BINTI MASIREN

MASTER OF ENGINEERING (CHEMICAL)

UNIVERSITI MALAYSIA PAHANG

UNIVERSITI MALAYSIA PAHANG

DECLARATION OF THESIS AND COPYRIGHT

Author's Full Name : EMYRA EZZATY BINTI MASIREN

Date of Birth : 10 DECEMBER 1990

Title : MOLECULAR DYNAMIC SIMULATION OF
AMINE-BASED ABSORPTION PROCESS

Academic Session : Semester II 2016/2017

I declare that this thesis is classified as:

- CONFIDENTIAL (Contains confidential information under the Official Secret Act 1997)*
- RESTRICTED (Contains restricted information as specified by the organization where research was done)*
- OPEN ACCESS I agree that my thesis to be published as online open access (Full Text)

I acknowledge that Universiti Malaysia Pahang reserves the following rights:

1. The Thesis is the Property of Universiti Malaysia Pahang
2. The Library of Universiti Malaysia Pahang has the right to make copies of the thesis for the purpose of research only.
3. The Library has the right to make copies of the thesis for academic exchange.

Certified by:

(Student's Signature)

(Supervisor's Signature)

901210-01-5090
Date: 23-01-2017

DR. NOORLISA HARUN
Date: 23-01-2017

NOTE : * If the thesis is CONFIDENTIAL or RESTRICTED, please attach a thesis declaration letter.

SUPERVISOR'S DECLARATION

I hereby declare that I have checked this thesis and in my opinion, this thesis is adequate in terms of scope and quality for the award of the degree of Master of Engineering in Chemical

(Supervisor's Signature)

Full Name : DR. NOORLISA BINTI HARUN

Position : SENIOR LECTURER

Date : 23-01-2017

(Co-supervisor's Signature)

Full Name : DR. WAN HANISAH BINTI WAN IBRAHIM

Position : SENIOR LECTURER

Date : 23-01-2017

STUDENT'S DECLARATION

I hereby declare that the work in this thesis is based on my original work except for quotations and citations which have been duly acknowledged. I also declare that it has not been previously or concurrently submitted for any other degree at Universiti Malaysia Pahang or any other institutions.

(Student's Signature)

Full Name : EMYRA EZZATY BINTI MASIREN

ID Number : MKC14001

Date : 23-01-2017



UMP

MOLECULAR DYNAMIC SIMULATION OF
AMINE-BASED ABSORPTION PROCESS
FOR CO₂ CAPTURE



EMYRA EZZATY BINTI MASIREN

Thesis submitted in fulfillment of the requirements
for the award of the degree of
Master of Engineering (Chemical)

UMP

Faculty of Chemical and Natural Resources Engineering

UNIVERSITI MALAYSIA PAHANG

JANUARY 2017

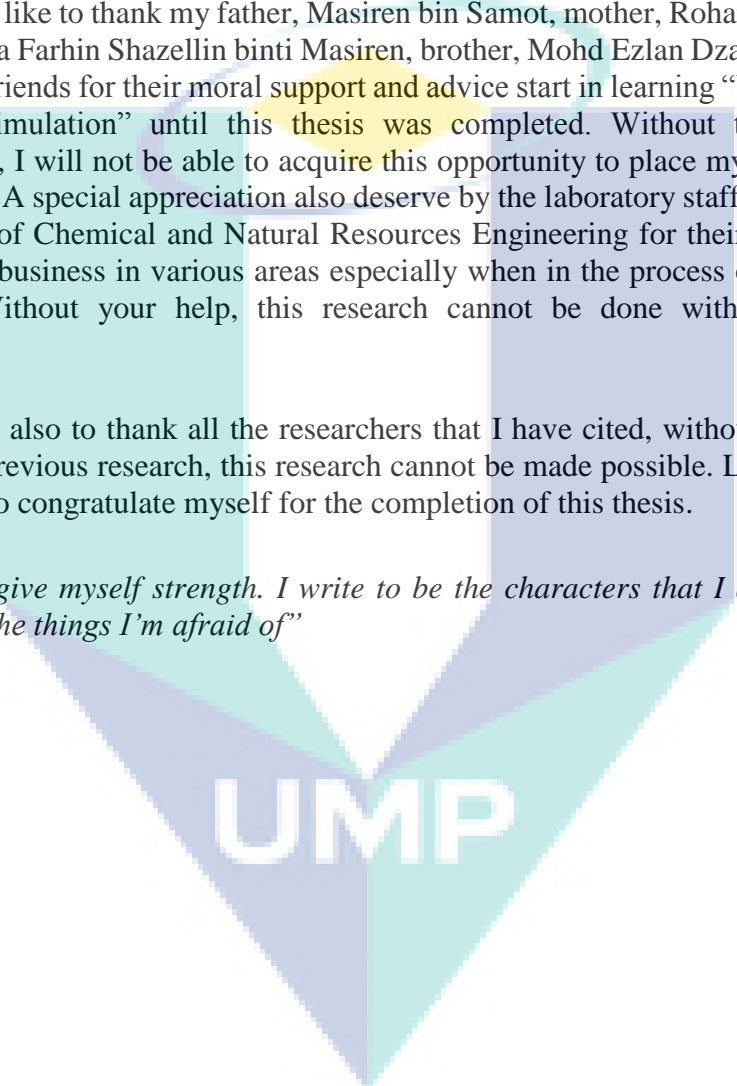
ACKNOWLEDGEMENTS

First and foremost, I would like to acknowledge my main supervisor, Dr. Noorlisa binti Harun and my co-supervisor, Dr. Wan Hanisah binti Wan Ibrahim. Their patience, guidance, ideas and also critics have made this research possible. I also want to express my thanks to Dr. Fatmawati binti Adam and Siti Hana binti Abu Bakar for their cooperation and guidance during the simulation runs and also for the help in searching for related information for the work.

I also would like to thank my father, Masiren bin Samot, mother, Rohana binti Mohd Ali, sister, Ezeera Farhin Shazellin binti Masiren, brother, Mohd Ezlan Dzaqwan bin Masiren and fellow friends for their moral support and advice start in learning “What is Molecular Dynamic Simulation” until this thesis was completed. Without their support and contribution, I will not be able to acquire this opportunity to place myself in the place I stand today. A special appreciation also deserve by the laboratory staff, and other staff in the Faculty of Chemical and Natural Resources Engineering for their contribution that ease up my business in various areas especially when in the process of completing this research. Without your help, this research cannot be done without thousands of difficulties.

I would like also to thank all the researchers that I have cited, without the information from their previous research, this research cannot be made possible. Last but not least, I would like to congratulate myself for the completion of this thesis.

“I write to give myself strength. I write to be the characters that I am not. I write to explore all the things I’m afraid of”

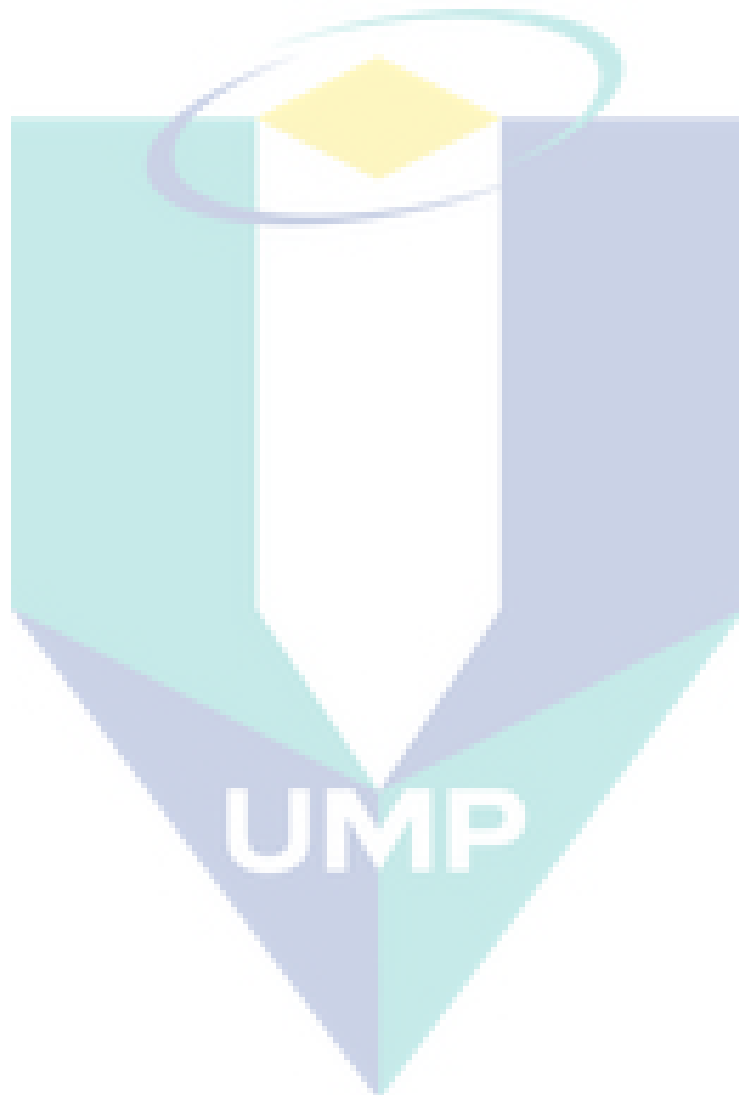
The logo of Universiti Malaysia Perlis (UMP) is a large, downward-pointing triangle. It is composed of four smaller triangles meeting at a central point. The top-left triangle is light blue, the top-right is light purple, the bottom-left is light green, and the bottom-right is light blue. The letters 'UMP' are written in white, bold, sans-serif font across the center of the triangle.

UMP

ABSTRAK

Karbon dioksida (CO_2) ialah salah satu komponen gas rumah hijau yang menyumbang kepada kesan pemanasan global. Penyerapan gas CO_2 penting bagi mengurangkan kepekatan CO_2 dalam atmosfera. Proses penyerapan menggunakan pelarut amina merupakan satu teknologi yang dipercayai keberkesanannya untuk menyerap gas CO_2 . Banyak kajian melibatkan pembangunan model dan simulasi proses pada skala makro telah dijalankan. Tujuan kajian ini dijalankan adalah untuk mengkaji proses penyerapan CO_2 menggunakan pelarut amina pada skala molekul bagi mengetahui interaksi antara molekul semasa proses penyerapan. Kajian interaksi antara molekul dalam proses penyerapan CO_2 dijalankan dengan menggunakan simulasi Molekul dinamik (MD) melalui perisian Material Studio (versi 7.0). Beberapa kajian kes telah dijalankan untuk mengkaji kesan suhu, kepekatan pelarut amina, kepelbagaian jenis pelarut amina, perbandingan antara amina tunggal dan campuran amina ke atas proses penyerapan. Kesan perbezaan molekul karbamat untuk proses penyerapan turut dikaji. Simulasi MD dijalankan pada keadaan NVE (molekul, jisim, tenaga) (selama 200 ps) dan NVT (molekul, jisim, suhu) (selama 1 ns) *ensemble*. Model COMPASS digunakan untuk mengira medan daya manakala model Ewald digunakan sebagai kaedah penjumlahan pengiraan tenaga dalam kotak simulasi. Enam langkah telah dilaksanakan dalam metodologi kajian ini iaitu lakaran struktur molekul, pengoptimuman geometri, pembentukan kotak simulasi dan pengurangan tenaga didalam kotak simulasi, simulasi pada fasa keseimbangan dan fasa penghasilan struktur molekul untuk dianalisis, dan analisis RDF. Graf RDF yang diperolehi akan menunjukkan hubungkait antara r iaitu jarak antara satu atom dengan atom yang lain dan $g(r)$ adalah kadar kebarangkalian untuk interaksi antara molekul berlaku. Perbincangan hasil kajian dibahagikan kepada enam bahagian. Parameter simulasi 1: hasil dari kajian menunjukkan bahawa, kekuatan interaksi antara molekul pelarut MEA dan CO_2 meningkat apabila meningkatnya suhu sistem penyerapan. Parameter simulasi 2: keputusan yang sama juga didapati dengan peningkatan kepekatan pelarut amina. Peningkatan kepekatan pelarut amina menyebabkan sifat akali MEA meningkat. Oleh itu, kecenderungan untuk berlakunya daya tarikan dengan molekul berasid (CO_2) juga bertambah. Parameter simulasi 3: hasil daripada kajian menunjukkan bahawa MEA merupakan pelarut yang mempunyai potensi paling tinggi untuk berinteraksi dengan gas CO_2 berbanding dengan DEA dan MDEA. Ini kerana MEA mempunyai keupayaan untuk bertindakbalas secara langsung dengan CO_2 dan membentuk ion karbamat. Amina pengaktif iaitu PZ dan *steric hindered* amina iaitu AMP juga menunjukkan kebarangkalian yang tinggi untuk berinteraksi dengan gas CO_2 . Disebabkan kekurangan ikatan nitrogen-hidrogen ($-\text{NH}$) pada MDEA menyebabkan pelarut ini kurang reaktif. Ketiadaan atom hydrogen yang terikat dengan tom nitrogen menyebabkan tidak berlaku pembentukan ion karbamat. MDEA tidak boleh berinteraksi secara langsung dengan CO_2 . Justeru, disarankan MDEA dicampurkan dengan pelarut lain yang lebih reaktif untuk meningkatkan kereaktifan MDEA terhadap CO_2 . Parameter simulasi 4: hasil daripada kajian ini menunjukkan bahawa campuran AMP dan PZ ke dalam larutan MDEA mampu meningkatkan kereaktifan MDEA dalam proses penyerapan gas CO_2 . Molekul AMP dan PZ berfungsi untuk membantu interaksi antara MDEA dan CO_2 . Parameter simulasi 5: interaksi *intra*- dan *inter*- molekul dalam proses penyerapan CO_2 menunjukkan ion MEA karbamat sukar memutuskan ikatan molekul jika dibandingkan dengan AMP dan PZ amina. Kecenderungan tinggi untuk interaksi *intra*- dan *inter*- molekul bagi pelarut AMP dan PZ, membuatkan amina ini menjadi pilihan untuk dicampurkan dengan pelarut amina yang kurang reaktif. Hasil

kajian ini dapat memberi penjelasan asas kimia kepada keputusan eksperimen dan simulasi yang dilaporkan dalam kajian terdahulu. Aplikasi MD simulasi dalam proses penyerapan menggunakan pelarut amina mampu meningkatkan pemahaman mengenai proses ini pada peringkat molekul dengan mengkaji pengaruh interaksi fizikal antara molekul dalam proses penyerapan gas CO₂ menggunakan analisis RDF. Interaksi fizikal antara atom atau molekul akan berlaku sebelum berlakunya tindakbalas kimia. Kajian mengenai interaksi fizikal penting untuk lebih memahami mengenai proses penyerapan menggunakan pelarut amina.



ABSTRACT

Carbon dioxide (CO₂) is a major greenhouse gas that causes global warming effect. It has to be captured to reduce its concentration in the atmosphere. Amine absorption process is a promising technology to be applied for CO₂ mitigation. Modeling and simulation of amine absorption process for CO₂ removal at macro-scale is well established. This study was aimed to investigate the amine-CO₂ absorption process at the molecular level and their intermolecular interaction during the absorption process. The study on the intermolecular interaction in amine absorption process for CO₂ capture was performed using molecular dynamic (MD) simulation via Material Studio (version 7.0) software. Several case studies were conducted to investigate the effect of temperature, amine concentration, different types of alkanolamines for CO₂ absorption process and comparison between single and blended amines for absorption process. Next, effect of different carbamate molecules for CO₂ desorption process were also performed. The MD simulation was carried out at NVE (moles, volume, energy) 200 ps (picosecond) and NVT (moles, volume, temperature) 1 ns (nanosecond) ensemble. COMPASS and Ewald models were used within simulation box for force field and summation method calculation. Six steps were performed to simulate the selected molecules representing the CO₂ absorption system which were molecular structure sketch, geometry optimisation, simulation box creation and energy minimization, simulation at equilibrium and production phase, and analysis of the last trajectory for output data for RDF (radial distribution function). RDF plot shows the relationship between r which is the distance between atom pairs in each of the trajectory distance of atom with other neighbouring atom and $g(r)$ is the tendency of atom to interaction/probability to have interaction between atoms. The discussion of result was divided into six sections. For simulation parameter 1, the simulation results shows the strength of intermolecular interaction between MEA (monoethanolamine) solution-CO₂ was increased with the increased in temperature. For simulation parameter 2, the simulation results shows the similar behavior is observed as the amount of amine concentration is increased. Due to high concentration, high basicity of MEA was produced. Hence, it tended to have strong intermolecular attraction with acidic, CO₂. For simulation parameter 3, the simulation results shows the MEA solvent showed the highest tendency to interact with CO₂ compared to DEA (diethanolamine) and MDEA (methyl diethanolamine) because it can directly react with CO₂ and easily form carbamate ions. A good performance of activator amine, PZ (piperazine) and steric hindered amine, AMP was observed in this study. Both showed high tendency to have intermolecular interaction with water and CO₂. Due to the lack of -HN bond in MDEA, this solvent was determined to be less reactive. This is because MDEA has lack of hydrogen atom attached in amino group there will be no formation of carbamate ion. MDEA cannot directly absorb CO₂. Therefore, it is suggested to be blended with other reactive amines in order to increase reactivity of MDEA with CO₂. For simulation parameter 4, the simulation results shows the blended MDEA/AMP and MDEA/PZ improved the efficiency of MDEA in CO₂ absorption process. The addition of AMP and PZ assisted MDEA to have intermolecular interaction with CO₂. For simulation parameter 5, the simulation results shows the inter- and intra-molecular interaction on stripping process showed that carbamate ions of MEA were difficult to break compared to AMP and PZ. The high tendency for inter and intra molecular interaction happened on AMP and PZ, making them a good choice to be blended with other amine solvent to overcome the limitation of other less reactive amines. The simulation results obtained from this study gave fundamental explanation on the

experimental and simulations results reported in the literature. The application of MD simulation in amine absorption process is capable to improve the understanding and give insight about this process at molecular level. The research gap in this study is to investigate the influence of physical interaction between molecules on CO₂ capture process by analysing system with RDF. Physical interaction between atoms or molecules will happen before chemical reaction occur. Learning about physical interaction was essential to understand the amine-based absorption process.

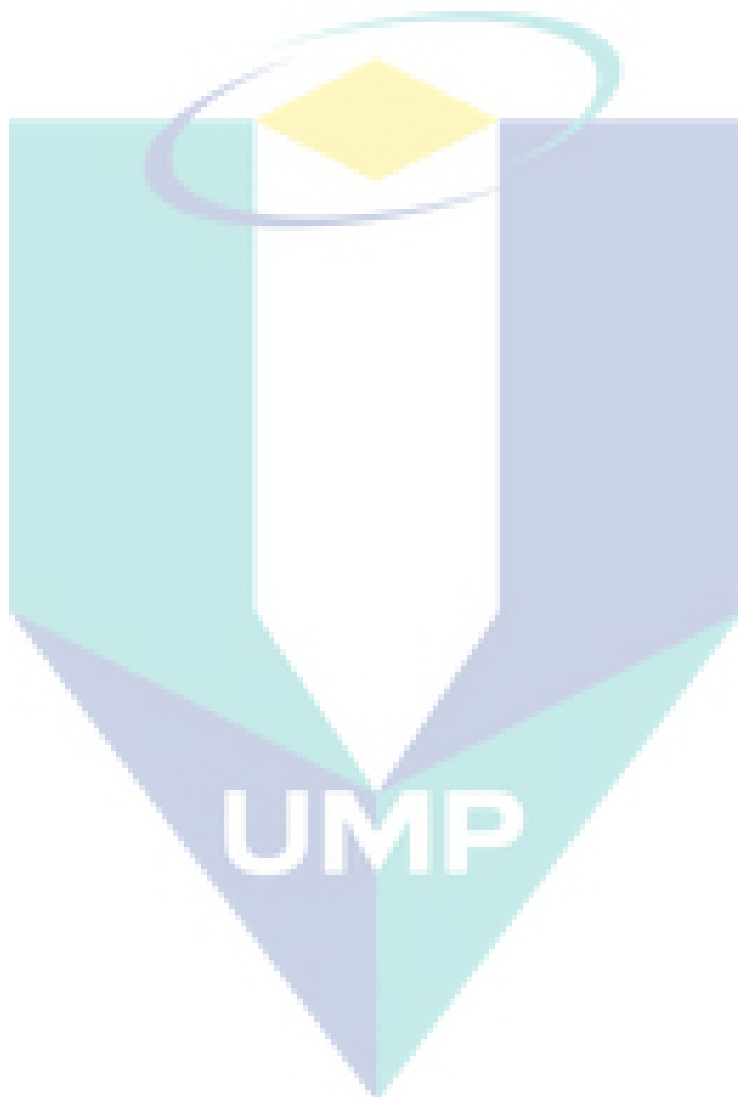


TABLE OF CONTENT

DECLARATION	
TITLE PAGE	
ACKNOWLEDGEMENTS	ii
ABSTRAK	iii
ABSTRACT	v
TABLE OF CONTENT	vii
LIST OF TABLES	xi
LIST OF FIGURES	xiii
LIST OF SYMBOLS	xv
LIST OF ABBREVIATIONS	xvi
CHAPTER 1 INTRODUCTION	1
1.1 Background of Study	1
1.2 Problem Statement	3
1.3 Research Objectives	4
1.4 Scope of Research	5
1.5 Significant of Study	6
1.6 Thesis Organization	7
CHAPTER 2 LITERATURE REVIEW	8
2.1 Introduction	8
2.2 CO ₂ Capture Process	8
2.3 CO ₂ Separation Technologies	9

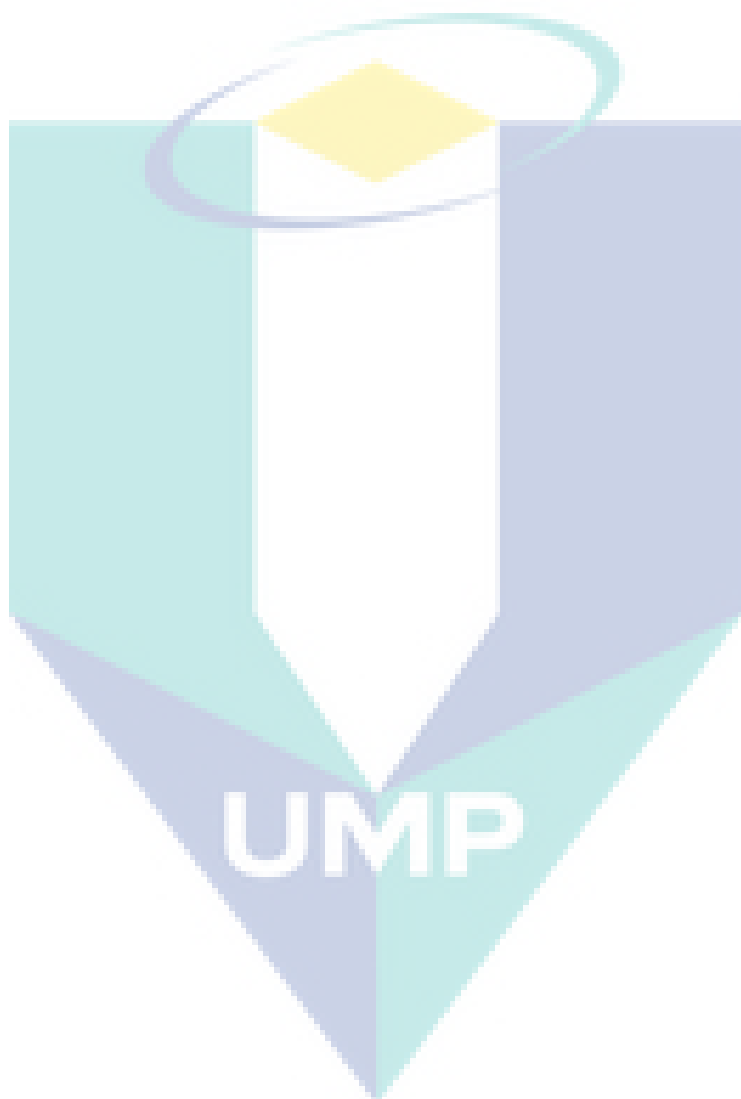
2.4	Amine-Based Absorption Process	13
2.4.1	Experiment Work using Single Amine	14
2.4.2	Experimental Work using Blended Amine	15
2.4.3	Computational Chemistry Study	18
2.4.4	The Gap of Study	20
2.4.5	Alkanolamines Solvent	20
2.4.6	The Reaction Mechanism between Alkanolamines and CO ₂	23
2.5	Stripping Process	26
2.6	Molecular Dynamic Simulation	26
2.6.1	Force Field	28
2.6.2	Time Integration Algorithm	29
2.6.3	Periodic Boundary	30
2.6.4	Thermodynamic Ensemble	31
2.6.5	Radial Distribution Function	32
2.7	Molecular Mechanics	34
2.7.1	Intramolecular Interaction	35
2.7.2	Intermolecular Interaction	38
2.8	Summary	42
CHAPTER 3 METHODOLOGY		43
3.1	Introduction	43
3.2	Material Studio Software	43
3.3	Flowchart of Methodology	43
3.4	Molecular Specification	45
3.4.1	Carbon Dioxide	45
3.4.2	Water	45

3.4.3	Alkanolamine	46
3.5	Molecular Dynamic Simulation	50
3.5.1	Molecular Structure Sketches	50
3.5.2	Geometry Optimization	51
3.5.3	Construction of Amorphous Cell Box	53
3.5.4	Equilibrium Phase	58
3.5.5	Production Phase	60
3.5.6	Trajectory Production Analysis	60
3.5.7	Calculation in RDF	62
3.6	Simulation Parameter 1: The Effect of Temperature	63
3.7	Simulation Parameter 2: The Effect of Amine Concentration	63
3.8	Simulation Parameter 3: The Effect of Different Types of Alkanolamines	65
3.9	Simulation Parameter 4: Comparison of Single and Blended Amines System	66
3.10	Simulation Parameter 5: Comparison of Different Types Carbamate Amine (Stripping Process)	68
CHAPTER 4 RESULTS AND DISCUSSION		70
4.1	Introduction	70
4.2	Simulation Parameter 1: Effect of Temperature on MEA/H ₂ O/CO ₂ System	70
4.2.1	Intermolecular Interaction between MEA and Water for Binary (MEA+H ₂ O) and Tertiary (MEA+H ₂ O+CO ₂) Systems	70
4.2.2	Intermolecular Interaction between MEA Solution and CO ₂ in Tertiary System	73
4.3	Simulation Parameter 2: Effect of Amine Concentration on MEA/H ₂ O/CO ₂ System	75
4.3.1	Intermolecular Interaction between MEA and Water for Binary (MEA+H ₂ O) and Tertiary (MEA+H ₂ O+CO ₂) Systems	75

4.3.2	Intermolecular Interaction between MEA Solution and CO ₂ in Tertiary System	77
4.4	Simulation Parameter 3: Effect of Different Types Alkanolamines	79
4.4.1	Intermolecular Interaction between Amine and Water for Binary (Amine+H ₂ O) and Tertiary (Amine+H ₂ O+CO ₂) Systems	79
4.4.2	Intermolecular Interaction between Amine Solution and CO ₂ in Tertiary System	81
4.5	Simulation Parameter 4: Comparison of Single and Blended Amines System	84
4.5.1	Intermolecular Interaction for Blended MDEA/AMP	84
4.5.2	Intermolecular Interaction for Blended MDEA/PZ	92
4.6	Simulation Parameter 5: Comparison of Different Types of Carbamate Amine (Stripping Process)	97
4.6.1	Intermolecular Interaction between Carbamate Ion with Water	97
4.6.2	Intramolecular Interaction between C-Carbamate and N-Carbamate	99
	CHAPTER 5 CONCLUSIONS AND RECOMMENDATIONS	102
5.1	Conclusions	102
5.2	Recommendations	103
	REFERENCES	105
	APPENDIX A RADIAL DISTRIBUTION FUNCTION (RDF) GRAPH	121
	APPENDIX B LIST OF PUBLICATIONS	140
	LIST OF CONFERENCE PRESENT	141

LIST OF TABLES

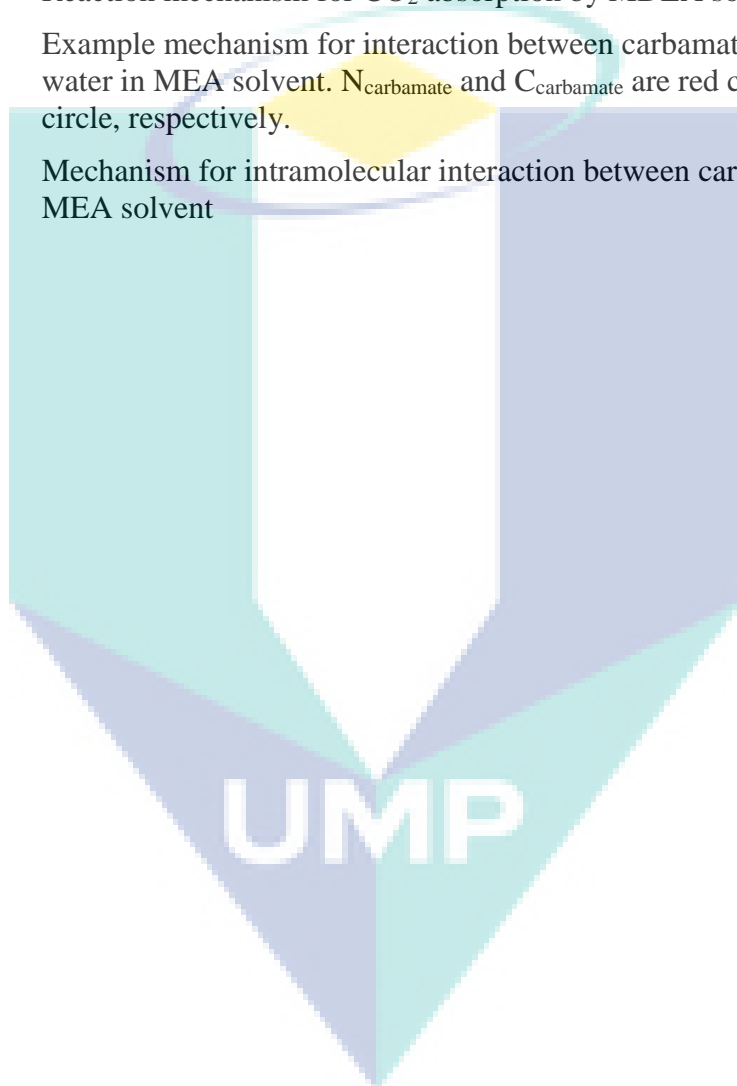
Table 3.1	Properties of alkanolamine molecules	47
Table 3.2	Input parameters used to analyse temperature effect on the system	63
Table 3.3	Input parameters used to analyse amine concentration effect on the system	65
Table 3.4	Input parameters to analyse the effect different types of amine on the system	66
Table 3.5	Molar ratio for single and blended system of MDEA, AMP, PZ, MDEA/AMP and MDEA/PZ solution	67
Table 3.6	Input parameters for single system of MDEA, AMP and PZ solution	67
Table 3.7	Input parameters for blended system of MDEA/AMP and MDEA/PZ solution	68
Table 3.8	Input parameters for carbamate amines system in stripping process	69
Table 4.1	Summary data of RDF result for binary and tertiary system at 298 K, 308 K, 313 K and 318 K of MEA	71
Table 4.2	Summary data of RDF result for intermolecular interaction between MEA and CO ₂	73
Table 4.3	Summary data of RDF result for binary and tertiary system at 10 wt.%, 20 wt.%, 30 wt.% and 40 wt.% of MEA	76
Table 4.4	RDF results for intermolecular interaction between MEA and CO ₂	77
Table 4.5	Summary data comparison RDF result for amine solution between binary and tertiary system	79
Table 4.6	Summary data of RDF result for intermolecular interaction of amine solutions with CO ₂	82
Table 4.7	Summary data of RDF result for binary system of MDEA and AMP, and blended MDEA/AMP system	85
Table 4.8	Summary data of RDF result for tertiary system of MDEA and AMP, and blended MDEA/AMP system	87
Table 4.9	Summary data of RDF result for intermolecular interaction between amine with CO ₂ for MDEA and AMP, and blended MDEA/AMP system	88
Table 4.10	Summary data of RDF result for binary system of MDEA and PZ, and blended MDEA/PZ system	93
Table 4.11	Summary data of RDF result for tertiary system of MDEA, PZ, and blended MDEA/PZ system	94
Table 4.12	Summary data of RDF result for reaction between amine with CO ₂ on MDEA and PZ, and blended MDEA/PZ system	95
Table 4.13	Intermolecular interaction between carbamate ion and water	97



LIST OF FIGURES

Figure 1.1	Percentage Greenhouse Gases 1990-2012 based on U.S. Inventories.	2
Figure 1.2	Trend of CO ₂ emissions from fossil fuel combustion.	2
Figure 2.1	CO ₂ separation and capture technologies.	10
Figure 2.2	Process flow diagram of amine post-combustion CO ₂ capture process from simulated process plant.	14
Figure 2.3	2-D periodic boundary condition.	31
Figure 2.4	Schematic explanation of $g(r)$ of a monoatomic fluid.	33
Figure 2.5	The atomic configuration and RDF pattern for (a) gas, (b) liquid, and (c) solid phase.	34
Figure 2.6	Example of covalent bond	37
Figure 2.7	Example illustration of metallic bond	38
Figure 2.8	Type of forces involve in intermolecular interaction	39
Figure 2.9	Example illustration for dipole-dipole force interaction.	40
Figure 2.10	Example illustration of hydrogen bond	40
Figure 2.11	Example illustration for instantaneous dipole-induce dipole forces.	41
Figure 2.12	Example illustration for ion-dipole forces.	42
Figure 3.1	The flowchart to MD simulation	44
Figure 3.2	The geometrical structure of CO ₂	45
Figure 3.3	The geometrical structure of H ₂ O	46
Figure 3.4	Replicate the molecular structure from Royal Society of Chemistry Database.	51
Figure 3.5	Step 1 for geometry optimisation of molecular sketches in MD simulation	52
Figure 3.6	Step 2 for geometry optimisation of molecular sketches in MD simulation	53
Figure 3.7	3-D amorphous cell box in MD simulation for MEA 30 wt.%	54
Figure 3.8	Step 1 for amorphous cell construction in MD simulation	54
Figure 3.9	Step 2 for amorphous cell construction in MD simulation	55
Figure 3.10	Amorphous cell minimization selection	56
Figure 3.11	“ <i>Smart Minimizer</i> ” setting with fine convergence level and 1000 maximum iterations	57
Figure 3.12	Step 1 for equilibrium phase in MD simulation	59
Figure 3.13	Step 2 for equilibrium phase in MD simulation	59
Figure 3.14	Step 3 for equilibrium phase and production phase in MD simulation	60

Figure 3.15	Step 1 for analysis sample in MD simulation	61
Figure 3.16	Step 2 for analysis sample in MD simulation	62
Figure 4.1	Single-step for reaction mechanism between CO ₂ , H ₂ O and amine	74
Figure 4.2	Molecular structure of MDEA	80
Figure 4.3	Molecular structure of MEA and AMP	83
Figure 4.4	N-O and N-C branches in (a) AMP and (b) MDEA molecular structure	90
Figure 4.5	Reaction mechanism for CO ₂ absorption by MDEA solution	91
Figure 4.6	Example mechanism for interaction between carbamate ions with water in MEA solvent. N _{carbamate} and C _{carbamate} are red circle and blue circle, respectively.	98
Figure 4.7	Mechanism for intramolecular interaction between carbamate ions in MEA solvent	101



LIST OF SYMBOLS



α_i	Acceleration
\AA	Amstrong
N_i	Atomic Population
r_i	Change In Particle Position
ρ	Density
E	Energy
fs	Femtosecond
f_i	Force Of Newton's Second Law Of Motion
K	Harmonic Force Constant
m_i	Mass Of Particle
μm	Micrometer
ns	Nanosecond
N	Number Of Mole
U_{AB}	Potential Energy
P	Pressure
r	Spherical Radius
T	Temperature
K_{Ga}	Volumetric Mass Transfer Coefficient
V	Volume
wt. %	Weight Percent
∇_i	3-Dimensions

LIST OF ABBREVIATIONS

AMP	2-Amino-2-Methyl-1-Propanol
AMPCOO ⁻	2-Amino-2-Methyl-1-Propanol Carbamate
CO	Carbon Monoxide
CH ₄	Methane
CO ₂	Carbon Dioxide
CCS	Carbon Capture And Sequestration
CFBC	Circulating Fluidized Bed Combustion
COSMO- RS model	Conductor-Like Screening Model For Realistic Solvents
DFT	Density Functional Theory
DMEA	N,N-Dimethylethanolamine
DEEA	N,N-Diethylethanolamine
DMAEOE	2-[2-(Dimethylamino) Ethanoxy] Ethanol)
H ₂ S	Hydrogen Sulfide
H ₂ O	Water
H ₂ CO ₃	Carbonic Acid
HCO ₃ ⁻	Bicarbonate Ion
HMDA	Hexamethylenediamine
ID	Inside Diameter
IBC	Isolated Boundary Condition
IGCC	Integrated Gasification Combined Cycle
IL	Ionic Liquid
LiF	Lithium Fluoride
MEA	Monoethanolamine
MEACOO ⁻	Monoethanolamine Carbamate
MM	Molecular Mechanic
MD	Molecular Dynamic
MDEA	Methyl-Diethanolamine
MIPA	Monoisopropanolamine
MgCl ₂	Magnesium Chloride
MgSO ₄	Magnesium Sulfate

MSD	Mean Square Displacement
NaCl	Sodium Chloride
NMP	Normal Methyl Pyrrolidone
NH ₃	Ammonia Compound
O ₂	Oxygen
RDF	Radial Distribution Function
PBC	Periodic Boundary Condition
PC	Propylene Carbonate
PSA	Pressure Swing Adsorption
PZ	Piperazine
PZH ⁺	Protonated Ion Of PZ
PZEA	(Piperazinyl-1)-2-Ethylamine
PZCOO-	Piperazine Carbamate
PCM	Polarizable Continuum Model
SiO ₂	Silicon Oxide
TEA	Triethanolamine
TBP	Tributyl Phosphate
TSA	Temperature Swing Adsorption
VAC	Velocity Autocorrelation
WWC	Wetted Wall Column
3DMAP	3-Dimethylamino-1-Propanol
1DMA2P	1-Dimethylamino-2-Propanol
¹³ C NMR	Carbon-13 Nuclear Magnetic Resonance
-OH	Hydroxyl Group
-NH	Amino Group

CHAPTER 1

INTRODUCTION

1.1 Background of Study

Anthropogenic carbon dioxide (CO₂) emissions occur when CO₂ is produced from burning activities and enters the atmosphere. The increased CO₂ concentration in the atmosphere leads to global warming effects. The main objective of CO₂ removal or capture from fuel gas is to reduce the acid gases in atmosphere and prevent global warming from happening. The concentration of CO₂ in atmosphere is increasing year by year. For example, in China, the CO₂ emission was increased by 3% in 2012 due to the increased use of electricity and fuel demand (Olivier et al., 2013). It was also estimated that, around 90% of the total CO₂ emissions was caused by fossil-fuel. This combustion was identified as the major sources of CO₂ emission (Lee et al., 2010).

Greenhouse gases that contribute to air pollution are carbon dioxide (CO₂), carbon monoxide (CO), sulphur dioxide (SO₂), nitrogen dioxide (NO₂) and burning of fossil fuels (Arapatsakos et al., 2012). Figure 1.1 shows the percentage of greenhouses gases which emit from fossil fuel combustion between 1990 and 2012 (U.S. Environmental Protection Agency, 2014). It shows that CO₂ has the highest percentage compared to others greenhouse gases.

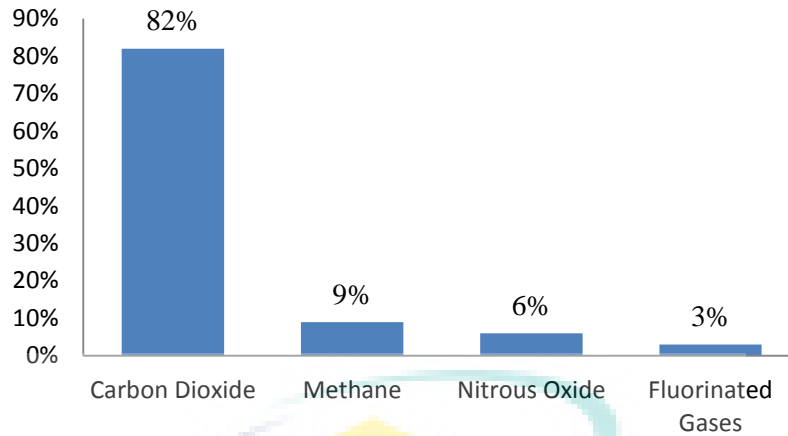


Figure 1.1 Percentage Greenhouse Gases 1990-2012 based on U.S. Inventories.
Source: U.S. Environmental Protection Agency, (2014)

The emission of CO₂ can increase the temperature of the earth and leads to climate change. The concentration of CO₂ in the atmosphere has risen by 40 per cent in 2007 (Barker, 2007). Figure 1.2 shows the trend of CO₂ emissions from fossil fuel combustion. The amount of CO₂ release is increasing dramatically by year. Therefore, the efforts to capture CO₂ are needed to prevent its release to the atmosphere and avoid negative effects to the people and the environment.

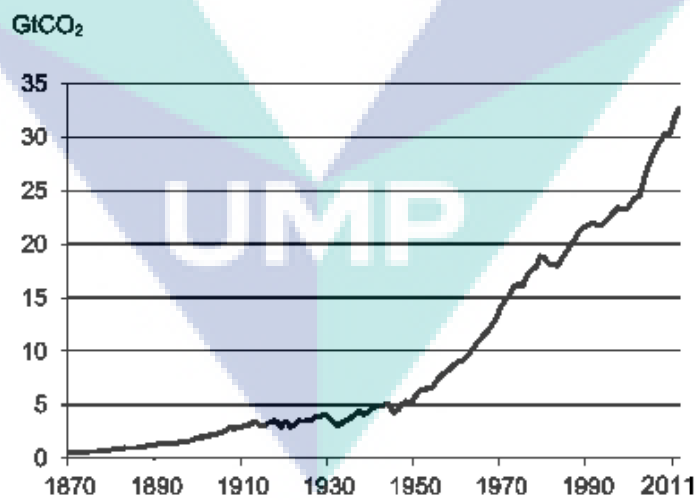


Figure 1.2 Trend of CO₂ emissions from fossil fuel combustion.
Source: IEA, (2015)

The main cause for greenhouse gases emission is the human activities especially the burning of fossil fuels. The fossil fuel power plant is the largest source of anthropogenic CO₂ emission into the atmosphere (Tran, Nguyen, & Le, 2013). High usage of fossil fuel, coal, natural gas and petroleum for power generation were identified

as the main cause for the increase in CO₂ emission which contributed to high global CO₂ emission as high as 86% in 2010 (International Transport Forum, 2010).

The statistics of CO₂ emission from fossil fuels sources has encourage many researchers to explore about technologies to capture CO₂. There are many technologies nowadays to capture and store CO₂ in order to prevent its emission to the atmosphere. The available technology used to capture CO₂ are physical and chemical absorption, low temperature (cryogenic) distillation, gas separation membrane and advance process such as using ionic liquids (Liang, 2003). At present, the most promising technology for CO₂ removal from coal-fired power stations is aqueous amine-based post combustion capture (Robinson, McCluskey, & Attalla, 2011). The process for post combustion capture occurs when fossil fuels and air are burned together before CO₂ is removed from fuel gases. Amine-based absorption process is a process where a chemical solvent is used to capture CO₂ from flue gas. Even though the amine-based absorption technology is already proven to capture and remove CO₂, more studies needs to be conducted in order to improve its efficiency and cost of the regeneration process by focusing on the chemical absorbent used in process.

Molecular dynamic (MD) is a computer simulation technique of complex systems that is modelled at the atomic level. This computational technique is an effective method to discover more details about absorption process and also CO₂ capture (Maginn & Elliott, 2010). Besides that, MD simulation offers a systematic and more accurate, calculation that gives results closer to the actual absorption process (Xing et al., 2013). MD simulations is also used to explain the theory in chemistry studies for the microscopic behaviour at the nano-scale, such as diffusion, (Li et al., 2010). It also helps in saving the experimental time and cost (Charpentier, 2002). The understanding of fundamental in chemistry at the molecular level gives benefit in the study of the removal of CO₂. Strength of attraction or repulsion interaction can be observed by analysing absorption process system with the radial distribution function analysis (RDF).

1.2 Problem Statement

Simulation works for amine absorption process for CO₂ capture at macro scale that emphasises on process simulation, optimization and control is well established. One of the challenges of amine-based absorption process for CO₂ removal is the stability of

the carbamate ion formed was strong and it requires high heat for the process of solvent regeneration (Desideri & Paolucci, 1999). Another challenge of this process is solvent degradation due to thermal and oxidation process in the presence of oxygen. The solvent degradation products can cause corrosion problem to the system. As many amine-based solvents are corrosive, there are limitations with regard to the concentration of amine that can be applied economically. Yu (2012) suggested that the future research should focus on the solvent formulation so that the chemical absorption process efficiency can be improved.

Considering the amine-based solvent characteristics, it is important to develop a clear understanding on the solvent molecular structure and its intermolecular interactions that influence the CO₂ absorption process. Molecular scale study will provide the insight of intermolecular interactions involve in the absorption process of CO₂ using amine-based solvent. So far, studies on amine absorption process at molecular level are still at an early stage and not many studies have been published.

Thus, this study was aim to apply MD simulation to describe the CO₂ absorption process at molecular level and definitely can give insight on molecular behaviour to improve the absorption process and overcome the limitation of this process in real plant. This simulation software has been reviewed as powerful and versatile tool to describe the chemical engineering processes at the atomic level.

1.3 Research Objectives

The objectives of the study are as follows:

1. To study the intermolecular interactions in amine-based solvent for CO₂ capture using MD simulation.
2. To investigate the effect of temperature, concentration and types of amines for CO₂ absorption process.
3. To evaluate the effect of single and blended amines on intermolecular interaction in amine absorption process.
4. To analyze the effect of carbamate molecules in the removal of CO₂ for regeneration process.

1.4 Scope of Research

This study focused on several scopes in order to achieve its objectives. The scopes are as follows:

1. To investigate the intermolecular interaction in amine solution and amine-CO₂ absorption process based on binary (amine + water) system and tertiary system (amine + water + CO₂) system.
2. To analyse the intermolecular interaction by using radial distribution function (RDF) analysis.
3. To study effect of different operating conditions on intermolecular interaction and diffusivity of CO₂ in amine solution.

(a) Temperature: 25, 35, 40 and 45°C

Temperature and pressure used in this simulation work is based on the actual process condition in absorption plant. From literature, study experimental a review of CO₂ capture by absorption and adsorption process at temperature and pressure in ranges 273 K-423 K and 1 bar (Yu, 2012) (Ye, Chen, & Yuan, 2012) (Aaron & Tsouris, 2005) (Silva et al., 2007).

(b) Amine concentration: 10, 20, 30 and 40 wt.%

Weight percent of solvent MEA aqueous is choose based on the literature data and actual absorption process in industry. Based on literature, study the MEA degradation oxygen (O₂) mass transfer effects under CO₂ conditions, the range weight percent of MEA aqueous used is 15 wt.%-30 wt.% (Goff & Rochelle, 2004).

4. To study effect different types of amine such as primary, secondary and tertiary amines were used.
 - (a) Primary amine: Monoethanolamine (MEA), 2-Amino-2-methyl-1-propanol (AMP), Piperazine (PZ)

(b) Secondary amine: Diethanolamine (DEA)

(c) Tertiary amine: Methyl diethanolamine (MDEA)

5. To compare the intermolecular interaction of pure and blended amines system for absorption process.

(a) PZ (10 wt.%) + MDEA (30 wt.%) + CO₂ (10 wt.%)

(b) AMP (15 wt.%) + MDEA (30 wt.%) + CO₂ (10 wt.%)

Speciation of the liquid phase in this thesis has been determined mainly based on reactions and experimental data given by (Lionel Dubois & Thomas, 2011).

6. To study effect different type of carbamate amines for stripping process.

(a) Primary amine: Monoethanolamine carbamate (MEACOO⁻)

(b) Sterically amine: 2-Amino-2-methyl-1-propanol carbamate (AMPCOO⁻)

(c) Activation amine: Piperazine carbamate (PZCOO⁻)

1.5 Significant of Study

Research on molecular modelling of amine absorption process for CO₂ capture was proposed in this study to give insight about this process at molecular level and to analyse the intermolecular interaction between CO₂ and amine solution. The strength of intermolecular interaction represents the effectiveness of absorption process. Better understanding on the solvent molecular structure and intermolecular interaction of solution mixture is crucial to improve CO₂ removal process using amine-based solvents to be more energy efficient and reduce losses and corrosion rates. The findings of this work explain the effect of varying process operating condition i.e.; temperature, concentration, and different types of solvent amines on absorption process for CO₂ capture. The outcomes from this research can be applied as guideline in the selection of solvent based on its characteristics that give significant effect to absorption process. This will help in improving the existing solvents and the consideration of using blended amine

solvent in the future so that the performance of this process can be improved. The research gap is to investigate the influence of physical interaction between molecules on CO₂ capture process by analysing system with RDF.

1.6 Thesis Organization

The thesis is organised in five chapters.

- Chapter 1 is the introduction part of this study. This chapter consist of research background, problem statement, research objective, scope of research and significant of research.
- Chapter 2 review the published information related to this work. Details description of amine based absorption process includes types of amine solvent and molecular dynamic (MD) simulation was provided in this chapter. The chemistry of the intermolecular interaction and thermodynamic properties involved in this process also are explained in this chapter.
- Chapter 3 provides the explanation for the methodology part. This chapter describes the simulation tool used in this study, molecular speciation, procedure to simulate the system, and analysis for simulation results. Explanation on the methods to analyse and interpret graphical results is also provided in this chapter.
- Chapter 4 discuss the results obtained from the MD simulations. The analyses involved the radial distribution function (RDF) results. Discussion on all simulation result gives insight on how MD simulation at molecular level can contribute to the absorption process.
- Chapter 5 is the conclusion part. The outcomes of this study are summarised and concluded in this chapter. The recommendations are also provided in order to improve the future work.

CHAPTER 2

LITERATURE REVIEW

2.1 Introduction

This chapter reviews the fundamental of amine-based absorption process and the application of molecular dynamic (MD) simulation in the absorption process. It starts with the technologies available for CO₂ capture and details description of amine-based absorption process including the types of amine solvents. It is followed by the review of main computational simulation used in this research, which is MD simulation. Conceptual of molecular mechanics and all theoretical information regarding to the component in MD simulation software is also briefly discussed.

2.2 CO₂ Capture Process

Many studies have been published to optimise the existing CO₂ capture process so that it can operate at optimum conditions. In addition, the target is to minimise the operating and capital cost and to have an environmentally friendly process (Energy, 2013). Three main methods for the capture of CO₂ from power plant generation are post combustion, pre-combustion, and oxy-fuel combustion.

Pre-combustion process to capture CO₂ occurs after the conversion of carbon monoxide (CO) into CO₂ in synthesis gas. Based on Kanniche et al., (2010), the treatment in gasification coal synthesis gas and reforming process with oxygen will produce CO and hydrogen. Then the CO will react with steam to convert to CO₂ and hydrogen (H₂). Pre-combustion technology requires high energy costing since it uses high conditions of pressure (2.5-5 MPa), CO₂ concentration (25-40%), and temperature (Babu et al., 2013; Kim et al., 2011). Babu et al. (2013) presented pre-combustion CO₂ capture by using the clathrate hydrate process and Kim et al. (2011) used gas hydrate crystallisation.

In oxy-fuel combustion, CO₂ capture occurs during the combustion of oxygen or air with recycled flue gas. It is also recognised as the combustion in air/CO₂ mixture (Fryda et al., 2010). The oxy-fuel combustion produces high concentration of CO₂. Disadvantages of oxy-fuel combustion are the limitation in finding the optimum amount of coal particles, the process requires pure oxygen, which is up to 90% purity to generate the absorption (Glarborg & Bentzen, 2007; Toftegaard et al., 2010), low energy efficiency, and leakage of air into the flue gas system (Chen, Yong, & Ghoniem, 2012).

Post-combustion process involves the capture of CO₂ from the flue gas of conventional pulverized-coal-fired power plants at low partial pressure (Harun et al., 2012). This process is divided into chemical absorption and physical absorption. Chemical absorption by using amine absorbent is getting attention for its efficiency to capture CO₂ for decades (Lawal et al. 2011; Merkel et al., 2010). Amine-based absorption process is a promising technology to capture CO₂ in term of development and applicability, and it can be retrofitted to the existing power plants (MacDowell et al., 2010). Furthermore, chemical absorption process is more energy efficient and less expensive compare to adsorption process, cryogenic separation and membrane separation (Herzog, 1999). Many initiatives are done under carbon capture and sequestration (CCS) using amine absorption process, but improvement has to be carried out to reduce the cost of processing and energy requirement. Currently, researchers are struggling to improve the efficiency of absorption process by developing highly efficient absorbents.

2.3 CO₂ Separation Technologies

On the basis of three CO₂ capture processes, post-combustion process was selected to be used due to its suitability to capture CO₂ produced from fossil fuel source. Many technologies are applied to pilot plants for fossil fuel power plants, but studies are being done for the large scale amine based absorption to capture CO₂ (Shao & Stangeland, 2009). This study employed the post-combustion process to investigate the effects of amine parameter and blends on CO₂ absorption process. Figure 2.1 shows the technologies to capture CO₂ that are available in the industries.

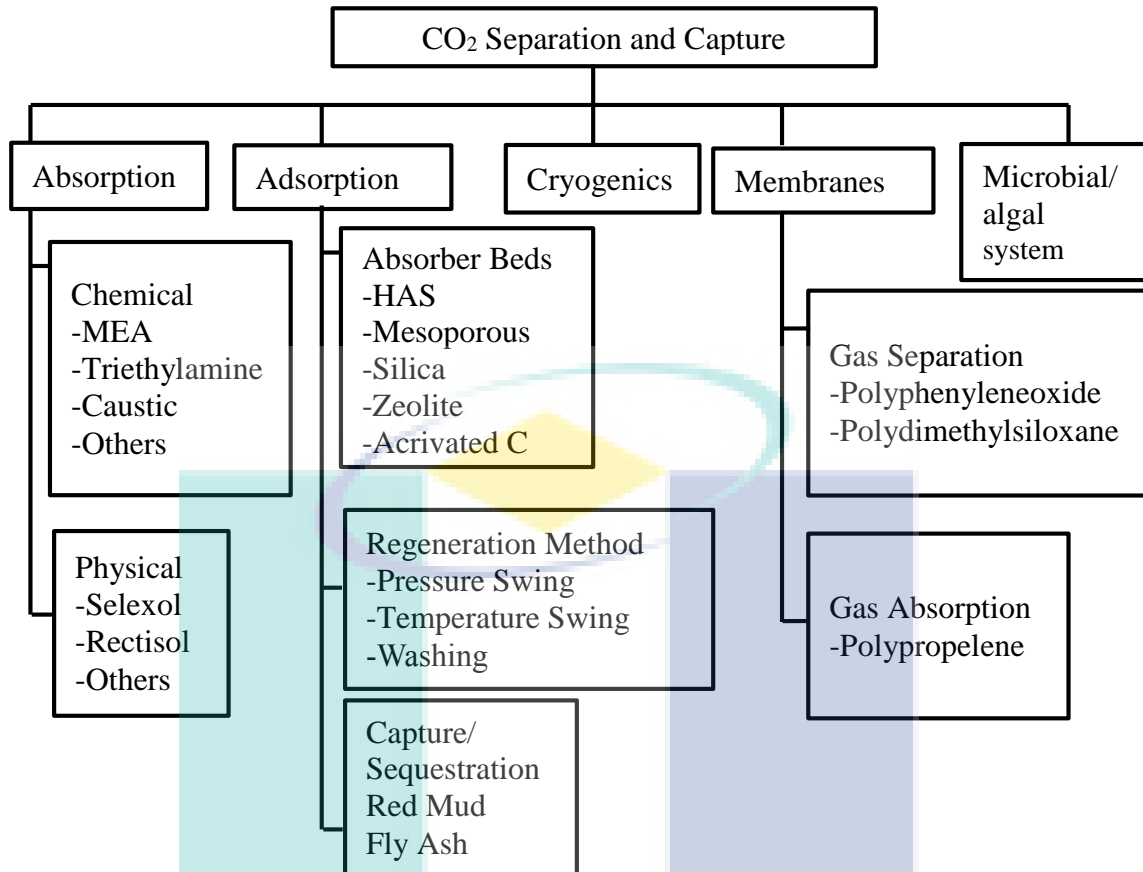


Figure 2.1 CO₂ separation and capture technologies.
Source: Rao & Rubin (2002)

Five types of technologies are available for CO₂ capture, which are adsorption, cryogenics, membranes, microbial/algal system, and absorption process. For gas separation using adsorption process, many conventional adsorbents can be used such as activated carbons (Rahman et al., 2005), metal oxides, pillared clays and zeolite (Nor Kamarudin, Khairul Sozana & Mat, 2009), aluminosilicate zeolite molecular sieves, and titanosilicate molecular sieves (Ebner & Ritter, 2009). The fundamental theory of adsorption process is the equilibrium between the amount of the adsorbed material and the pressure or concentration at constant temperature (Wang & Giammar, 2013). Adsorption process for CO₂ capture can be classified as either physical adsorption (physisorption) or chemical adsorption (chemisorption), depending on the type of forces between the adsorbent and CO₂. Physical adsorption from a gas occurs when the intermolecular attractive forces between molecules of the solid adsorbent and the gas are greater than those between molecules of the gas itself. In chemisorption, there is a transfer or sharing of electron, or breakage of the adsorbate into atoms or radicals which are bound

separately. The adsorption processes used in the separation of CO₂ are temperature swing adsorption (TSA), pressure swing adsorption (PSA), and hybrid of PSA/TSA (Ebner & Ritter, 2009). The advantage of adsorption process is that it is an economical purification process. The CO₂ content within purification process is reduce from 3 to 0.5% (Keskes, Adjiman, Galindo, & Jackson, 2006).

Membrane is a porous material that acts as a filter (Folger, 2013). The pressure differential across a membrane is the driving force for this separation process. Membrane technology was already established before 1980 and improvement to fabricate high-performance membranes is still on going. The important criteria in membrane process to produce high CO₂ absorption are high CO₂ selectivity, high CO₂ permeability, cost effective, and thermally and chemically robust (Baker, 2002; Powell & Qiao, 2006). In order to achieve high permeation rate, the effective thickness of membrane for gas separation has to be thin, for example less than 0.5µm. The weaknesses of using hollow fibre or flat asymmetric membranes are high cost and brittle (Powell & Qiao, 2006).

For gas separation, cryogenic separation uses the principle of cooling and condensation. Cryogenic separation is mostly used for O₂ separation from air and for oxyfuel combustion (Li et al., 2011). Temperature and pressure are manipulated to effectively liquefy the CO₂. The disadvantage of cryogenic separation is that it requires high energy for its cooling system (refrigeration energy) and to pressurise the system. However, this technique yields CO₂ that is ready to store and transport (Aaron & Tsouris, 2005; White et al., 2003).

Absorption is a process to transfer one or more compounds from one phase into another. The species transferred to the liquid phase are commonly called as absorbates. Physical absorption involves the transfer of gas molecules to liquid solvent. Organic or inorganic solvents are used to physically absorb CO₂. This process uses the concept of Henry's law, which the absorption occurs at high CO₂ partial pressure and low temperature (Li et al., 2011). The advantage of this process is that it requires low energy demand. Physical absorption is better compared to chemical absorption because it can produce higher CO₂ loading capacity at high CO₂ partial pressure (Keskes et al., 2006). The examples of solvents used commercially for physical absorption are tributyl phosphate (TBP), propylene carbonate (PC), normal methyl pyrrolidone (NMP), methanol, dimethyl ether, and mixture of polyethylene glycol dialkyl (Newman, 1985;

Olajire, 2010). The application of ionic liquids in CO₂ absorption can be done by combining both chemical and physical absorption, which is also known as physisorption/chemisorption of CO₂ (Pinto et al., 2014). 1-Ethyl-3-methylimidazolium acetate and 1-ethyl-3-methylimidazolium ethylsulfate are used for chemical and physical absorption, respectively.

Chemical absorption process is the most commonly used method for CO₂ removal. Absorber and stripper are two processes that utilise the principle of absorption. In an absorber, gas compound (solute) is injected and mixed with solvent. In a stripper, the opposite process occurs, in which the gas is separated from the solvent. The pressure and temperature normally used in chemical absorption processes are 1.0 bar and 40-60°C, respectively (Yu, 2012). Chemical reaction occurs between the substances present to be absorbed and the absorbing medium. Chemical absorption process is a chosen method for post-combustion process and already practised since the 1930's (Kothandaraman, 2010). The list of advantages and disadvantages of amine-based absorption process are as follows:

The advantages of amine-based absorption using amine as absorbent are:

- (a) The most matured technology for CO₂ capture and already established for many decades (Derks & Versteeg, 2009).
- (b) The chemical reaction of amine with CO₂ and absorption are faster even at low partial pressures of CO₂ (Kallevik, 2010).
- (c) This technology is suitable for retrofitting of the existing power plants (Mores, Scenna, & Mussati, 2011).
- (d) Pure CO₂ can be obtained by using different amines or blended amines and it is suitable application for industrial flue gas (Mores et al., 2011).
- (e) Amine solvent can be recycled because the reaction is reversible (Strazisar, Anderson, & White, 2001).

The disadvantages of amine-based absorption using amine as absorbent are:

- (a) The process is energy-intensive and the cost is expensive (Muñoz et al., 2009).
- (b) The amount of CO₂ capture is low. It requires high amount of amine solvent to capture CO₂ (kg CO₂ absorbed per kg amine) (James & Henry, 2004).

- (c) Potential to have corrosion in the equipment and degradation when excessive solvent containing O₂ is used (Mores et al., 2011).

By using amine-based absorption, almost 90% CO₂ capture can be achieved but the capital and operating costs were very high (Fisher, 2007). The selection of amine for absorption process were based on the characteristics of aqueous solubility, basicity and stability (Muñoz et al., 2009). Different amines have different reaction rate for CO₂ absorption process. The most commonly used amine in the chemical absorption processes is a primary amine. Primary amine is used for its fast reaction to bond with CO₂ compared to secondary or tertiary amine. MEA is always used as a benchmark in most studies (Dubois & Thomas, 2012). Nevertheless, MEA has limitation such as low CO₂ capacity loading, high energy demand during regeneration process, and corrosion of equipment (Fauth et al., 2005; Yeh et al., 2005).

2.4 Amine-Based Absorption Process

The post-combustion CO₂ capture process is one of the promising technologies. The aqueous amine solvent in the absorber and stripping can enhance the CO₂ capture. Nowadays, there are many industries use aqueous amine in their plants for CO₂ removal. Figure 2.2 shows an example of the process flow diagram for the simulated process plant of amine post-combustion CO₂ capture process (Lee et al., 2013). The flue gas from power plant is pre-cooled first in a contact condenser and compressed slightly before being sent to the bottom of the absorber column. Solvent with low CO₂ concentration, or lean amine, enters the top of the absorber and reacts with the amine solvent in the absorber. The solvent stream rich in CO₂, or rich amine, exits the bottom of the absorber. The CO₂ lean overhead flue gas stream exits the top of the absorber and capture with store in a tank for prevent CO₂ emitted to the atmosphere. The rich Amine solution is pre-heated in a cross flow heat exchanger by hot lean amine solution before entering the stripper. The CO₂ is thermally driven out of solvent, regenerating the amine and a moisture rich in CO₂ leaves the bottom of the stripper is cooled first before sending it back to the absorber as lean amine. The CO₂ from the overhead stream of the stripper column is captured. The established operating condition for CO₂ absorption process is by using 30 wt.% MEA amine solvent solution, with the temperatures of 40 °C and 120 °C

for the absorber and stripper at the atmospheric pressure, respectively (Puxty & Rowland, 2011).

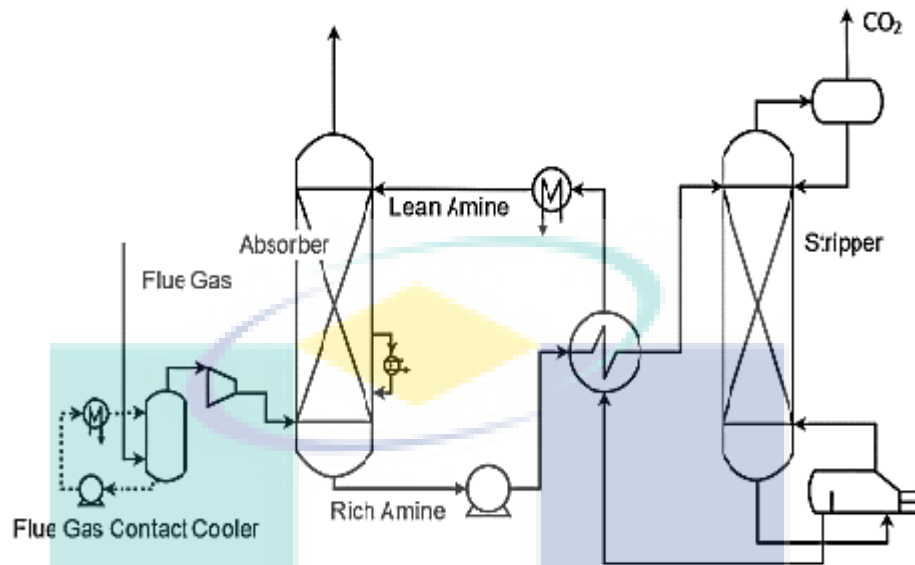


Figure 2.2 Process flow diagram of amine post-combustion CO₂ capture process from simulated process plant.

Source: Lee et al., (2013)

2.4.1 Experiment Work using Single Amine

There are a few reports that highlighted about the amine-based CO₂ absorption process. Cullinane and Rochelle (2004) studied the CO₂ absorption process in wetted-wall column using potassium carbonate and piperazine (PZ). The addition of 0:6 M PZ to 20 wt.% potassium carbonate increased the rate of CO₂ absorption at 60 °C. PZ has a cyclic diamine structure that may favor rapid formation of the carbamates. As a mild base, it may catalyse the proton extraction in the reaction mechanism. Also theoretically, one mole of amine can absorb two moles of CO₂. The promoted potassium carbonate is expected to retain its low energy of regeneration, and the reaction of carbonate in bulk solution is expected to increase the absorption capacity. Rayer and Henni (2014) studied the CO₂ absorption process using MDEA, Triethanolamine (TEA), 1-dimethylamino-2-propanol (1DMAP), and 3-dimethylamino-1-propanol (3DMAP) by experimental flow calorimeter. Eighty per cent of the operational cost comes from the cost of solvent regeneration. Therefore, there is a need to develop solvents that require low energy consumption during regeneration. Abdul Halim et al. (2015) studied the absorption experiments using MEA. The processes were performed in a 2.040 m high and 0.046 m

inside diameter (ID) packed column. At a high pressure of 5.0MPa, CO₂ removal percentage was increased with the increased of MEA concentration. The optimum temperature for CO₂ absorption was 40°C. López et al. (2015) studied the absorption process using new amine, Diisopropanolamine (DIPA) and Monoisopropanolamine (MIPA) in a bubble column reactor. The mass transfer coefficient was decreased with the increased amine concentration. The application of DIPA increased the viscosity and reduced the mass transfer coefficient. Rayer and Henni (2014) found that the heat of absorption was decreased when the steric hindrance group was increased by the alkyl group. The order of the heat of absorption values is TEA < MDEA < 3DMAP < DMAEOE < 1DMAP. As the number of -OH group increases, the heat of absorption values decrease. The position of the -OH group from the amino also influences the heat of absorption.

2.4.2 Experimental Work using Blended Amine

The success of amine solvent is due to meet criteria of give high rate of reaction in absorber and requires low heat of reaction in stripper. The combination of primary or secondary amine with tertiary amine is identified as a good way to improve the efficiency of amine solvent. The sequence of high to low degradation is straight chain di- and triamines > MEA > tertiary amines > alkanolamines with steric hindrance > long chain alkanolamines > cyclic amines with no side chains (Davis, 2009).

Barzagli et al. (2010) studied the CO₂ absorption process using DEA, MDEA, and AMP. AMP showed the highest absorption efficiency and MDEA was best for regeneration at any amine concentration and desorber temperature. At high amine concentration (2.00 M), lowest CO₂ absorption efficiency was observed. DEA showed modest performance compared to other amines. Blended AMP/MDEA showed highest absorption rate compared to AMP/DEA and AMP/MEA because DEA and MEA produced carbamate that influenced the efficiency of absorption and desorption processes. Choi et al. (2009) studied the CO₂ absorption/regeneration experiment using MEA and AMP. High CO₂ loading of blended MEA/AMP solutions was obtained compared to single MEA and AMP amines. This work also showed that MEA had more influence in CO₂ separation (regeneration part) but AMP was more dominant for fast reaction during the absorption. At high concentration of MEA, the reaction rate of blended MEA/AMP was increased and CO₂ loading was decreased. However, at high

concentration of AMP, the result was reversed. Because, for MEA can directly react with CO₂ through carbamate reaction and produced a stable carbamate. Due to this, CO₂ loading was limited by stoichiometry to 0.5 mole CO₂/mole amine. Meanwhile, AMP had unstable carbamate and fast hydrolysis reaction, which resulted in the stoichiometry of 1.0 mole CO₂/mole amine from the reaction of zwitterion mechanism. Nainar and Veawab (2009) carried out the electrochemical corrosion experiments using the potential dynamic polarisation technique for corrosion measurements for MEA and PZ. Blended MEA/PZ resulted in more corrosion compared to MEA alone. When the concentration of PZ was increased, the corrosion rate was increased. The corrosion rate of carbon steel was increased with the increased in the concentration of PZ, total amine concentration, CO₂ loading of solution, solution temperature, and the presence of heat stable salts. Tertiary amines have a lower regeneration energy requirement, but also a lower absorption rate. Meanwhile, primary and secondary amines are effective in the absorption process, but both are more difficult to regenerate because of the high heat of reactions involved. Dinca (2015) studied the MEA and DEA based absorption process using the circulating fluidized bed combustion (CFBC) technology. The increased concentration of DEA influenced the increased in absorption capacity of CO₂ in blended MEA/DEA solutions. The highest absorption capacity of CO₂ was 0.23 mole CO₂/mole DEA at 40 wt.% concentration. Conway et al. (2015) studied the absorption process using MEA, N,N-dimethylethanolamine (DMEA), N,N-diethylethanolamine (DEEA) and AMP in wetted wall column (WWC) contactor. The absorption capacity of blended MEA/AMP was significantly higher than single MEA solution. For CO₂ mass transfer analysis, a single MEA solution gave higher result compared to blended solvent amine at similar CO₂ loading and total amine concentrations. Zhang et al. (2016) studied the blended amine of MEA, 1-Dimethylamino-2-propanol (1DMA2P), and MDEA using ¹³C NMR technique. Solution that was blended with tertiary amine showed low energy consumption in the regeneration process. In addition, the bicarbonate ions breakdown with low heat duty was also observed compared to MEA. Blended MEA/1DMA2P produced more bicarbonate ions than MEA/MDEA which made 1DMA2P a better choice in the regeneration process.

Mandal et al. (2001) studied about the simulation of blended amine MDEA/AMP and AMP/MEA for CO₂ absorption process using the subroutine DDASSL in double precision FORTRAN. The results showed that the additional of MEA in MDEA or AMP

solution can increase the CO₂ absorption. Blended amine solution of AMP/MEA gave high absorption rate compared to MDEA/MEA solution. Mandal et al. (2003) reported about the effect of blended amines of AMP/DEA solution on the CO₂ absorption process. Blended AMP/DEA showed high rate of CO₂ absorption compared to blended amine MDEA/DEA. Sterically amine such as AMP can enhance the CO₂ absorption rate compared to DEA solution. Mandal and Bandyopadhyay (2005) studied the effect of blended amine AMP/DEA on the simultaneous CO₂ and Hydrogen sulfide (H₂S) absorption process. They found that blended amine AMP/DEA was an effective solvent used to absorb CO₂ and H₂S. Mandal and Bandyopadhyay (2006) studied the effect of aqueous blended amine of AMP/MEA in CO₂ absorption process. The results showed that AMP/MEA blended amine was a potential solvent to absorb CO₂ with fast reaction rate of 9500 m³/kmol.s at 313K and high amount of CO₂ was being absorbed.

Aroonwilas and Veawab (2004) studied about single and blended amine in a packed column CO₂ absorption process. They found that sequence of CO₂ absorption rate capacity for single amines are MEA > DEA > AMP > DIPA > MDEA. Blended amines such as MEA/MDEA, DEA/MDEA, MEA/AMP, and DEA/AMP were also tested. The result showed that high CO₂ absorption performance on blended AMP solvent especially MEA/AMP was observed compared to blended MDEA solvent.

Dubois et al. (2010) studied the CO₂ absorption into single and blended amines of (piperazinyl-1)-2-ethylamine (PZEA), AMP, MEA, and MDEA. They reported that blended amines of AMP/MEA solution gave effective absorption efficiency compared to blended amine AMP/MDEA. For amine activation, PZEA solution produced high CO₂ absorption rate compared to AMP solutions. Higher amine concentration increased the liquid phase reaction and yielded good absorption efficiency. Based on CO₂ absorption performance, PZEA and AMP efficiencies were in between the MEA and MDEA solutions.

Barzagli et al. (2010) studied the absorption and regeneration process of CO₂ by single and mix DEA, MDEA, and AMP amines. Compared to pure amine, AMP solvent was good for absorption process and MDEA solvent was effective in regeneration process. Meanwhile, high performance for absorption and regeneration was exhibited by blend amine AMP/MDEA compared to AMP/DEA alone.

2.4.3 Computational Chemistry Study

Other than experiment works, several studies were conducted to analyse this process using computational approach. This section will describe previous studies done for CO₂ absorption process at micro level.

Farmahini (2010) studied about the blended PZ/MDEA absorption processes for CH₄ and CO₂ using MD simulation. From this dissertation, it shows that small amount of PZ can accelerate the CO₂ absorption process by MDEA solvent. The following year, Farmahini et al. (2011) reported that blended of MDEA and PZ gives good combination for CO₂ absorption process. PZ molecule forms protonated piperazine (PZH⁺) and piperazine carbamate (PZCOO⁻) that cause high solubility in water. Formation of PZCOO⁻ accelerated the absorption process.

Maiti et al. (2010) conducted atomistic modelling research for CO₂ capture using primary and tertiary amines. This research was done using Quantum chemical and classical MD simulation. The speciation was evaluated based on the fraction of ionic species, density and volume changes and ionic association. The density of carbamate was increased in MEA compared to bicarbonate ion in MDEA. It shows that MEA was able to absorb more CO₂ than MDEA. Similar methodology approach used by Singh (2011) but using solvent Hexamethylenediamine (HMDA) for CO₂ absorption process. Absorption rate was decreased with the increased in chain length of amine. The potential of HMDA was also investigated in that study. Interaction of amine and CO₂ was discussed using molecular dynamic simulation. (Singh, Niederer, & Versteeg, 2007, 2009) performed the modelling studied of CO₂ absorption using alkanolamine solutions. Their simulation work used the Density Functional Theory (DFT) with dielectric continuum solvation models and Conductor-like Screening Model for Realistic Solvents (COSMO-RS) model. They found that the alcohol chain length of alkanolamine affected the yield of CO₂ absorption process.

Yamada et al. (2013) performed computational investigation of CO₂ absorption using alkanolamine solutions. This simulation work used Density Functional Theory (DFT) with dielectric continuum solvation models and Conductor-like Screening Model for realistic solvents (COSMO-RS) model. From that study, it was found that alcohol chain length of alkanolamine affected the yield of CO₂ absorption process. Calculation

was based on intramolecular for hydrogen bond (NCOO--HO) in carbamate. Matsuzaki et al. (2013) applied Polarizable Continuum model (PCM), Ab initio molecular orbital method to study inter conversion of carbamate and bicarbonate for MEA. They proposed a new pathway mechanism, in which proton ion was transferred from carbamate to form bicarbonate ion and MEA. Besides that, study reported by Emmanuelle Masy (2013) shows that MEA has high CO₂ diffusivity compared to MDEA and ethylamine due to small spatial configuration and low amount of hydroxyl group in amine structure. Hydroxyl group contribute more significant affect to diffusivity than geometry of amine.

Sumon et al. (2014) studied about reaction mechanism involved in CO₂ absorption process using Ab initio in MD simulations. Structures for carbamate zwitterions (R₁R₂NHCOO[±]) and carbamic acid (R₁R₂NCOOH) was observed. This report was aimed to improve mechanism for kinetic model. Hwang et al. (2015) also studied about chemical reaction mechanism. From quantum chemical calculation, a zwitterion-mediated two-step mechanism is used in reaction of amine with CO₂ absorption and desorption process. It was observed that proton was transferred in MEA+CO₂+H₂O by H-bonded water bridges. Current research done by Kachko et al. (2016) using an Aspen Plus model32–34 with chemometrics approach for the simulation of CO₂ absorption by aqueous MDEA. Solutions activated by PZ were used for the properties estimation of the liquid solvent under pilot plant conditions. The model used was the unsymmetrical electrolyte NRTL (eNRTL) method and the PC-SAFT equation of state was used to compute liquid and vapour properties, respectively. Prakash and Venkatnathan (2016) studied CO₂ absorption process using ionic liquid (IL). The CO₂ was absorbed in the bulk IL layers during the first ten nanoseconds. The interaction of CO₂ was more on cations of the IL compared to anions.

Idem et al. (Idem, Edali, & Aboudheir, 2009) conducted experimental and simulation work at various concentration of MDEA/PZ, temperature and CO₂ loading to determine the reaction rate constant. Edali et al. (Edali, Idem, & Aboudheir, 2010) developed a 2D model for the blended amines MDEA/PZ using COMSOL software to study the concentration profiles of all the species considering both the radial and axial directions. It was revealed that PZ may be depleted when a loading of the solvent blend MDEA/PZ was greater than 0.015 mol/mol is exposed to CO₂ from the top of the laminar jet absorber.

2.4.4 The Gap of Study

Most of the previous research work has focused on the computational chemistry, notably regarding the calculation of ionic and enthalpy effect for the CO₂ absorption process. This study aims to apply the computational chemistry studies focusing on the physical inter- and intra-molecular interaction in the CO₂ regeneration process. There is research gap for the physical molecular interaction in the open literature for CO₂ absorption and regeneration process.

2.4.5 Alkanolamines Solvent

Alkanolamine is an amine/ammonia compound that contain hydroxyl (-OH) and amino (-NH) functional groups on an alkane chain. The hydrogen atom in ammonia compound (NH₃) is replaced first by alkyl or aryl group to form an amine compound. The alkanolamine can be classified into three categories, which are primary (1°), secondary (2°), and tertiary (3°) amines based on the number of alkyl group replacing the hydrogen atom (Farmahini, 2010). Besides that, there are sterically hindered amines that act as catalyst to enhance the reaction of amine solution with CO₂ gases. Sterically hindered amine can save the regeneration cost up to 40%.

2.4.5.1 Primary Amine

Primary amine is a molecule containing one substituent alkyl group and two hydrogen atoms attached to the nitrogen atom. MEA is one of the primary alkanolamines (Toon, 2003). Alkanolamine is a base compound that forms a weak base when dissolved in water. The functional groups in MEA are one (-OH) group and one (-NH) groups. MEA is a primary alcohol and it is corrosive in the presence of H₂O.

2.4.5.2 Secondary Amine

Secondary amine is a molecule that has two substituents alkyl group and one hydrogen atom bonded to the nitrogen atom (Toon, 2003). DEA is a secondary alkanolamine with two hydrocarbons attached to the nitrogen atom. Other names of DEA are bis(hydroxyethyl)amine and diolamine. DEA exhibits the properties of amine and alcohol. Due to the alcohol group, it can be soluble in water as hydrophilic molecule.

Besides that, DEA is known as an effective solvent in absorption process with pressure of more than 30 kPa (Lunsford & Bullin, 2006).

The chemical reactions of primary and secondary amines are similar as both will form a stable carbamate. The comparison of primary and secondary amine with tertiary amine is these amine capable to react with CO₂ since it has free hydrogen attach at nitrogen atom and can form a stable carbamate ion. But, primary and secondary are difficult to break the bond and remove CO₂ from the solvent. In addition, high energy is required at the regeneration process. The CO₂ loading capacity product by primary/secondary amines is also low at 0.5 mole CO₂/mole amine (Bougie & Iliuta, 2012).

2.4.5.3 Tertiary Amine

Tertiary amine is a molecule that has three substituent alkyl groups attached to a nitrogen atom (Toon, 2003). MDEA is a tertiary amine that has three hydrocarbons attached to the nitrogen atom. Other name of MDEA is bis (2-hydroxyethyl) methylamine. TEA is also a tertiary amine, but the difference is that MDEA has two hydroxyl (-OH) bonds and TEA has three hydroxyl (-OH) bonds. Other names of TEA are triethylamine and 2, 2', 2''-trihydroxy-triethylamine.

The chemical reaction of tertiary alkanolamine is the opposite of the reactions of primary and secondary amines. The reactivity of tertiary amine with CO₂ is significantly slow compared to primary and secondary amines due to absence of carbamate ion and only involves bicarbonate ion formation. Nevertheless, it requires less energy to break the bond of amine-CO₂ during the regeneration process. Bicarbonate formation has low heat of reaction and it leads to low solvent regeneration cost (Vaidya & Kenig, 2007). In addition, CO₂ loading capacity by absorption tertiary amine was high with the value of 1 mole CO₂/mole amine (Bougie & Iliuta, 2012).

2.4.5.4 Sterically Hindered Amine

Sterically hindered amine is a new class of amine that gets great attention. The chemical reactions of sterically hindered amines with CO₂ form unstable carbamate (low stability) due to presence of hindrance beside (-NH) group. However, the hydrolysis process with unstable carbamate leads to the formation of bicarbonate ion.

AMP is one example of sterically hindered amine. Other names of AMP are isobutanol-2-amine and aminomethyl propanol. AMP is a primary amine which contains one (-NH) group bonded to the tertiary carbon atom and one (-OH) group. AMP acts as additive in the absorption process and co-dispersant for particulate system. Moreover, AMP can be a corrosive inhibitor for steam-condensate equipment (“AMP Properties,” 2000).

2.4.5.5 Cyclical Amine

Cyclical amine is an amine in which the nitrogen atom is allocated in a ring structure. Cyclical amines can be secondary or tertiary amines. The aim of blending cyclical amine with tertiary amine is to improve the absorption rate. Cyclical amine acts as activator in amine solvent. One example of cyclical amine is PZ. PZ is an advanced amine that is always blended with conventional amine, such as MEA and MDEA, and acts as promoter to increase absorption rate.

Other names of PZ are piperadine and diethylenediamine. PZ is also known as a cyclical diamine or primary cyclical. PZ is an organic compound that only has (-NH) group and without the (-OH) group like other alkanolamines compound. PZ is presence in cyclic with six-member ring structure. Cyclical amine is mainly used in pharmaceutical field (Tangallapally, Yendapally, Lee, Lenaerts, & Lee, 2005). Rayer et al. (2011) demonstrated the kinetic reaction of CO₂ with amines using the stopped flow technique at 303.15 K. They reported that cyclic amine gave the highest reaction rate compared to primary, secondary, and tertiary amines due to the high quantity of -CH₃ and -CH₂ groups that increase the electron donor to the nitrogen atom. Tan & Chen (2006) also studied about CO₂ absorption process using PZ. The results showed that PZ was the most effective absorbent compared to MEA, AMP, and MDEA. The sequence of amines based on the reaction rate was PZ > MEA > AMP > MDEA, with PZ gave the highest reaction rate. Overall volumetric mass transfer coefficient (K_{Ga}), value of PZ was much higher compared to other amines. Amine scrubbing study by Rochelle et al. (2011) reported that double reaction kinetic was obtained by the reaction of PZ with CO₂ compared to MEA. Also, PZ is unaffected by oxidation and thermal degradation. Cyclic amine also has lower molecular weight and high absorption rate compared to polyamines. In addition, Dugas & Rochelle (2009) studied the comparison between absorption and desorption rates of

CO₂ with MEA and PZ. They reported that the CO₂ absorption capacity by PZ was 75% higher than MEA and the reaction rate was also 2-3 times faster than MEA at 40°C.

2.4.6 The Reaction Mechanism between Alkanolamines and CO₂

Thorough understanding about the reaction and mechanism is important to produce better solvent and improve its efficiency. The CO₂ reaction for absorption process is an exothermic reaction (Eswaran, Adhikari, Chowdhury, Pal, & Thomas, 2010). The reaction of alkanolamines with CO₂ affects the process of amine-based absorption. It is also known as CO₂-amine-H₂O chemistry reaction. The kinetics of the reaction affect the absorber height. As a consequence, the capital cost of the capture unit is high. Alkanolamines have different reactions and mechanisms with CO₂ due to the differences of the molecular structure. The reaction of CO₂ with amine solution produces carbonate, carbamate, and bicarbonate ions through acid-base mechanism reaction (Aroua, Ramasamy, Haji-Sulaiman, & Ramasamy, 2002). Primary, secondary, and sterically hindered amines go through zwitterion mechanism while tertiary amine undergoes the base-catalysed hydration of CO₂ process (Vaidya & Kenig, 2007).

2.4.6.1 The Reaction Mechanism of Primary and Secondary Amines

Reaction and mechanism of primary and secondary amines proposed by Caplow (1968) is also known as two-step mechanism. The mechanism starts with the reaction of CO₂ with an amine as an intermediate reaction or zwitterion instantaneous reaction. Then, proton from zwitterion will be transferred to base to form carbamate ion. This step is also known as deprotonation of zwitterion. The base can be water (OH), hydroxyl ion (OH⁻), or amine functionality (Gutowski & Maginn, 2008; Vaidya & Kenig, 2007). This step is also called as deprotonation of amine. Mechanisms for zwitterion and carbamate formation are shown in Equation (2.1) to (2.4).

Zwitterion pathway:



Carbamate formation water as base:



Carbamate formation amine as base:



Carbamic acid formation:



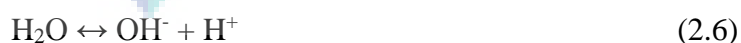
2.4.6.2 The Reaction Mechanism of Tertiary Amine

Reaction and mechanism of tertiary amine with CO_2 were presented by Donaldson and Nguyen (1980). Tertiary amine cannot form carbamate ion directly because of the lack of N-H bond to be displaced by CO_2 . Therefore, it promotes the hydrolysis of CO_2 first to form carbonic acid. This step is also called as base-catalysed hydration mechanism. The function of CO_2 hydration mechanism is to be the catalyst for hydrogen bonding between tertiary amine and water (Donaldson & Nguyen, 1980). Hence, it will reduce the H-O bond strength and the reactivity of nucleophilic between water and CO_2 will be increased. Next, the carbonic acid will react with another amine to form bicarbonate ion and protonated amine, but the kinetics of the reaction is slower than primary and secondary amine. Second-order rate constant used for tertiary amine was reported by García-Abuín et al. (2011). Two important products from tertiary amine are carbonic acid (H_2CO_3) and bicarbonate ion (HCO_3^-) Mechanism reactions involve in tertiary amine is shown in Equations (2.5) to (2.8).

Carbonic acid formation:



Ionisation of water:



Bicarbonate formation:



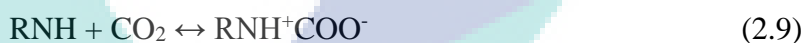
Dissociation of bicarbonate:



2.4.6.3 The Reaction Mechanism of Sterically Hindered Amine

The reaction and mechanism of sterically hindered were proposed by Vaidya and Kenig (2007). As the sterically hindered amine is characterised as primary or secondary amines, it will form carbamate first by reacting with CO_2 . But due to the unstable carbamate ion, it will react with base by hydrolysis process to form bicarbonate ion and free amine molecule. Consequently, the zwitterion undergoes rapid reaction with base compared to conventional primary or secondary amine. This reaction is also known as hydrolysis of carbamate ion. Free amine molecules react with CO_2 and leads to high CO_2 loading. The production of these amines is found to be a great finding in the development of good solvent due to high CO_2 absorption capacity, fast amine- CO_2 reaction, and low heat regeneration cost. The mechanisms involve in sterically hindered amine is shown in Equations (2.9) and (2.10).

Zwitterion pathway:



Bicarbonate formation water as base:



2.4.6.4 The Reaction Mechanism of Cyclical Amine

The rate constant for the reaction of PZ- CO_2 is identified to be the first order (Bishnoi & Rochelle, 2000). The reaction will produce PZ carbamate and protonated PZ. The reaction and mechanism of carbamate formation for cyclical amine is shown in Equation (2.11).

Carbamate formation:



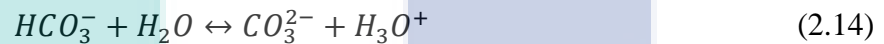
2.5 Stripping Process

The stripping process occurs after amine has successfully bound with CO₂. At this stage, a breakdown of bond between amine and CO₂ happens and amine will be recycled back to the absorber. In industrial processes, high temperatures of more than 100 °C are used to regenerate amine solutions (Singh et al., 2007). The reaction and mechanism of amine and CO₂ are shown in Equations (2.12) to (2.14):

The absorption of CO₂ in amine solution.



The regeneration process of CO₂ removal



2.6 Molecular Dynamic Simulation

There is a huge amount of experimental work done to study the CO₂ absorption process by amine absorbent. Recently, computer simulations are widely used all over the world including Molecular Dynamic (MD) simulation. MD is a modelling technique for complex systems and is modelled at the atomic level. It will explain the molecular interaction and atomic in macroscopic and microscopic behaviours of the physical systems. This computational tool applies the concept of motion to molecules (Lewars, 2010). It is used to investigate the structure, dynamics, and thermodynamics of materials/chemical and biological system. MD simulation is initially started as the need to incorporate physical theory (electron and nuclei) to explain the details in chemistry (Berendsen et al., 1987).

The macroscopic behaviour is replicated to microscopic system and constructed in manageable box in MD simulation. MD simulation computes the initial configuration and system properties of the molecules based on the calculation of length and angle of

bonds, forces applied, and other parameters as input data. Molecular forces applied depend on the interaction that occurs in the system with a given force field. The calculation in MD simulation was initially developed to integrate Newton's second law of motion by B.J Alder and T.E Wainwright in the 1950s. The integration simulates the dynamic of molecules by calculating the particle positions and forces acting on the particles within. The law is shown in Equation (2.15) and (2.16) (Toon, 2003).

$$f_i = m_i a_i = m_i \frac{d^2 r_i}{dt^2} \quad (2.15)$$

$$f_i = \nabla_i V(r_i) \quad (2.16)$$

Where the mass of a particle is represented as m_i , a_i is acceleration, t is time, f_i is the force acting on the particle and $V(r_i)$ is the potential energy with respect to the particle's position. The structure constraints and molecular interactions use the Newton equation of motion in the integration of simulation.

MD simulation is employed to calculate the chemical reaction, kinetic energy, and diffusion coefficient. This computational method has become an effective tool to explore about absorption process and also CO₂ capture. In MD simulation, a modern simulation technique for high-quality simulation will be employed. It consists of double time step algorithm for fast and slow modes, electrostatic interaction by an optimized Ewald method, and a constant temperature-constant-pressure algorithm.

There are many advantages using computer as tool for research purposes. Computer simulations can be used to study the real process through the process model that is related to theoretical and laboratory work. The theory can be verified by doing simulation and compare the model by experimental results. MD simulation benefits the researchers to understand more about the properties of molecule, its structure, and the microscopic interaction between molecules (Allen, 2004). MD simulation acts as a virtual experiment to analyse system at atomic scale (Tu, 2011) and is used to study the properties of nano-scale materials which cannot be observed in experimental work (Kim et al., 2009). Furthermore, MD simulation can be used to study the thermodynamic properties of pure molecule and mixtures (Lopez-Rendon, 2008). RDF analysis is performed to analyse the results from the simulation of interatomic interactions and intra-atomic interactions. The benefits of computational tools compared to experimental work

are less expensive (does not require to buy materials, equipment, and laboratory apparatus), environmentally friendly, and less time consuming (Lewars, 2010). MD simulation also acts as a computer graphic image software to show the progress of the process (Mizukami et al., 2001).

2.6.1 Force Field

In MD simulation, it applies the molecular mechanic concept with forces as important elements. Every potential energy functions are required to incorporate into force field concept to become the driving force of simulation. Force field is an equation used to calculate the potential energy between atoms and functional groups which also consist of parameter and partial atomic charges (Farmahini et al., 2011). The types of force field available in MD simulation are OPLS/AA, AMBER, CHARMM, Compass, Compass26, Compass27, Dreiding, Universal, cvff, pcff, and pcff30. The selection of force field depends on the degree of complexity and systems applied. The force field can be described as mathematical expression which depends on energy of the system and coordinates of atoms (González, 2011). The molecules involved have bonded interaction (bond stretching, angle bending, proper torsional angle, and improper torsional angle) and non-bonded interactions (van der Waals and electrostatic) as shown in Equation (2.17).

$$V_{FF} = V_{\text{bond}} + V_{\text{angle}} + V_{\text{torsion}} + V_{\text{improper}} + V_{\text{vdW}} + V_{\text{elec}} \quad (2.17)$$

The force field element in MD simulation involves the calculation of the potential energy of system during specific time step. But, there are some problem faced by researchers or experimentalists to describe and analyse the results from computer simulation. Therefore, the current features of force fields are available now in the software calculation such as Charmm, NAMD, Amber, Gromacs, Gromos, and DL_POLY (González, 2011). Each type of force field has its own sensitivity of some properties to the specific trajectory (Price & Brooks, 2002). In each force field, there is a calculation algorithm to follow. The calculation algorithm suits the system or the objective of the simulation research. Furthermore, recently, many studies have been done to improve the knowledge about MD simulation, such as the algorithmic and force field used in MD simulation (Lucas, Bauer, & Patel, 2012).

2.6.2 Time Integration Algorithm

The application of time integration algorithms was widely used in the molecular dynamic computational analysis (Chung & Hulbert, 1994). The condition for stable algorithms was the size of the time step that was inversely proportional to the highest frequency of the discrete system (Hilber, Hughes, & Taylor, 1977). To analyse the interaction of system from MD simulation, the Newton's equations of motion can be used with some initial conditions. The time of integration method has gained attention for the past several of years (Bajer, 2002). The common time integration algorithms available for MD simulation are Verlet, Velocity Verlet, and Leap-Frog algorithm (Young, 2014).

The conditions for using integration algorithms were (Martini, 2009):

- (a) Computational efficient
- (b) Enable a “long” time step of integration
- (c) Only used one force in evaluation per time step and energy conservation

The movement of particle is shown in number of trajectories result which was analysed and displayed with averaged properties (Farmahini, 2010). By this algorithm, the changing of particle position with time is defined as $r_i(t)$ and the velocities as $v_i(t)$. Verlet algorithm from Taylor expansion is used to calculate the velocity explicitly which may affect the simulation with constant pressure. Modest operation mode and storage are required for velocity of Verlet. This allows the usage of a relatively long time steps duration as the position (r), velocities (v), and acceleration (a) are calculated at the same time with high precision. Besides this, the capability to conserve energy with numerically stable and time reversible properties becomes the reason for the software developer to use this algorithm (Farmahini, 2010). The Verlet algorithm was used for the calculation of the atomic motion.

The simple Verlet algorithm uses the atomic positions and accelerations at time t and the positions from the prior step, $x(t - \Delta t)$, to determine the new positions at $t + \Delta t$ as shown in Equation (2.18) (Adcock & McCammon, 2006).

$$x(t + \Delta t) = 2x(t) - x(t - \Delta t) + \frac{d^2x(t)}{dt^2} \Delta t^2 \quad (2.18)$$

2.6.3 Periodic Boundary

The periodic boundary is used to visualize the interaction of molecules of the whole system. Therefore, this boundary is used to simulate the chemical molecule in a small part of the large system. The simulation box is where the molecules are initially placed in a periodic boundary model. The interactions of atom with their neighbour occur in the simulation box. The simulation box represents the whole atoms/molecules (bulk system). Attractive or repulsive interactions can be seen when the molecule is simulated in periodic boundary box. Before creating the simulation box, it is important to ensure amount of molecule inserted in simulation box was fix to density box and specific operating condition because the periodic boundary box was representative to the whole model system. Therefore, by calculate the pair correlation functions can identify the size simulation box. The size of simulation box was referring to the amount of molecule in amorphous box. In principle, size of the simulation box should be appropriately chosen so that the box can contain dimensions of the fluctuations or interactions which are supposed to be observed during the simulation (Farmahini, 2010).

There are two major types of boundary conditions which are isolated boundary condition (IBC) and periodic boundary condition (PBC). In MD simulation, periodic boundary condition (PBC) will be used to simulate a bulk environment but replicate in only small number of molecules. Figure 2.3 shows the 2-D periodic boundary condition. The temperature was controlled by means of scaling the atom velocities under 3-D periodic boundary conditions. The calculations were made with the time step of 1.0 fs (Mizukami et al., 2001).

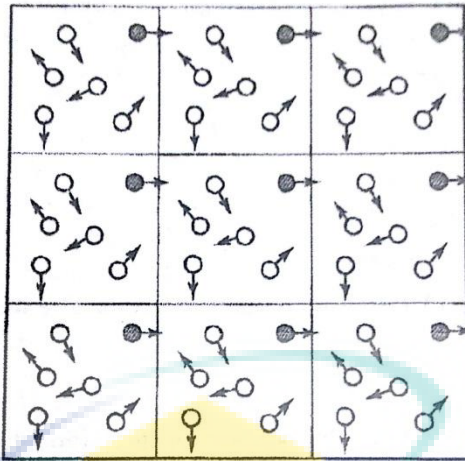


Figure 2.3 2-D periodic boundary condition.

Source: Farmahini, (2010)

2.6.4 Thermodynamic Ensemble

There are three common ensembles available in MD simulation, which are NVE (Mole, Volume, Energy), NPT (Mole, Pressure, Temperature), and NVT (Mole, Volume, Temperature). It is important to decide the types of ensemble in MD simulation to ensure the stability in term of moles, volume, temperature, pressure, and enthalpy of the system. The time integration algorithm will generate the trajectories of NVE, NPT, and NVT (Machado, 2012).

NVE ensemble can be described as controlling the constant of mole, volume, and energy. NVE is also known as the microcanonical ensemble. This assemble corresponds to an isolated physical system which involves the space coordinates and the velocities of the particles (Griebel & Hamaekers, 2005). In NVE, the number of particles, the volume, and the total energy are constant over time.

NPT ensemble can be described as controlling the constant of mole, pressure, and temperature dynamics. NPT is also known as the isothermal-isobaric ensemble. In NPT, it controls the pressure and temperature thermodynamics (Griebel & Hamaekers, 2005). The MD simulation is run to obtain the equilibrium thermodynamic properties for temperature and pressure. The NPT ensemble better or suitable to study molecule interaction by MD simulation. There were many studies of MD simulation that used the isothermal-isobaric (NPT) at constant temperature and pressure (Machado, 2012).

NVT ensemble is known as canonical ensemble. It involves the constant moles, volume, and temperature dynamics. NVT ensemble is suitable to be used in the study of diffusivity coefficient and is widely used in biological molecular simulations

2.6.5 Radial Distribution Function

Radial distribution function (RDF) is an analysis run in MD simulation with the objective to know the intramolecular/intermolecular interactions of molecules. RDF plot shows the relationship between the distances (r) of atom pairs in each of trajectory, the distance of atom with other neighbouring atom, and the tendency of atom to interaction/probability to have interaction between atoms, $g(r)$.

Radius in RDF graph represents the distance between atomic valences of the molecule. The interaction can be seen by setting the main atomic position. The radius reflects the distance between an atom and the neighbouring atoms. When the value of peak Armstrong can be seen, it means that there is interaction and when the value of peak Armstrong cannot be detected, it means that no interaction between the atoms. RDF depends on the distance between atoms/molecules. The distance of radius atoms actually based on origin atom (chosen atom). RDF analysis is done to know the intensity of the interactions at certain distance from the origin atom.

RDF is important for three main reasons. First, it is useful for pairwise additive potentials. Knowledge of RDF is sufficient to provide information to calculate thermodynamic properties, particularly the energy and pressure. Second, RDF is a very well developed integral equation theory that permits estimation of the RDF for a given molecular model. Last but not least, RDF can be measured experimentally using neutron-scattering techniques. Figure 2.4 shows the schematic explanation of $g(r)$ of a monoatomic fluid. In this current research, the maximum distance of atoms was 20\AA represents the typical radial distribution function from MD simulation of the liquid. The atom at the origin is highlighted by a black sphere. The dashed regions between the concentric circles indicate which atoms contribute to the first and second coordination number shells.

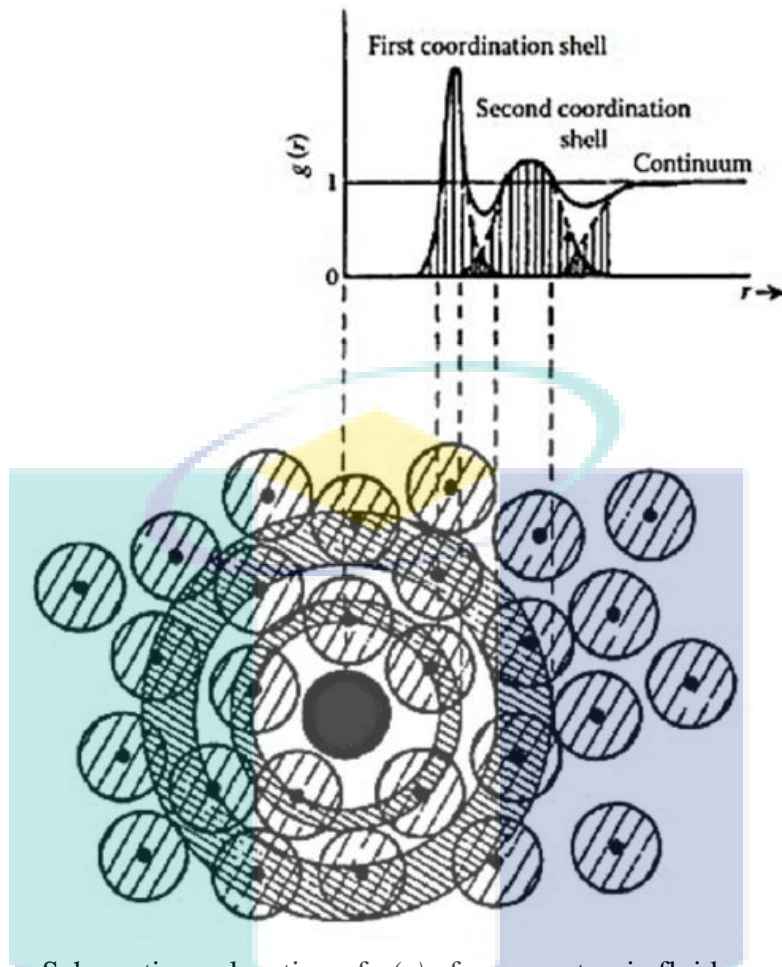


Figure 2.4 Schematic explanation of $g(r)$ of a monoatomic fluid.

The $g(r)$ pattern basically depends on the phase of the system. The ideal gas will approach $g(r) = 1$. These patterns can be seen in Figure 2.5. The RDF pattern for solid phase fluctuates more frequently as compared to liquid and gas phase. According to kinetic molecular theory of matter, the atoms of solid phase are arranged accordingly so they will vibrate constantly. Vibration between the atoms will cause repulsive forces against each other. Therefore, many fluctuations occur as shown in Figure 2.5 (c). Because liquid atoms are closely arranged to each other and gas atoms are far apart from each other, their RDF patterns are quite stable as compared to solid phase.

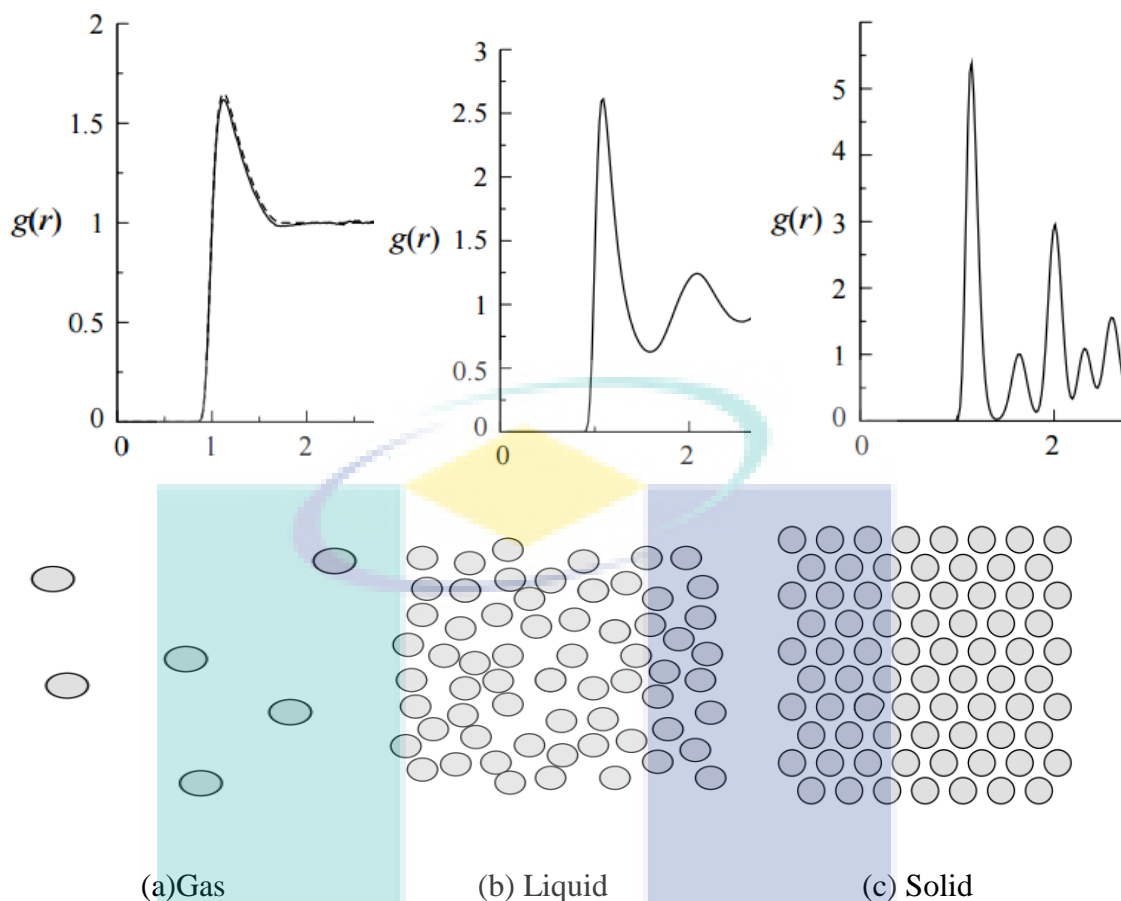


Figure 2.5 The atomic configuration and RDF pattern for (a) gas, (b) liquid, and (c) solid phase.

2.7 Molecular Mechanics

Molecular modelling, which is also known as computational chemistry, is a tool use to solve the problems related with chemical processes by a computer. The basic concept of molecular mechanics is based on a set model of balls (atoms) that are attached together by springs (bonds) (Lewars, 2010). It starts with the calculation of length of spring, angle, and the energy of stretch and bend. Molecular mechanic (MM) applies force field methods for the prediction of energy between molecules and it calculates the structure and geometries of large molecule. In molecular dynamic simulation, it will calculate the motion of large molecules such as DNA and proteins. Molecular dynamic simulation is one of the computer programmes used to study molecular mechanics, in which the potential energy on large molecules that describes the intramolecular and intermolecular interactions will be studied (Sherill, 2001). The intramolecular interaction is the interaction forces between atoms inside a single molecule whereas the intermolecular interaction is the interaction forces between different molecules. With

additional information to calculate the energy of molecules, suitable calculation modules are molecular mechanics, Ab initio or the density functional theory, and Schrödinger equation (Lewars, 2010).

The principles used for molecular mechanic are (Bansal, 2011):

- (a) Atom-like particles are spherical (the radii are obtained from measurements) and have a net charge.
- (b) Interactions must be obtained from specific set of atoms.
- (c) Interactions is analysed from spatial distribution of atom and energies.

The limitations of molecular mechanics models are (Hehre, 2003):

- (a) The study of the equilibrium geometries and equilibrium conformations
- (b) The calculation of chemical bonding or electron distribution in molecules
- (c) The available force field cannot be obtained from non-equilibrium forms

It is crucial to understand about the molecular mechanic to study the features of organic chemistry. The concerns in molecular mechanics theory are molecular structure, dynamic, and energies. The sum of potential energy of molecule such as bond stretching, bond bending, torsion, van der Waals' forces, and electrostatic interaction are particularly the constituents to form a force field. Force field is one of the important elements required to run the molecular dynamic simulation.

Intra and intermolecular interactions will result in the bonding of chemical molecules. Chemical bond is defined as a binding of more than one atom by the attraction forces to form chemical compound (Toon, 2003)

2.7.1 Intramolecular Interaction

The intramolecular interaction is due to the attraction between cations and anions, nuclei and electron pairs, and cation-delocalized valence electron, or also known as ionic bonding, covalent bonding, and metallic bonding, respectively (Istadi, 2007).

2.7.1.1 Ionic Bond

Ionic bond is also known as electrovalent bond. Electrovalent bond is formed by the transfer of one or more electrons in the valence or outermost shell of one atom to another. Moreover, the transfer of electron from metal compound with low ionisation energy to non-metal compound with high electron tendency can form an ionic compound (Toon, 2003).

Ionic bonds are formed when there are attractions between different charges or cation and anion particles (Lee, 1991). It also involves the transfer of the opposite charges between two atoms. The attractions between two ions can form Coulomb force. Coulomb's laws describes the relationship of charge ions and the distance of the ions itself (Charless, 2003). This force is much stronger compared to the force of covalent bond. The example of ionic bond is the interaction between Na^+ (metal) and Cl^- (non-metal) ions and example ionic compounds are Lithium Fluoride (LiF), Sodium chloride (NaCl), Magnesium chloride (MgCl_2), and Magnesium sulfate (MgSO_4). The boiling point of a compound is high when the force is strong.

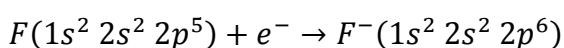
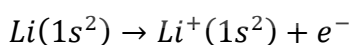
The flow for the formation of ionic compound is as follows (Toon, 2003):

1. The electronic structure for lithium and fluorine

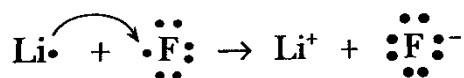
Lithium (Li) $1s^2 2s^1$

Fluorine (F) $1s^2 2s^2 2p_x^2 2p_y^2 2p_z^1$

2. Electron from $2s^1$ orbital is transferred to a fluorine atom to form a lithium ion. Because of the oppositely charged ions, Li^+ ions (positive charge) and F^- ions (negative charge), electrostatic attractions between two atoms will occur.



3. The transfer of electron 2s orbital (lithium) to 2p orbital (fluorine) occurs to form ionic compound.



2.7.1.2 Covalent Bond

Single covalent bond is formed by sharing a pair of electron between two atoms. Both atoms will achieve the electronic configuration of a noble gas to form a molecule. Within the molecule, a pair of electron is held together by the electrostatic attraction covalent bond. It commonly involves the non-metallic elements (Toon, 2003). Covalent bond also involves electron sharing between polar atom joined with other atom that has different electronegativity (Istadi, 2007). Molecular polarity occurs when there is a net imbalance of charge electron. Polar covalent bond occurs when electron on each atom shifts between partial negative charge and partial positive charge. Non-polar covalent bond occurs when two atoms share a pair of electrons with each other. The example of covalent bond is Bromine (Br). Figure 2.6 shows the example of covalent bond.

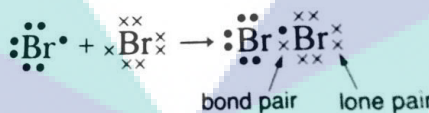


Figure 2.6 Example of covalent bond

2.7.1.3 Metallic Bond

The metallic bonds occur when the metal cation is attracted towards the 'sea' of electron of delocalised electrons. In metal, valence electron cannot connect with others by ionic or covalent bonds. But, metal is easily ionised in delocalised valence electrons. Delocalised valence electrons are free to move from negative to positive electrodes where metal can be an electrical potential. The metal has tendency to have high melting points and boiling points because the metallic bond is strong (Clark, 2012). The example of metallic bond is iron, copper, tin, and zinc. Figure 2.7 shows the example of a metallic bond.

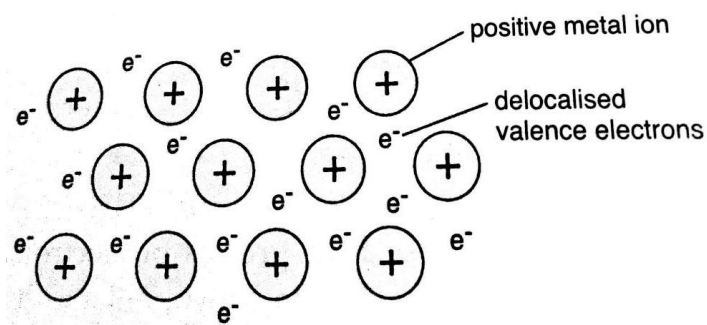


Figure 2.7 Example illustration of metallic bond

2.7.2 Intermolecular Interaction

Intermolecular force is either attractive or repulsive interaction between a molecule and its neighbouring molecule (or covalent molecules) (Toon, 2003). Intermolecular forces include polar and non-polar molecules, ionic force, dipole-dipole force, hydrogen bond force, dipole-induced dipole force, instantaneous dipole-induced dipole force, and ion-dipole force (Adams, Williams, & Rory Adams, 2011). Polar molecules force is the interaction between atoms in the molecule which has different electronegativity. The force of attraction in polar molecules is high since it has interaction between positive and negative charges. Repulsive interaction occurs for non-polar molecules which have the same electronegativity charge. Intermolecular interaction also plays an important role in physical properties such as boiling point, solubility, and melting point (Toon, 2003). The sequence of strength from the strongest to weakest force is charge-charge (ion-ion) > charge-dipole (ion-dipole) > hydrogen bonding > dipole-dipole > charge induced dipole > dipole-induced dipole > instantaneous dipole-induced dipole or van der Waal's (Israelachvili, 1992). Figure 2.8 shows the type of forces involves in intermolecular interaction.

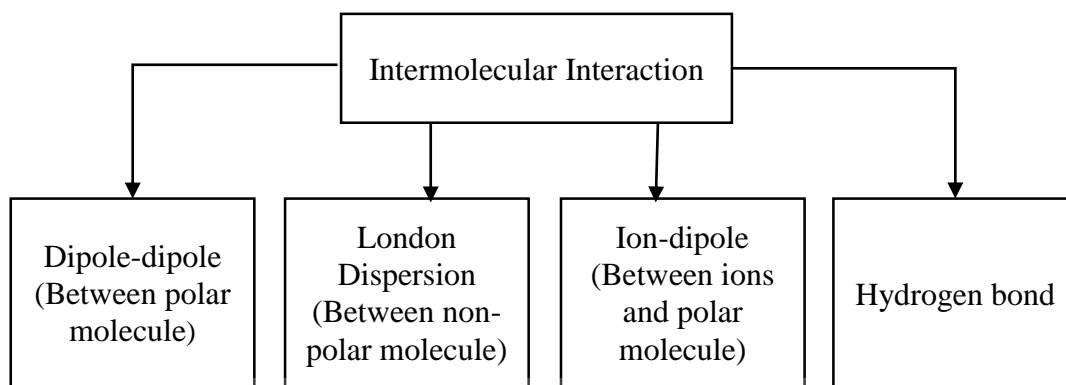


Figure 2.8 Type of forces involve in intermolecular interaction

2.7.2.1 Dipole-Dipole Force

Dipole-dipole interaction depends on the internal electronic of the atoms. The molecule has positive and negative ions called dipole (Brennen et al., 2000; Brown & Lemay, 2001). The dipole-dipole forces occur when the dipole molecule with positive end charge attracts with another dipole molecule with negative end charge. The greater the polarity of the molecule, the higher the boiling point. The main factor for strength of a dipole-dipole force is dipole moment size of the molecule (Toon, 2003). Polar molecule has electronegativity imbalance due to the different charges of atoms in the molecule. In organic molecule, polar group normally contains O or N atom (Brittain, 2007). An organic molecule that has hydrocarbon is non-polar and it does not has dipole-dipole forces. The examples of molecules that exhibit dipole-dipole attractions are $\text{CH}_3\text{CH}_2\text{CH}_3$, CH_3OCH_3 , and CH_3CN . Figure 2.9 illustrates the example for dipole-dipole force interaction.

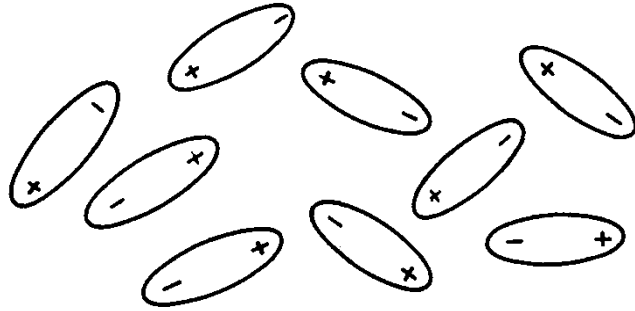


Figure 2.9 Example illustration for dipole-dipole force interaction.

Source: Toon, (2003)

2.7.2.2 Hydrogen Bond

Hydrogen bond will occur when there is electrostatic attraction between covalent bond of hydrogen atom with high electronegativity atom of neighbouring atom such as nitrogen (N), oxygen (O), fluorine (F), or chlorine (Cl). H-bonding is a very strong attraction interaction forces in which the small hydrogen atom is bound to a large atom such as oxygen and nitrogen (Israelachvili, 1992). Hydrogen atom with partial positive charge is attracted to the oxygen atom which has partial negative charge. The dipole force tends to align themselves in order to make the positive charge closed to the negative charge of other molecules (Roussel, 2012). The strength of the hydrogen bond is higher than van der Waals' bond but lower than covalent bond (Toon, 2003). The examples of molecules that possesses hydrogen bonding are H_2O , NH_3 , and HF . Figure 2.10 illustrates the hydrogen bonds in water molecules.

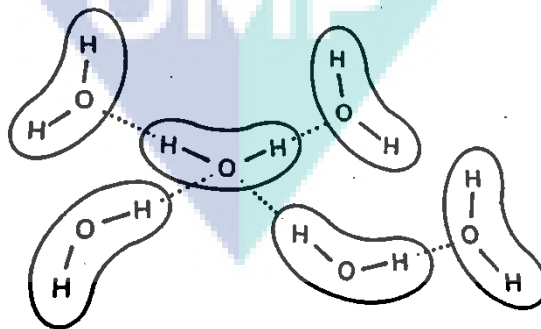


Figure 2.10 Example illustration of hydrogen bond

2.7.2.3 Dipole-Induced Dipole Force

The dipole-induced dipole force is also known as London dispersion forces. A polar molecule will induce other dipole molecule or non-polar molecule. This interaction force is weak. The first molecule is polar and the second molecule is non-polar. Dipole-dipole interaction forces occur when the second molecule is polar. The induced dipole happens when the polar molecule tends to create electric field force of electron of other molecules (Roussel, 2012). The calculation of how large the induced dipole is produced from an electric field is called as polarisability. The induced dipole causes the attraction force in polar molecule.

2.7.2.4 Instantaneous Dipole-Induced Dipole Force

Instantaneous dipole-induced dipole force occurs due to the interaction of molecules by dispersion forces. When a cloud of electron exists, the electron clouds can be seen as thick and thin (Brittain, 2007). Once the negative charges of electron overshadow the positive charges, it will form a thick cloud. On the other hand, when the positive charges of electron overshadow the negative charges, it will form a thin cloud. Instantaneous dipole-dipole interaction is weak attraction forces because the electron is instantly having reaction between each other and constantly moving in the clouds. This type of forces is available for hydrocarbon molecules and non-polar molecules. The example of instantaneous dipole-induced dipole attractions are halogens and Nobel gases such as Ar, He, and Kr. Figure 2.11 illustrates an instantaneous dipole-induced forces.

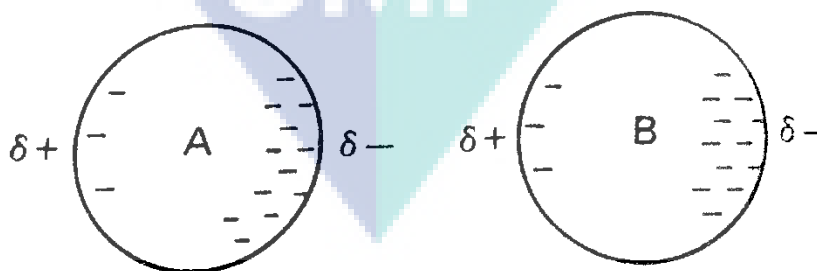


Figure 2.11 Example illustration for instantaneous dipole-induced dipole forces.

Source: Toon, (2003)

2.7.2.5 Ion-Dipole Force

Ion-dipole force involves an electrical interaction between partial charges on the end of a polar molecule and an ion (Toon, 2003). This is the strongest forces between ions and dipoles and it is proportional to the charge of the ion and the strength of the dipole (Roussel, 2012). The interaction of ion-dipole force is faster than ion-ion forces. The intermolecular force of ion and polar solvent is strong when the distance between them are small. The example of ion-dipole force is the interaction of ionic compound that dissolves in water (Istadi, 2007). The ions are separated when the attraction of ions and the opposite charge poles of the water molecule overcome the attraction of ions-ions. Figure 2.12 illustrates the ion-dipole forces.

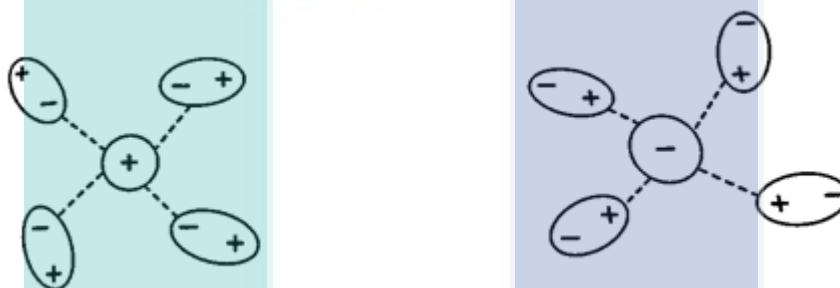


Figure 2.12 Example illustration for ion-dipole forces.

Source: Toon, (2003)

2.8 Summary

In conclusion, several studies have been conducted to improve the amine absorption process for CO₂ capture. However, there are several issues that need to be resolved to enhance the process of CO₂ absorption. Fundamental understanding of molecular behaviour of this process is not well explored, especially on the effects of different types of molecule at different operating conditions on the performance of CO₂ absorption process. Most of the studies conducted experimental and simulation work of this process at macro scale. Several studies on computational chemistry focused on the ionic carbamate stability without considering the physical interaction of molecules during absorption. MD simulation is a computational tool selected to analyse the physical interaction involved in CO₂ absorption process. By using MD simulation, inter- and intra-molecular interactions can be observed between pure amine, blended amine, water, and CO₂.

CHAPTER 3

METHODOLOGY

3.1 Introduction

This chapter describes the methodologies applied to study the CO₂ absorption process by amine solution. The intermolecular interaction of amine/CO₂/H₂O system via MD technique was performed in this work. The methods can be divided into two parts, which are molecular speciation and process simulation. After the simulation was completed, the results obtained were analysed in terms of RDF to determine the intermolecular interaction. The purpose of using MD simulation was to understand the microscopic interaction between molecules involved in CO₂ absorption process.

3.2 Material Studio Software

MD simulation study of amine-based absorption for CO₂ capture were performed using Material Studio version 7.0 software on HP Z400 workstation with 8 GHz dual core processor . Material studio software was supplied by Accelrys (Accelrys, 2014). Setting parameter used in this simulation was atom based summation method (for geometry optimization), Ewald summation method (for equilibrium and production phase), COMPASS force field (for energy interatomic potential calculation), and velocity Verlet algorithm (for time integrator algorithm calculation).

3.3 Flowchart of Methodology

MD simulation was used as a computational tool to analyse the intermolecular interaction of amine-CO₂-water systems. Figure 3.1 shows the process flow of the MD simulation steps. The details for every simulation steps are discussed in the following subsections.

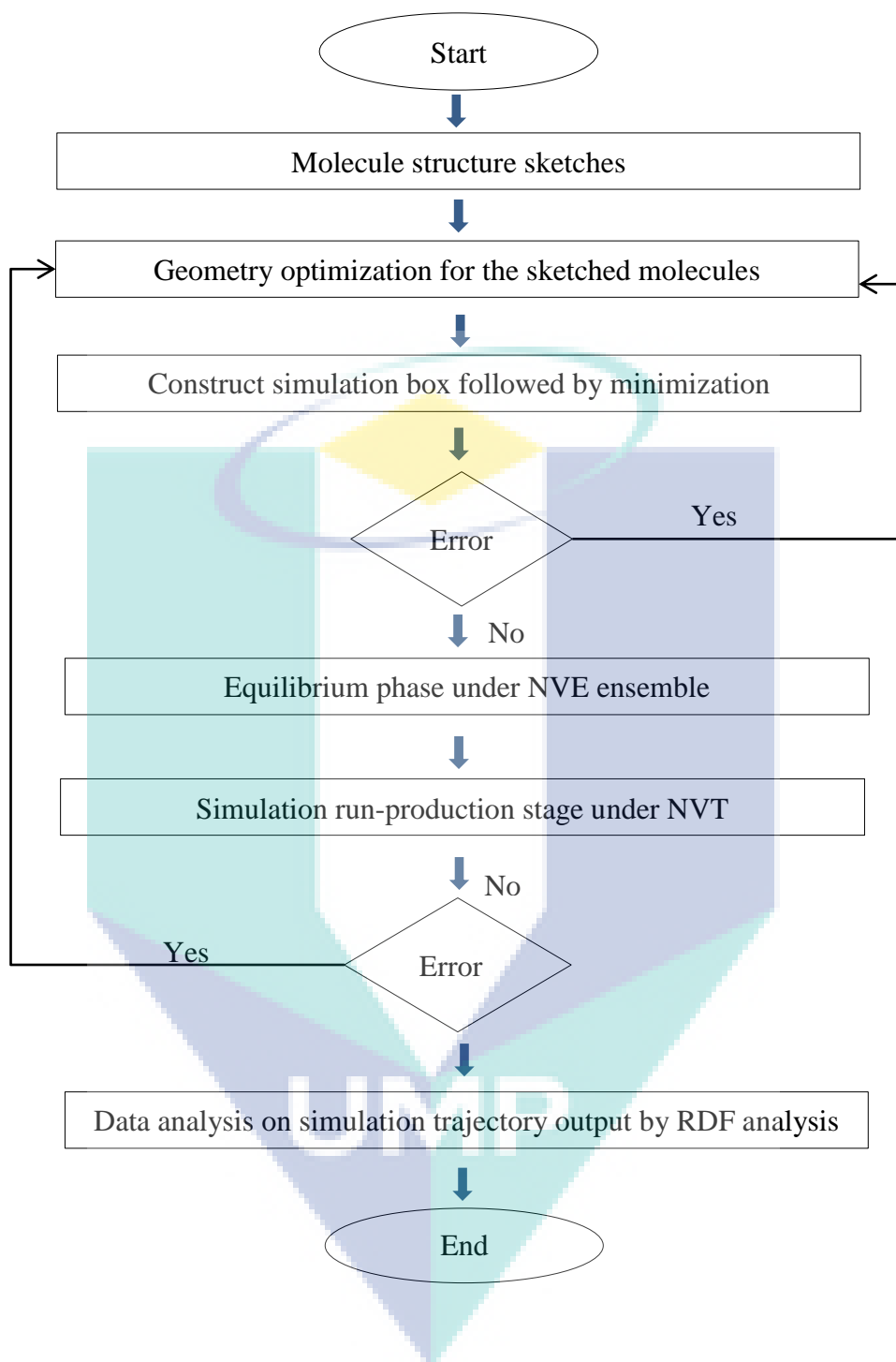


Figure 3.1 The flowchart to MD simulation

Error in MD simulation occurred due to:

- (a) Density of the solution is not accurate
- (b) The geometry of molecular structure such as length of bond and angle between bonds was not optimized.
- (c) The type of force field, time integration algorithm and thermodynamic ensemble choose was not suitable to process used.

3.4 Molecular Specification

In order to replicate true behaviour of the system in actual condition, specification of the system needs to be determined accurately based on experimental results of CO₂ absorption process using amine solutions published in literature. Three different molecules were identified which is alkanolamine, H₂O, and CO₂.

3.4.1 Carbon Dioxide

Carbon dioxide (CO₂) is a main molecule in this simulation. CO₂ molecule consists of C-O polar bonds. Figure 3.2 shows the geometrical structure of CO₂ molecules. Carbon atom that is located at the centre of the molecule electrophilic (electron-lover) has tendency to bond with high electronegativity oxygen atom.



Figure 3.2 The geometrical structure of CO₂

3.4.2 Water

A water (H₂O) molecule consists of two hydrogen atoms bonding to oxygen atom. The bond of oxygen-hydrogen is resulted from electron sharing. The oxygen atom has higher tendency to electron compared to hydrogen atom (Shakhashiri, 2011). The electron in oxygen-hydrogen bond has more tendencies to attract with oxygen atom. Water is a polar molecule when it has different electron charge. The attraction interaction in water is high because the hydrogen atom that has positive charge interacts with oxygen

atom which has high tendency for electron. Oxygen-hydrogen bond has high attraction interaction. Figure 3.3 shows the geometrical structure of H₂O.

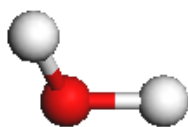
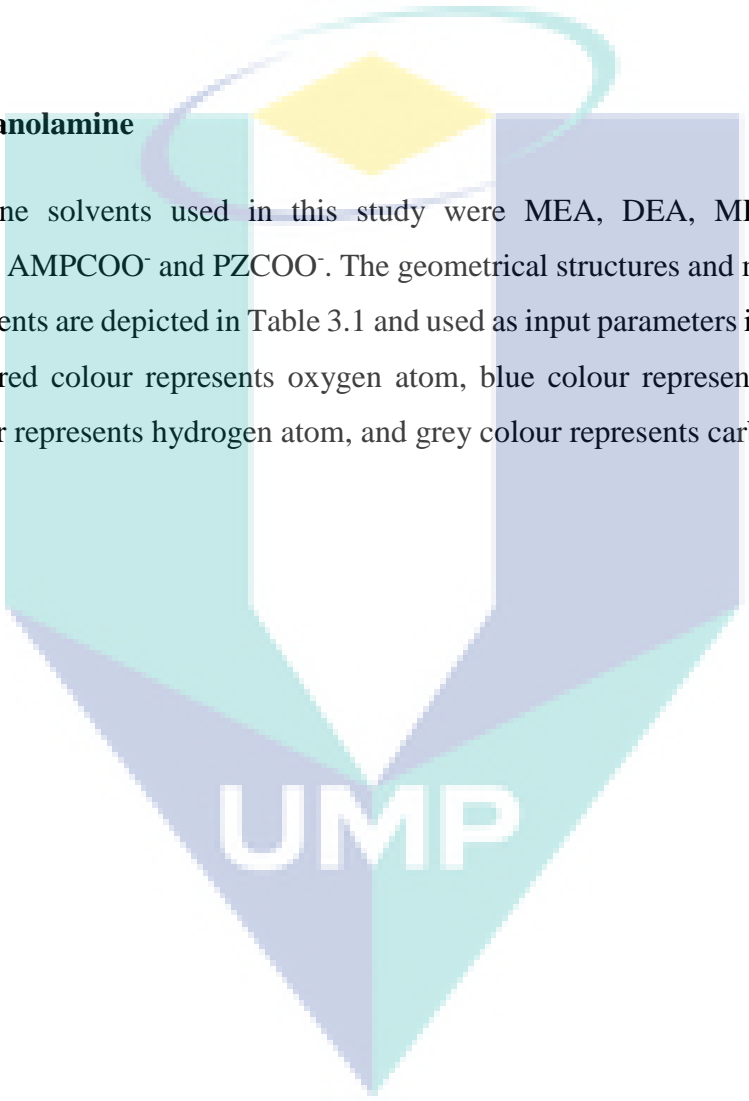


Figure 3.3 The geometrical structure of H₂O

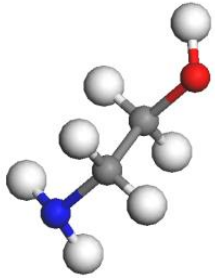
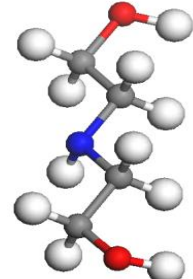
3.4.3 Alkanolamine

Amine solvents used in this study were MEA, DEA, MDEA, AMP, PZ, MEACOO⁻, AMPCOO⁻ and PZCOO⁻. The geometrical structures and molecular weights of each solvents are depicted in Table 3.1 and used as input parameters in MD simulation. Noted that red colour represents oxygen atom, blue colour represents nitrogen atom, white colour represents hydrogen atom, and grey colour represents carbon atom.

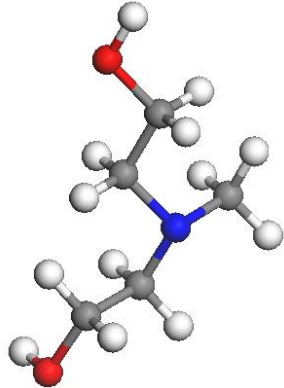
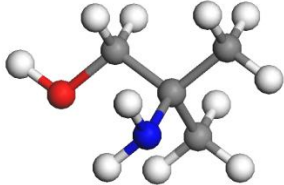
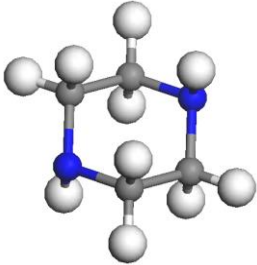


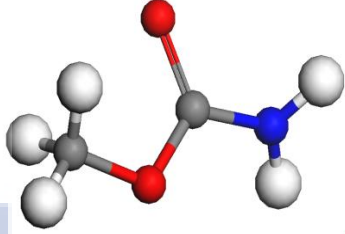
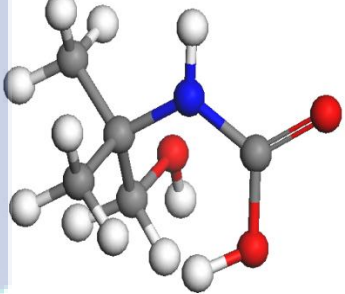
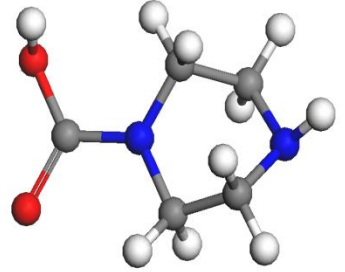
UMP

Table 3.1 Properties of alkanolamine molecules

Alkanolamine	Type of amine	Molecular formula	Geometrical structure	Molecular weight (g/mole)
Monoethanolamine (MEA)	Primary	C_2H_7NO		61.08
Diethanolamine (DEA)	Secondary	$C_4H_{11}NO_2$		105.14

UMP

Alkanolamine	Type of amine	Molecular formula	Geometrical structure	Molecular weight (g/mole)
Methyl Diethanolamine (MDEA)	Tertiary	$C_5H_{13}NO_2$		119.61
2-Amino-2-Methyl-1-Propanol (AMP)	Primary, sterically hindered	$C_4H_{11}NO$		89.14
Piperazine (PZ)	Primary, cyclical	$C_4H_{10}N_2$		86.14

Alkanolamine	Type of amine	Molecular formula	Geometrical structure	Molecular weight (g/mole)
Methyl carbamate (MEACOO)	Primary	$C_3H_6NO_3$		104.08
2-amino-2-methyl-1-propanol carbamate (AMPCOO)	Primary, sterically hindered	$C_5H_{10}NO_3$		132.14
Piperazine carbamate (PZCOO)	Primary, cyclical	$C_5H_8N_2O_2$		112.13

3.5 Molecular Dynamic Simulation

Once the speciation of the system was determined, MD simulation of the selected molecules was performed using Material Studio software. Procedures for MD simulation involved four main steps. The first step was sketching and optimising the molecular structure. All interaction parameters were decided through a suitable force field. Second step was the creation of simulation box, followed by forcite simulation and lastly was trajectory output analysis.

3.5.1 Molecular Structure Sketches

The MD simulation was started with replicating the structure of actual molecule. The structure must be accurate and similar with the real structure. The structure of molecules were obtained from Royal Society of Chemistry database (Chemspider, 2016). Three dimensions (3D) atomisation of the actual structure molecule were downloaded from this database. The advantage of using molecular structure obtained from this database was to prevent error in the sketches. A 3D molecule structure was used in this simulation because it involved a movement of the molecule and required in MD simulation. Then, the molecular structures were imported to MD simulation file. Figure 3.4 shows the page of Royal Society of Chemistry database (<http://www.chemspider.com/>). The step were insert or type name of chemical, click for 3D button and save as .mol file. To insert molecular structure (.mol file) which download from ChemSpider database, click File and import. After insert the molecular structure, the file will label as .xsd.

The screenshot shows the ChemSpider website interface. At the top, there is a navigation bar with links for Home, Sign in, Publishing, ChemSpider, Education, Community, News, and More... The main header features the ChemSpider logo and the tagline 'Search and share chemistry'. Below this is a secondary navigation bar with links for About, More Searches, Web APIs, and Help, along with a search bar containing 'eg. Pyridine' and a Search button. The main content area displays the search results for 'co2', indicating it was found by an approved synonym. The entry for Carbon dioxide includes its ChemSpider ID (274), molecular formula (CO₂), average mass (44.009 Da), and monoisotopic mass (43.989830 Da). A 3D ball-and-stick model of the CO₂ molecule is shown. The page also lists the systematic name (Methanedione) and provides links for SMILES and InChIs, and a 'Cite this record' option. On the right side, there are featured data source boxes for ChemSpider SyntheticPages and a 'Want to comment on this record?' section with a 'Leave Feedback' button. Advertisements for Waters and Bruker are also visible on the right.

Figure 3.4 Replicate the molecular structure from Royal Society of Chemistry Database.

Source: “ChemSpider Database,” (2014)

3.5.2 Geometry Optimization

Geometry optimisation step was carried out on each of the molecule to ensure the stability of molecular geometry to be used in further simulation steps. The well-equilibrated molecular structure was required for starting the simulation work. Figure 3.5 and Figure 3.6 show the steps for geometry optimisation. The force field used in optimization step is Forcite calculation. Forcite calculation used in this simulation because capable to calculate the dynamics simulations, energy and geometry optimization. This Forcite calculation allow to analyze simple properties such as density variations and also complex properties such as dipole autocorrelation functional (Accelrys, 2014). Time integration algorithm used in geometry optimization step is verlet algorithm from Taylor expansion. It is used to calculate the velocity explicitly which may affect the simulation with constant pressure. This allows the usage of relatively long time steps duration as the position (r), velocities (v), and acceleration (a) are calculated at the same time with high precision. Besides this, the capability to conserve energy with numerically stable and time reversible properties becomes the reason for the software developer to use this algorithm (Farmahini, 2010). The Verlet algorithm was used for the calculation of the atomic motion. The step were click module, Forcite, Calculation. Setup,

Task: geometry optimization, Quality: Fine. Energy, Forcefield: COMPASS, Charges: Forcefield assigned, Quality: Fine, Summation method: Atom based. Job control, ok. Then, click Run. Finish, click OK.

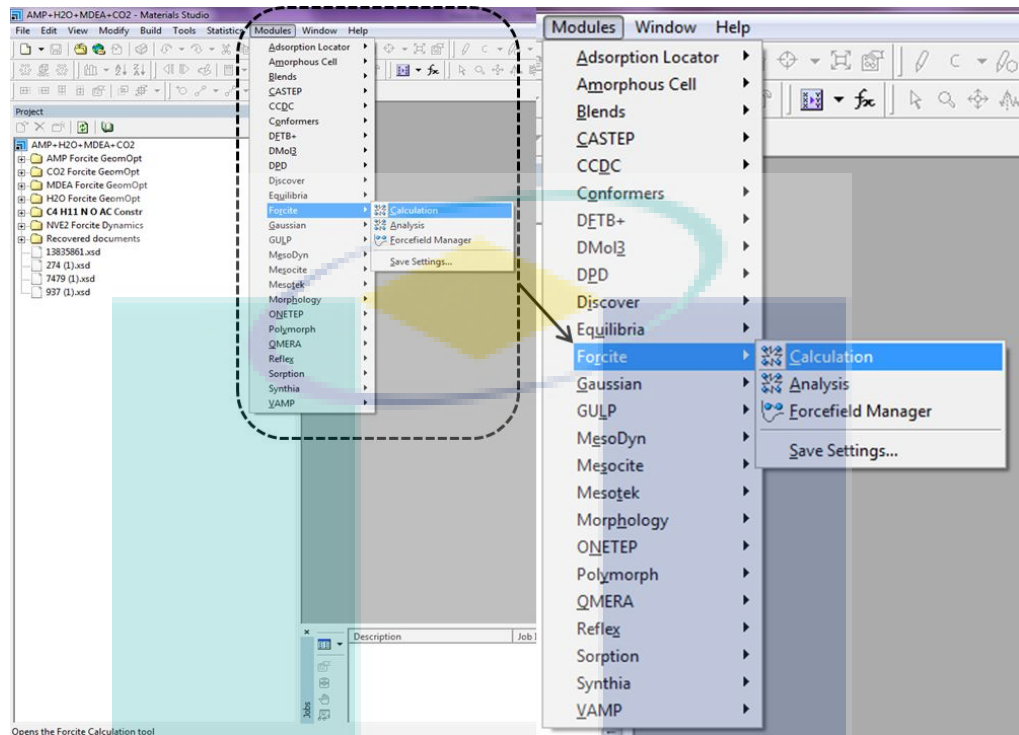


Figure 3.5
simulation

Step 1 for geometry optimisation of molecular sketches in MD

UMP

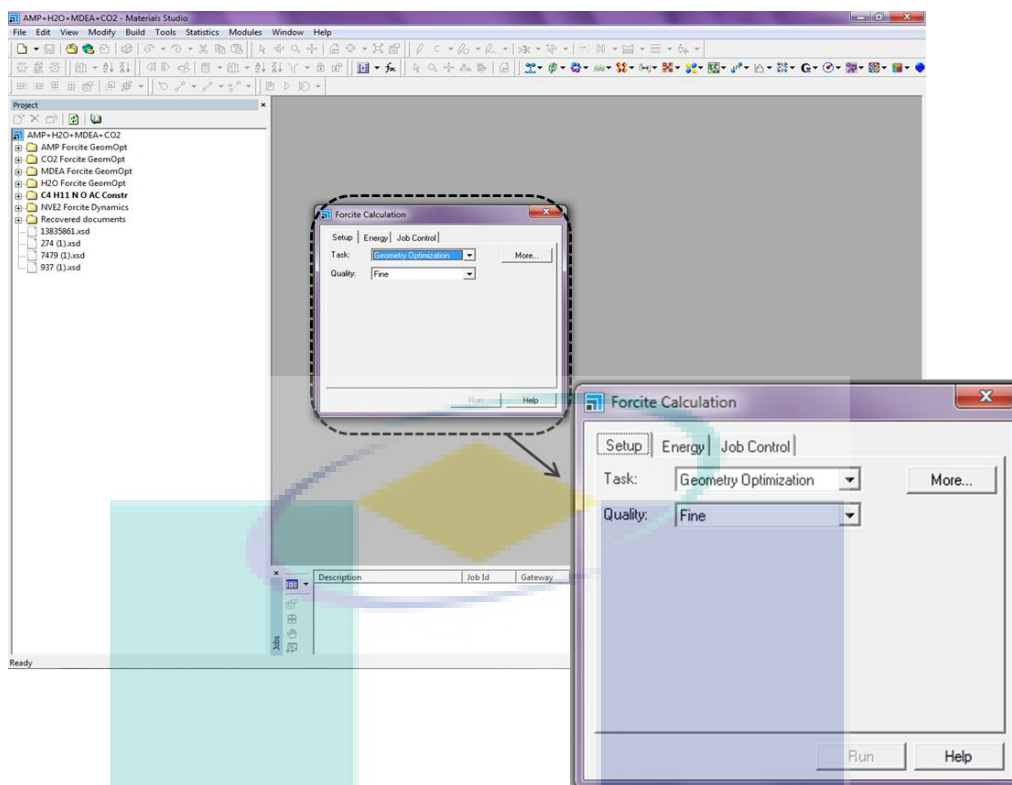


Figure 3.6 Step 2 for geometry optimisation of molecular sketches in MD simulation

3.5.3 Construction of Amorphous Cell Box

There were two steps involved in box creation stage, which were box creation and energy minimisation. The simulation box was constructed using the amorphous cell calculation model in Material Studio software. The cubic periodic boundary condition was enabled to overcome the surface effect. The size of simulation box depended on the amount of molecules inserted. The simulation box size should be chosen correctly because the dimension and fluctuation of the box will be observed through simulation run (Farmahini, 2010). Figure 3.7 shows the box creation for MEA molecule in MD simulation process. Figure 3.8 and Figure 3.9 show the step for the construction of amorphous cell. The simulation box represents the whole atoms/molecules (bulk system). The step were double click on .xsd file. To continue for construction box step. Click Modules, Amosphous Cell and Construction (available for 4.4 version only). Input data need are: number (how many molecule which you want to simulate), temperature (depend on temperature for what process you want to study), target density (the density of simulation box. If you want to simulation two (2) type of molecule such as H2O and CO2, So have to insert density of this mixture). Click Add (make sure the file .xsd is appear) and click Run.

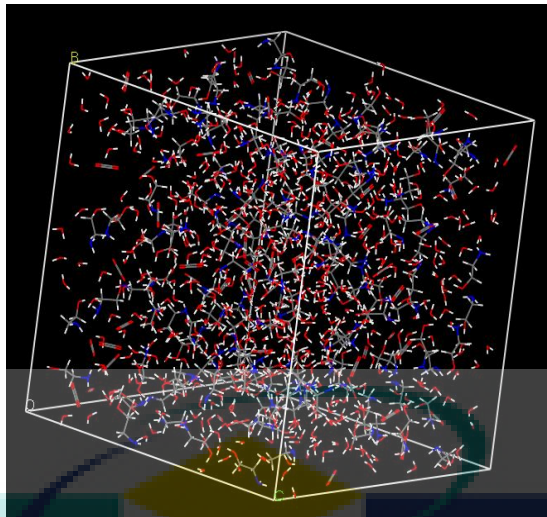


Figure 3.7 3-D amorphous cell box in MD simulation for MEA 30 wt.%

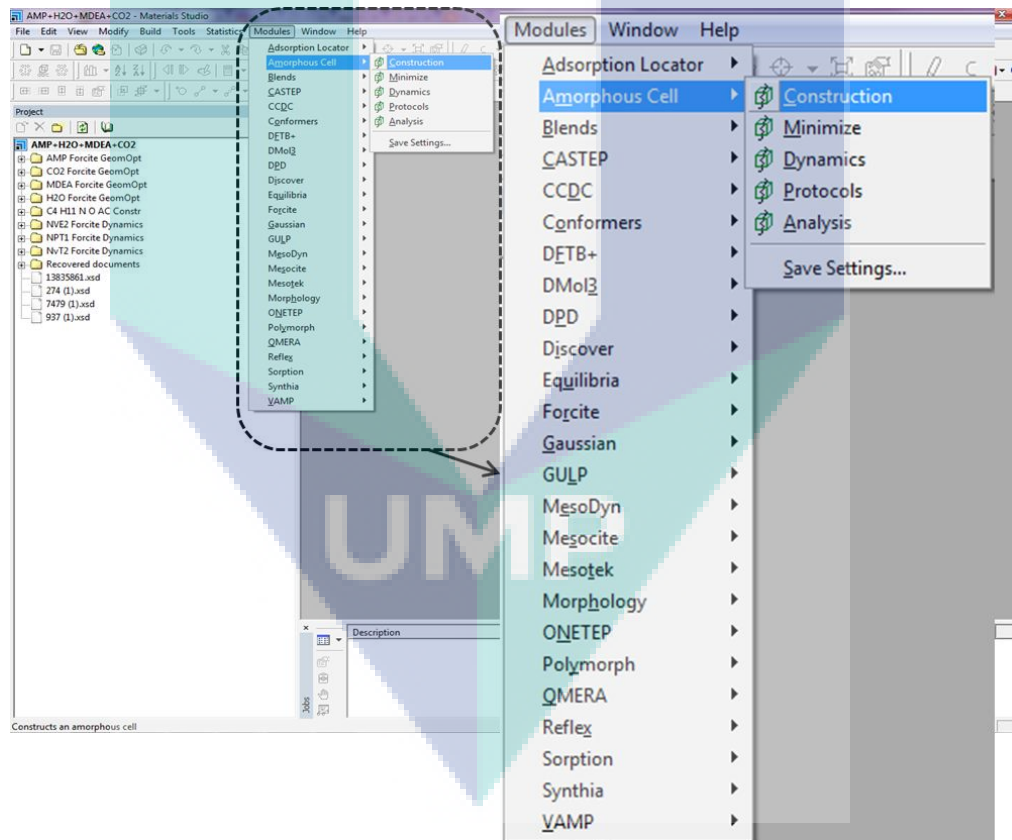


Figure 3.8 Step 1 for amorphous cell construction in MD simulation

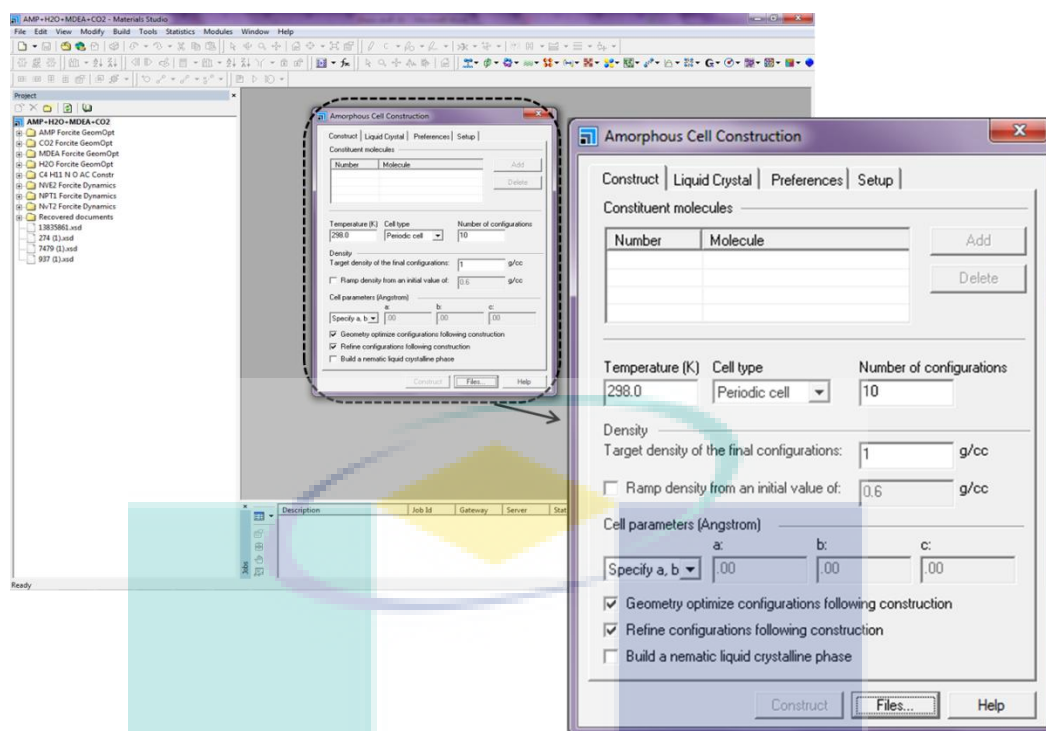


Figure 3.9 Step 2 for amorphous cell construction in MD simulation

After the simulation box was developed, this model was simulated for box energy minimisation. *Smart Minimize* module was used for energy minimisation step and the convergence was set at fine level. Minimisation step was run to minimise the energy of structure in the amorphous box. Energy minimisation method was also used to correct the unrefined molecular structure with distorted bond angles and lengths or with steric clashes between atoms (Adcock & McCammon, 2006). The minimum interaction was set up to 10,000. 10,000 is maximum value of energy in simulation box. The minimization step was done to minimize the energy in box until 10,000. If energy in box higher than 10,000, the simulation will be error. Figure 3.10 and Figure 3.11 show the steps for energy minimisation. The step were double click .xtd file, click Modules, Amorphous Cell, Minimize. Method: Smart Minimizer, Convergence level: Fine, Maximum iterations: 10000.

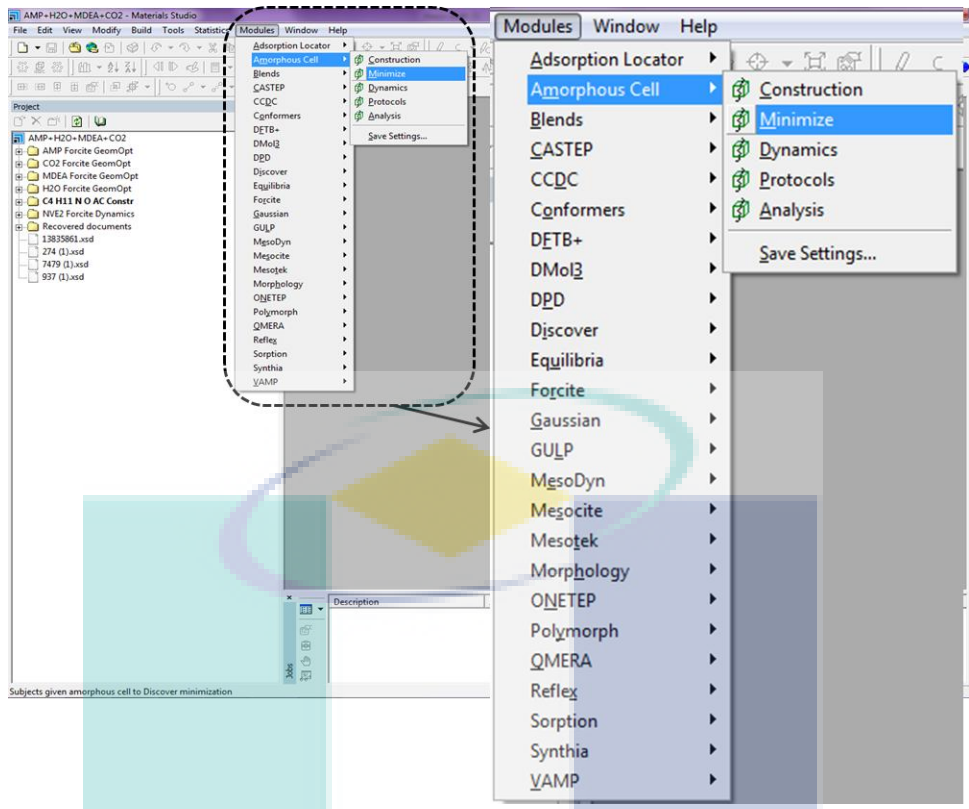


Figure 3.10 Amorphous cell minimization selection

UMP

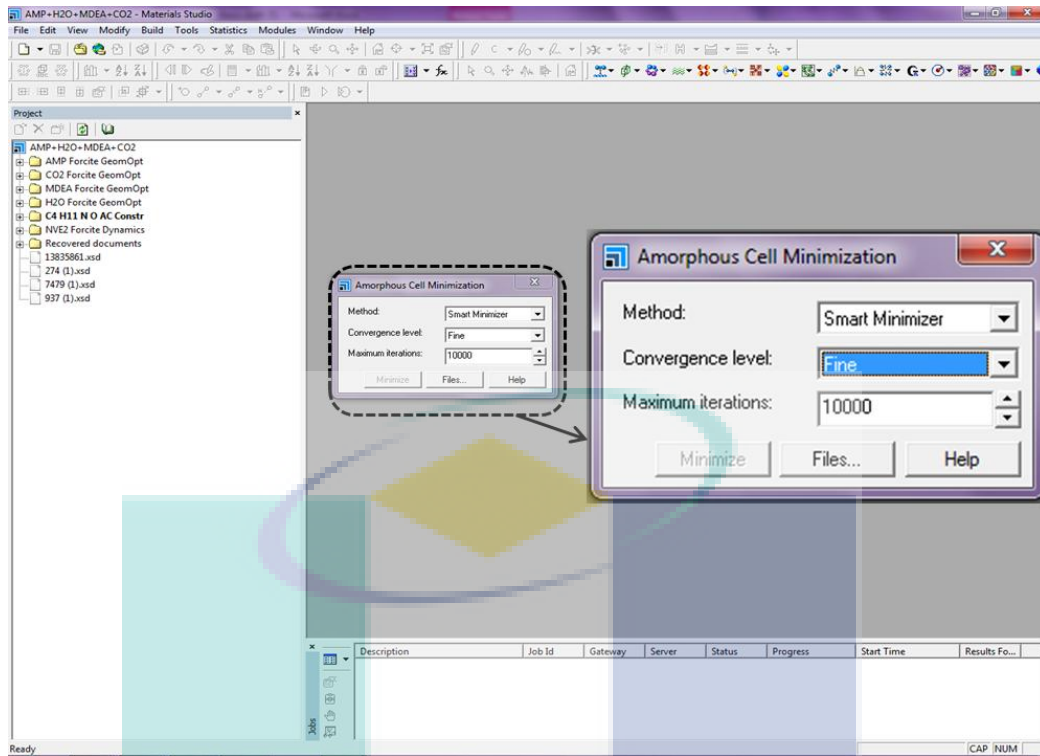


Figure 3.11 “Smart Minimizer” setting with fine convergence level and 1000 maximum iterations

The steps to construct the amorphous cell box required a few input parameters such as temperature, pressure, number of molecule, and density. Temperature and pressure that were obtained from the literature. The density of mixture was calculated as follows:

- (a) Weight per cent of solution was based on literature. Conversion of mass of molecule to particles using Equation (3.1) as follows:

$$\text{mass} \xrightarrow{\div \text{molar mass}} \text{moles} \xrightarrow{\times \text{Avogadro's number}} \text{number of particles} \quad (3.1)$$

- (b) Density of liquid mixtures. i is species of liquid and x is number of particles. The density values were taken from ‘Thermodynamic Properties of Chemical and Hydrocarbon’ book based on specific temperature used.

$$\sum \left(\rho_i \times \frac{x_i}{x_{total}} \right) \quad (3.2)$$

where ρ_i is density for species i , x_i is number of particles for species i and x_{total} is the total amount of particles used.

3.5.4 Equilibrium Phase

The next step after constructing and minimising amorphous cell was to simulate equilibrium phase. The simulation was started with the equilibration of the system under constant NVE (number molecules, volumes, and total energy) ensemble for 200 ps with random initial velocities. The purpose of equilibration step was to ensure the system configuration was stable with energy conservation. The number of time steps between each output was 1 fs. The time step employed in MD simulation is 1 fs because in this simulation was run using the Verlet algorithm calculation. This algorithm calculation was used to calculate the positions and velocities of all atoms. Therefore, generally the time step was set to 1 fs which is very small and it is represent to bond stretching motions of C-H bonds vibration vibration (Jean M., 2015). The equilibrium phase was also known as molecular relaxation. Ewald summation method was used to evaluate both van der Waals and electrostatic interactions (Essmann et al., 1995). Figure 3.12, Figure 3.13 and Figure 3.14 show the steps to simulate the equilibrium phase. COMPASS was types of force field used. COMPASS is condensed-phase optimized molecular potentials for atomic simulation studies. COMPASS suitable to be used for inorganic gas molecule, polymers and organic molecule. COMPASS force field is adds to the cross coupling term for the prediction of structural variation and vibration frequencies (Matthew, 1997). COMPASS also a licensed force field and it is a third generation of force field. In this study, type of time integration algorithm will be used is Verlet algorithm. The step were double click on .xsd file, click Modules, Forcite, Calculation. Setup, Task: Dynamic, Quality: Fine, Click MORE. Ensemble, choose NVE for equilibrium phase, Initial velocities (I dont know, But usually i choose current), Temperature: based on your system temperature, Time Step: 1 fs, Total simulation time: 200 ps, Number of steps/ Frame output every = usually I used 100 frame, Run. Energy, Forcefield: COMPASS, Charges: Forcefield assigned, Quality: Fine, Summation method: Ewald. Job control. Run in parallel on: put 8, Click Run. To proceed simulation or next run, Double click on .xtd file.

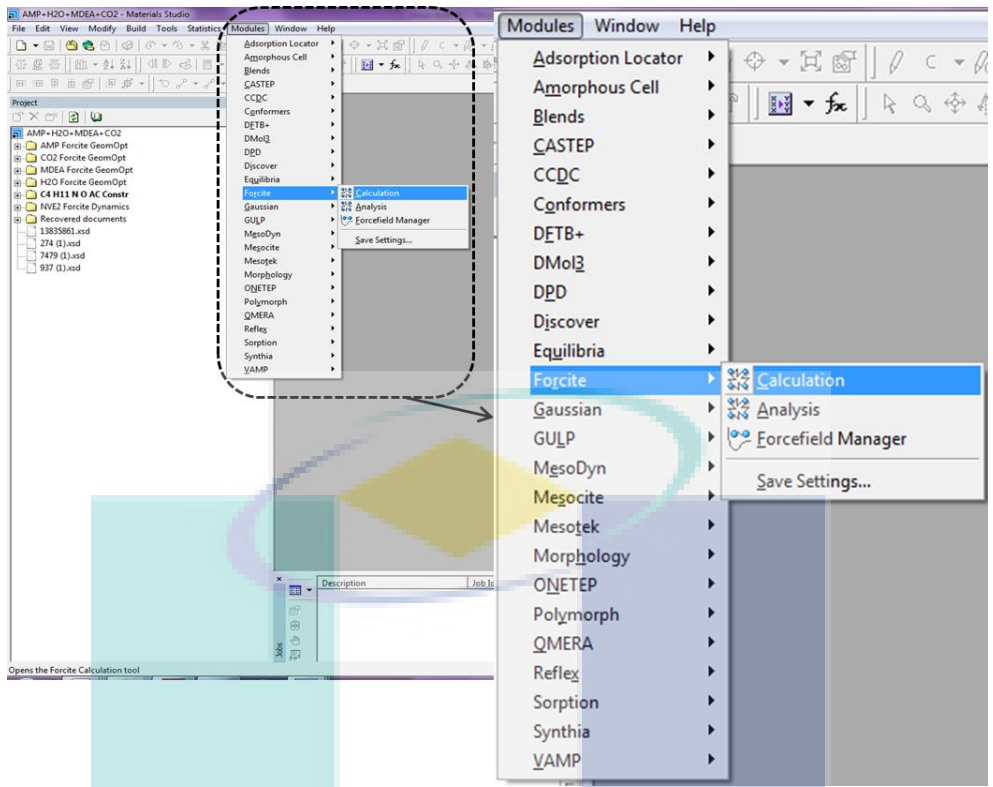


Figure 3.12 Step 1 for equilibrium phase in MD simulation

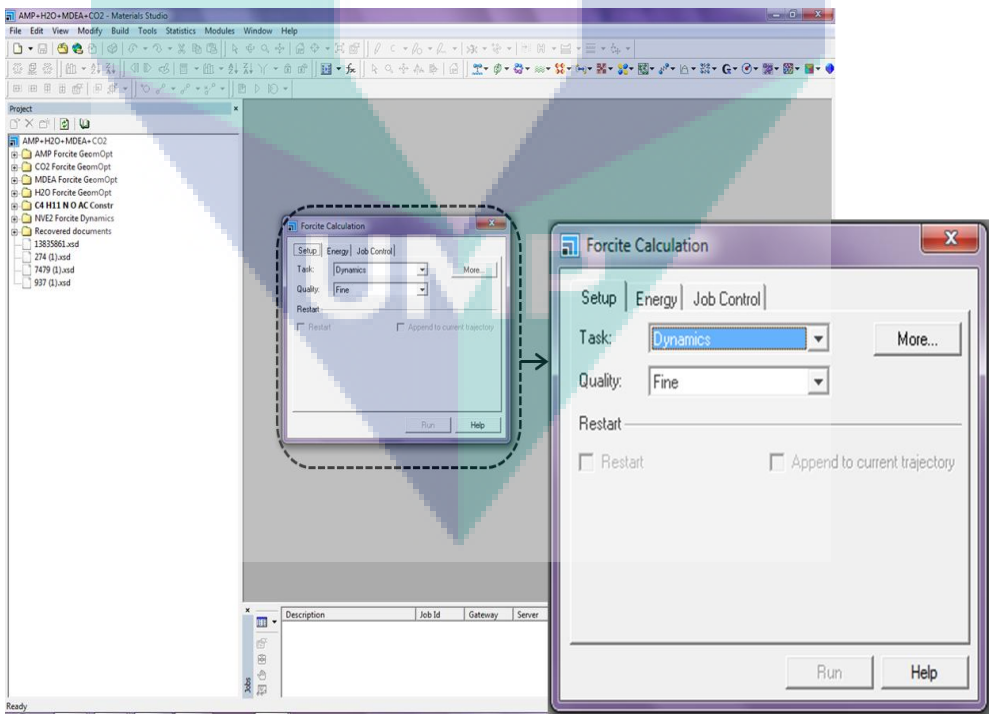


Figure 3.13 Step 2 for equilibrium phase in MD simulation

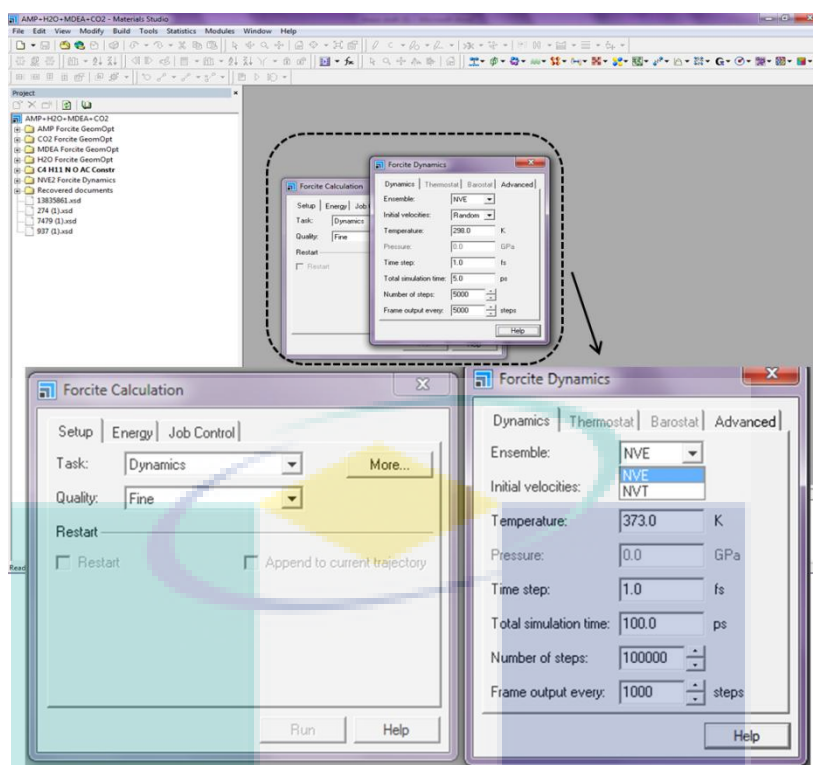


Figure 3.14 Step 3 for equilibrium phase and production phase in MD simulation

3.5.5 Production Phase

After the system was simulated for 200 ps in equilibrium phase, the simulation process was continued in the production phase under constant canonical ensemble, NVT (number of moles, volume and temperature) for 1 ns and a time step of 1 fs. Ewald summation method was applied in this study to simulate the molecular solution. Ewald summation method was only available when a periodic box was present. After completing the simulation until 1 ns, final structure was obtained for step analysis and evaluation (Wongsinlatam & Remsungnen, 2013). Figure 3.14 shows the step for production phase. The step was renamed .nvt file as nvt1. Step production phase was similar as equilibrium phase except ensemble: NVT.

3.5.6 Trajectory Production Analysis

The final structures were obtained from the trajectory output for analysis when the simulation under NVE and NVT ensembles were completed. RDF results were used to analyse the final structure and its molecular interactions. In the RDF calculation, the cut off interval was set to half of the box length with an interval of 0.5 Å. Cutoff distance

was set to 20.0 Å. Cutoff distance is a distance, in Å, at which how long the interaction energies would be calculated. Molecular interaction was determined by selecting inter/intramolecular interaction box and periodic table. The RDF graph was used to analyse the attractive and repulsive interaction of molecule. The radial distribution function became equal to one at the edge of the box (Allen & Tildesley, 1991). Whereas, MDS graph was used to analyse the diffusivity of CO₂ in amine-based absorption process. The program used real units of kiloJoules and angstroms for RDF analysis. Figure 3.15 and Figure 3.16 show the steps to generate data for analysis.

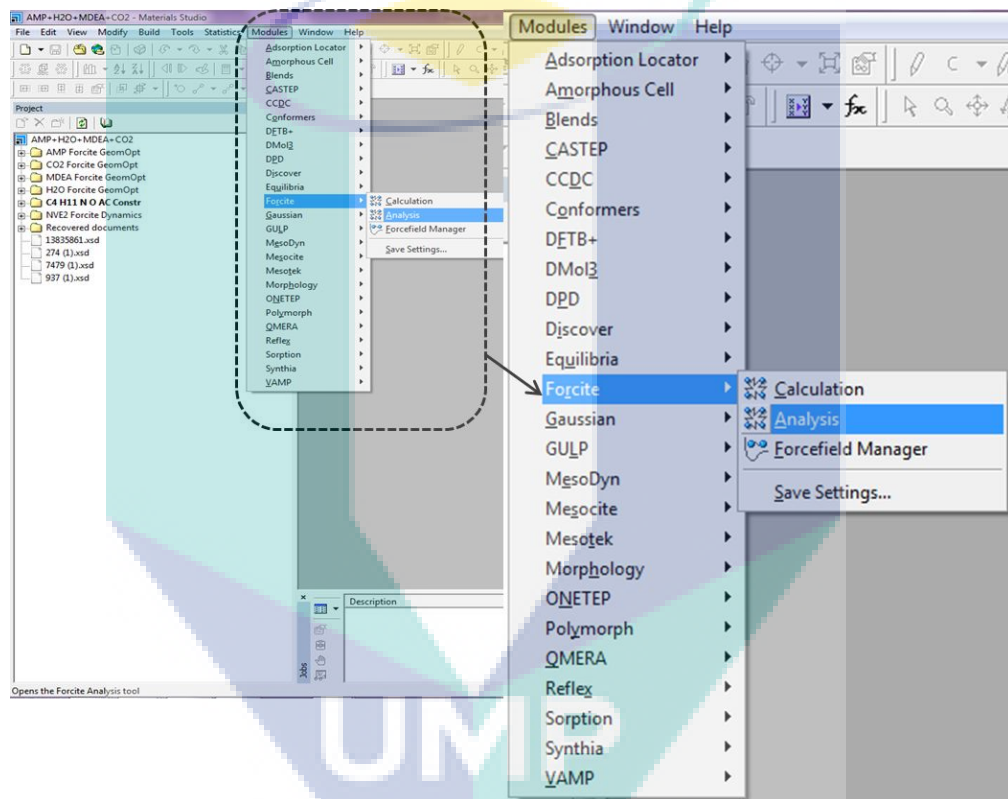


Figure 3.15 Step 1 for analysis sample in MD simulation

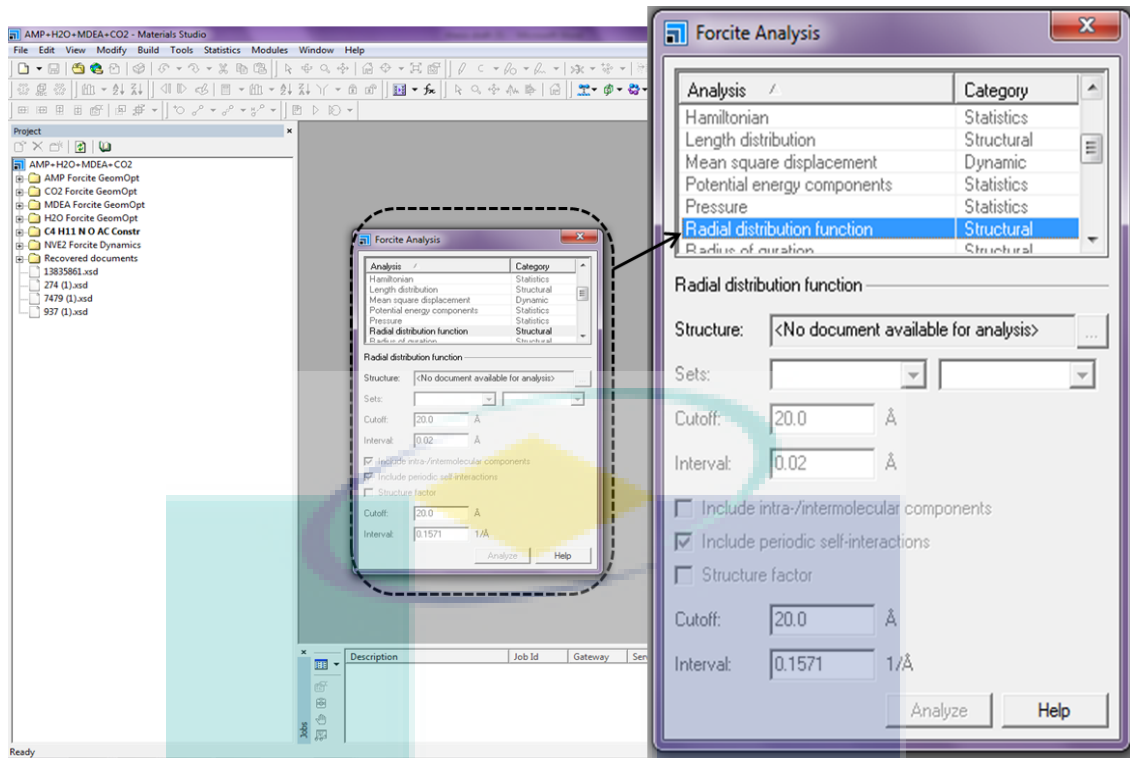


Figure 3.16 Step 2 for analysis sample in MD simulation

3.5.7 Calculation in RDF

RDF plot shows the relationship between r and $g(r)$. As assume the model system was in a homogeneous distribution of the atoms/molecules, the $g(r)$ represents the probability to find an atom in a shell dr at the distance r of another atom chosen as a reference point. Equation (3.3) shows the calculation for RDF. The number of atom $dn(r)$ at a distance between r and $r + dr$ from a reference atom can be calculate by dividing the model system volume into shell dr .

$$dn(r) = \frac{N}{V} g(r) 4\pi r^2 dr \quad (3.3)$$

where, where N represents the total number of atoms, V the model volume and where $g(r)$ is the radial distribution function. The volume of the shell of thickness dr is approximated as Equation (3.4):

$$V_{shell} = \frac{4}{3} \pi (r + dr)^3 - \frac{4}{3} \pi r^3 \cong 4\pi r^2 dr \quad (3.4)$$

3.6 Simulation Parameter 1: The Effect of Temperature

The selection of temperatures used in this case study was based on literatures. According to Kim et al. (2013) and Yu (2012), more CO₂ were absorbed for the system at the temperatures between 313 and 333 K. Therefore, temperature of 298, 308, 313, and 318 K were selected to study the effect of temperature on intermolecular interaction of water and CO₂. Temperature of the system affected the diffusion coefficient of CO₂ in amine solution, reaction rate constant, and Henry's constant (Ye et al., 2012). Number of molecules for all system was kept constant. Mass ratio for binary system was 30 wt.% of MEA and 70 wt.% of H₂O while for tertiary system was 30 wt.% of MEA, 60 wt.% of H₂O, and 10 wt.% of CO₂. Table 3.2 shows the input parameters used for case study 1.

Table 3.2 Input parameters used to analyse temperature effect on the system

Pressure:	1 atm			
Temperature	298 K	308 K	313 K	318 K
Density mixture for binary system (g/ml)	1.01244	1.00477	1.00089	0.99698
Number of molecule for binary system	A: 50	A: 50	A: 50	A: 50
	B: 400	B: 400	B: 400	B: 400
Density mixture for tertiary system (g/ml)	1.00610	0.99737	0.99297	0.98855
Number of molecule for tertiary system	A: 110	A: 110	A: 110	A: 110
	B: 800	B: 800	B: 800	B: 800
	C: 50	C: 50	C: 50	C: 50

where, A is amine; B is H₂O; C is CO₂

3.7 Simulation Parameter 2: The Effect of Amine Concentration

Amine concentration is one of the important parameters to determine the performance of amine absorption process to capture CO₂. High concentration of MEA is commonly used because it gives high production of CO₂ absorption process. However concentration higher might cause corrosion problem. CO₂ absorption process using MEA

absorbent was normally applied with the amine concentration in the range of 10-30 wt.% (Goff & Rochelle, 2004). Four different amine concentrations were selected in this work in term of weight per cent (wt.%) which refers to the mass of the species divided by the total mass of all species. For example:

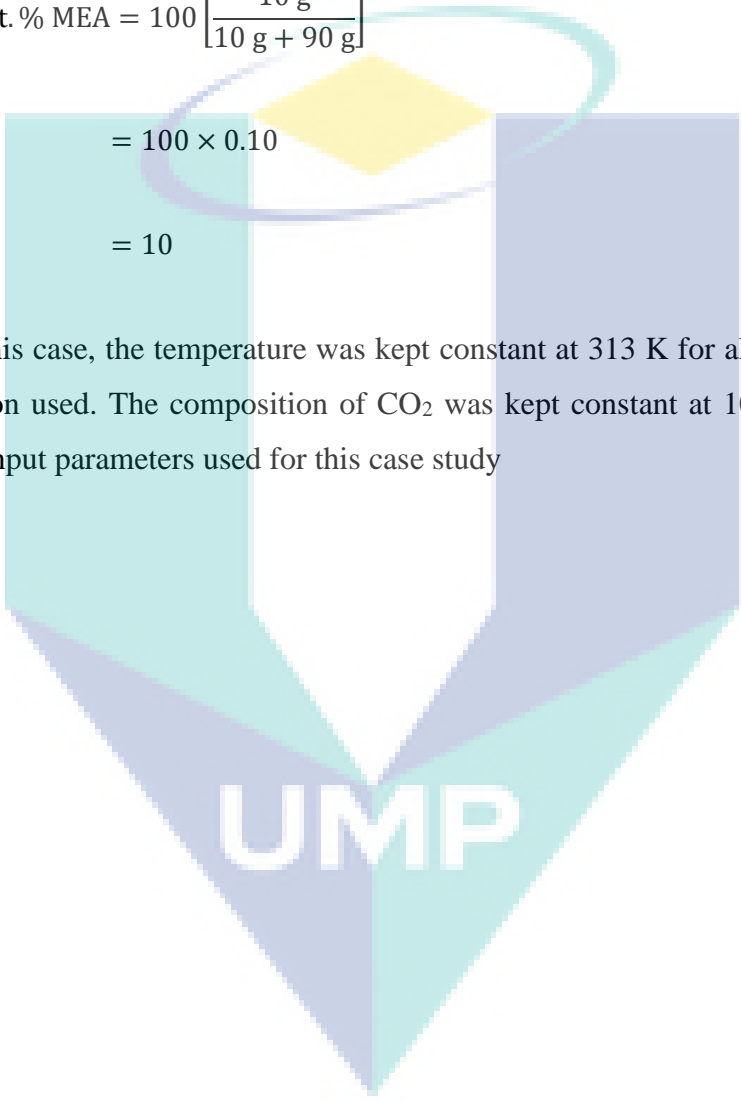
10 wt.% MEA in H₂O = 10 g MEA in 90 g H₂O

$$\text{wt. \% MEA} = 100 \left[\frac{10 \text{ g}}{10 \text{ g} + 90 \text{ g}} \right]$$

$$= 100 \times 0.10$$

$$= 10$$

In this case, the temperature was kept constant at 313 K for all different amines concentration used. The composition of CO₂ was kept constant at 10 wt.%. Table 3.3 shows the input parameters used for this case study

The logo of UMP (Université de Moncton) is a large, downward-pointing arrow shape. It is composed of four colored triangular sections: a light blue section on the top left, a light purple section on the top right, a teal section on the bottom left, and a light blue section on the bottom right. The letters 'UMP' are written in white, bold, sans-serif font across the center of the arrow.

UMP

Table 3.3 Input parameters used to analyse amine concentration effect on the system

Temperature	313 K			
Pressure	1 atm			
Molar ratio for amine	10 wt.%	20 wt.%	30 wt.%	40 wt.%
Density mixture for binary system (g/ml)	1.00078	1.00083	1.00088	1.00096
Number of molecule for binary system	A: 50	A: 50	A: 50	A: 50
	B: 1500	B: 650	B: 400	B: 250
Density mixture for tertiary system (g/ml)	0.99354	0.99295	0.87576	0.88565
Number of molecule for tertiary system	A: 50	A: 50	A: 50	A: 50
	B: 1350	B: 590	B: 340	B: 220
	C: 70	C: 35	C: 23	C: 20

Where, A is amine; B is H₂O; C is CO₂

3.8 Simulation Parameter 3: The Effect of Different Types of Alkanolamines

Different type of amine classes used, such as primary, secondary, tertiary and activator amines, gives different effects in the efficiency of the CO₂ absorption process. The reaction of amine with CO₂ and water will produce carbamate, bicarbonate, and carbonic ions. The aim of this case study was to determine the best amine that has fast intermolecular interaction with CO₂ and water, and to discover causes for it to happen. The ion molecules form has its own stability which affected the stripping process later. In this case study, amine concentrations for all systems were kept constant at 30 wt.%. Mass ratio for binary system was 30 wt.% of MEA and 70 wt.% of H₂O, while for tertiary system was 30 wt.% MEA, 60 wt.% of H₂O, and 10 wt.% of CO₂. Table 3.4 shows the input parameters for different alkanolamines case study.

Table 3.4 Input parameters to analyse the effect different types of amine on the system

Temperature	313 K				
Pressure	1 atm				
Type amines	MEA	DEA	MDEA	AMP	PZ
Density mixture for binary system (g/ml)	1.00088	1.00642	1.00157	0.99366	0.99401
Number of molecule for binary system	A: 50	A: 50	A: 50	A: 50	A: 50
	B: 396	B: 681	B: 772	B: 578	B: 554
Density mixture for tertiary system (g/ml)	0.99244	0.99786	0.99259	0.98399	0.98455
Number of molecule for tertiary system	A: 50	A: 50	A: 50	A: 50	A: 50
	B: 340	B: 580	B: 660	B: 490	B: 478
	C: 23	C: 40	C: 45	C: 34	C: 33

Where, A is amine; B is H₂O; C is CO₂

3.9 Simulation Parameter 4: Comparison of Single and Blended Amines System

Several studies such as Dubois et al. (2010) and Barzagli et al. (2010) proposed the use of blended amine to increase efficiency of single amine for CO₂ absorption process. This case study aimed to analyse how the addition of other amine will affect the intermolecular interaction between amine and CO₂. MDEA is a tertiary amine that is known as a less reactive compared to other amines. Two amine activators, i.e., AMP and PZ were identified to be able to increase the efficiency of MDEA (Mandal & Bandyopadhyay, 2006). Mass ratio of the species in system was decided accordingly from the literature review (Dubois and Thomas, 2011). In this case study, temperature and pressure were set at 313 K and 1 atm, respectively. Table 3.5 shows the mass ratio specified for single and blended system to intermolecular interaction between amine and water. Table 3.6 and Table 3.7 show the input parameters for single and blended system, respectively to intermolecular interaction between amine solution and CO₂.

Table 3.5 Molar ratio for single and blended system of MDEA, AMP, PZ, MDEA/AMP and MDEA/PZ solution

Single	Binary	MDEA: 30 wt.% H₂O: 70 wt.%	AMP: 30 wt.% H₂O: 70 wt.%	PZ: 30 wt.% H₂O: 10 wt.%
	Tertiary	MDEA: 30 wt.% H ₂ O: 60 wt.% CO ₂ : 10 wt.%	MDEA: 30 wt.% H ₂ O: 60 wt.% CO ₂ : 10 wt.%	MDEA: 30 wt.% H ₂ O: 60 wt.% CO ₂ : 10 wt.%
Blended	Binary	MDEA: 30 wt.% AMP: 15 wt.% H ₂ O: 55 wt.%		MDEA: 30 wt.% PZ: 10 wt.% H ₂ O: 60 wt.%
	Tertiary	MDEA: 30 wt.% AMP: 15 wt.% H ₂ O: 45 wt.% CO ₂ : 10 wt.%		MDEA: 30 wt.% PZ: 10 wt.% H ₂ O: 50 wt.% CO ₂ : 10 wt.%

Table 3.6 Input parameters for single system of MDEA, AMP and PZ solution

Single system	MDEA	AMP	PZ
Density mixture for binary system (g/ml)	1.0016	0.9934	0.9985
Number of molecule for binary system	MDEA: 50 H ₂ O: 772	AMP: 50 H ₂ O: 578	PZ: 50 H ₂ O: 1750
Density mixture for tertiary system (g/ml)	0.9926	0.9842	0.9911
Number of molecule for tertiary system	MDEA: 56 H ₂ O: 733 CO ₂ : 50	AMP: 74 H ₂ O: 733 CO ₂ : 50	PZ: 50 H ₂ O: 1150 CO ₂ : 80

Table 3.7 Input parameters for blended system of MDEA/AMP and MDEA/PZ solution

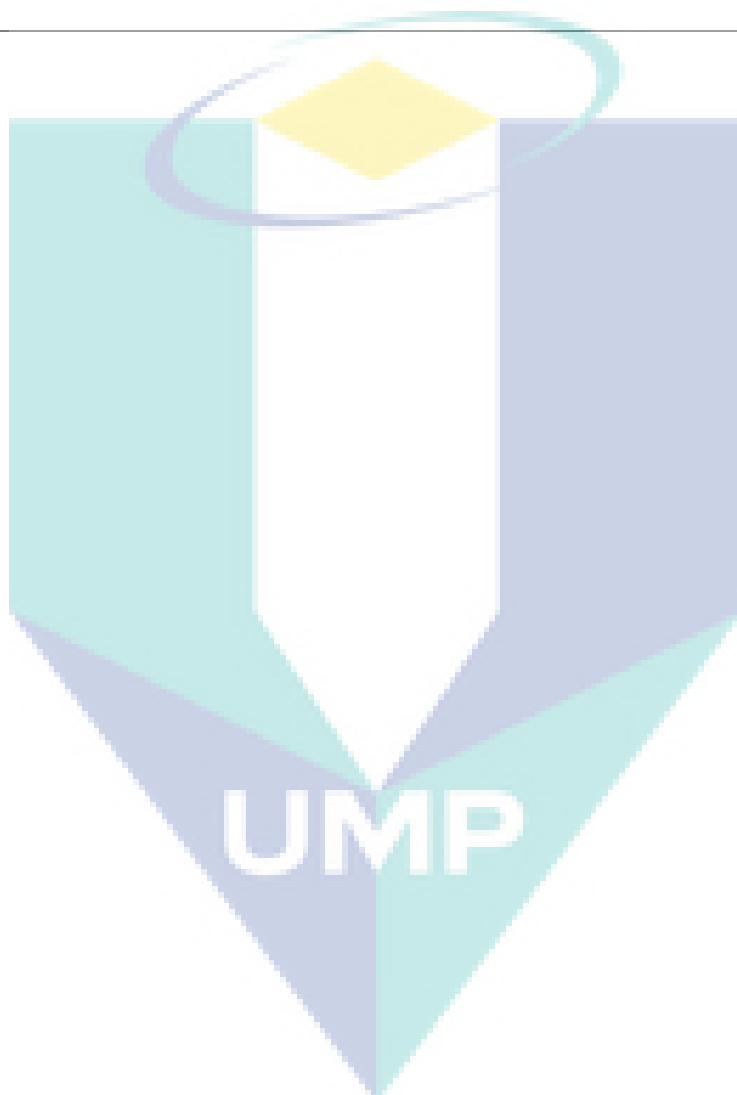
Blended system	MDEA/AMP			MDEA/PZ				
Density mixture for binary system (g/ml)	0.9974			0.9942				
Number of molecule for binary system	MDEA	AMP	H ₂ O	MDEA	PZ	H ₂ O		
	45	30	543	60	30	870		
Density mixture for tertiary system (g/ml)	0.9857			0.9886				
Number of molecule for tertiary system	MDEA	AMP	H ₂ O	CO ₂	MDEA	PZ	H ₂ O	CO ₂
	30	20	296	28	44	20	478	40

3.10 Simulation Parameter 5: Comparison of Different Types Carbamate Amine (Stripping Process)

One of the challenges in amine absorption process is high energy requirement for stripping process to remove CO₂ from the carbamate ion. Process at desorption column occurred at high temperature and the mixture of amine and acid gas was separated at this stage. MEA, AMP, and PZ carbamate amines were used in this case study due to the stability of carbamate ions that required high heat for separating CO₂ from amine solution. The study of intermolecular and intramolecular reaction of amine carbamate with water can show the tendency of carbamate to break the bond and release CO₂. Temperature and pressure were kept constant at 393 K and 1 atm, respectively. Molar ratio for three carbamate amines were similar for all systems. Table 3.8 shows the input parameters for carbamate amines system in stripping process.

Table 3.8 Input parameters for carbamate amines system in stripping process

Type carbamate amine	MEACOO ⁻		AMPCOO ⁻		PZCOO ⁻	
Density mixture (g/ml)	0.9337		0.9088		0.9241	
Number of molecule	MEACOO	H ₂ O	AMPCOO	H ₂ O	PZCOO	H ₂ O
	428	1000	272	1000	170	1000



CHAPTER 4

RESULTS AND DISCUSSION

4.1 Introduction

This chapter is organized as follows: Section 4.2 discusses the effect of temperature on MEA/H₂O/CO₂ absorption process. Section 4.3 presents the effect of amine concentration on MEA/H₂O/CO₂ absorption process. Next, Section 4.4 discusses the effect of different types of alkanolamines. Section 4.5 explains the comparison of using single and blended amines while Section 4.6 evaluates the results of different type of carbamate amine for desorption process. The elaboration of intermolecular interaction between amine/water/carbon dioxide molecules may give more understanding into CO₂ absorption process by amine-based solution.

4.2 Simulation Parameter 1: Effect of Temperature on MEA/H₂O/CO₂ System

4.2.1 Intermolecular Interaction between MEA and Water for Binary (MEA+H₂O) and Tertiary (MEA+H₂O+CO₂) Systems

This section discusses the effect of temperatures on intermolecular interaction for MEA-water-carbon dioxide systems. The temperatures selected were 298, 308, 313, and 318 K. Temperature of the system can affect the diffusion coefficient of CO₂ in amine solution, reaction rate constant, and Henry's constant (Ye et al., 2012). Binary system was used to represent the solubility of MEA solvent in water. The interaction of nitrogen and oxygen atoms in MEA and oxygen atom in H₂O was analysed through characterisation of RDF. RDF plot shows the relationship between r which is the distance between atom pairs in each of the trajectory distance of atom with other neighbouring atom and $g(r)$ is the tendency of atom to interaction/probability to have interaction between atoms. MEA and H₂O molecules represented the aqueous mixture that could

form hydrogen bonding (chemical bonding). Table 4.1 shows the RDF result for temperature 298, 308, 313 and 318 K. Binary system's data acts as a reference to interpret tertiary system.

HO_{mea}: Hydrogen atom at oxygen in MEA

O_{water}: Oxygen atom in water

HN_{mea}: Hydrogen atom at nitrogen in MEA

Table 4.1 Summary data of RDF result for binary and tertiary system at 298 K, 308 K, 313 K and 318 K of MEA

	Binary		Tertiary	
	Homea-Owater	Hnmea-Owater	Homea-Owater	Hnmea-Owater
298K	1.75, 1.4073	3.25, 0.9993	1.75, 1.6381	3.25, 0.9993
308K	1.75, 1.4168	3.25, 1.0111	1.75, 1.5527	3.25, 0.9558
313K	1.75, 1.4989	3.25, 1.0368	1.75, 1.5970	3.25, 1.0160
318K	1.75, 1.6447	3.25, 1.0468	1.75, 2.2408	3.25, 1.1456

Based on RDF plot as shown in Table 4.1, the probability to find the first neighbouring atom for HO_{amine}-O_{water} was higher compared to HN_{amine}-O_{water}. Hydroxyl group (-OH) was more influenced in this simulation compared to amino group (-NH). The stronger interaction of -OH group with water was observed due to the hydrogen bonding. In addition, water had stronger intermolecular force of polar bond with -OH group of amines compared with -NH group since the electronegativity for the oxygen atom was bigger than the nitrogen atom. Electronegativity is an influence to attract electron in order to achieve maximum stability. Referring to the periodic table for orbital energy levels and the Pauli principle, atomic number and electron configuration for oxygen and nitrogen are shown as follows:

O atomic number: 8, $1s^2 2s^2 2p^4$

N atomic number: 7, $1s^2 2s^2 2p^3$

Nitrogen has a half filled p-orbital containing 3 electrons and oxygen has an incomplete p-orbital containing 4 electrons. P-orbital can accommodate a maximum of 6 electrons. In Pauli's principle, half-filled and completely filled orbital are more stable and has greater ionisation energy (Toon, 2003). In this case, the nitrogen atom is already

stable and the oxygen atom was not. The oxygen atom requires two electrons to have a completely filled p-orbital. Therefore, oxygen was more electronegativity than nitrogen. This results proved that the interaction of $\text{HO}_{\text{mea}}\text{-O}_{\text{water}}$ was higher compared to $\text{N}_{\text{mea}}\text{-O}_{\text{water}}$.

Stronger interaction was observed at 318 K compared to other temperatures. For binary system, the r and $g(r)$ value for $\text{HO}_{\text{amine}}\text{-O}_{\text{water}}$ were (1.75, 1.4073), (1.75, 1.4168), (1.75, 1.4989), and (1.75, 1.6447) at the temperatures of 298, 308, 313, and 318 K, respectively. Around 16.87% increment of strength intermolecular interaction between temperature 298 K and 318 K. Based on RDF results, as the temperature increased, stronger intermolecular interaction was observed and it was expected that MEA to dissolve faster in water.

For tertiary system, it was observed that the probability of intermolecular interaction to occur between MEA and water was changed with the addition of CO_2 in the amine solution. CO_2 molecules caused the probability interaction between neighbouring H_2O molecules and MEA to be higher compared to binary system. Intermolecular interaction of $\text{HN}_{\text{amine}}\text{-O}_{\text{water}}$ was slightly changed with the presence of CO_2 . The temperature effect on tertiary system was similar with binary system. The probability of intermolecular interaction between MEA and water molecules was increased as the temperature increased.

As the temperature increased, the kinetic energy of the molecules will increase. When more heat was supplied to system, the rate of collisions, attractions, and repulsion of atoms to each other were also increased. Therefore, as temperature increased, the rate of intermolecular interaction was also increased. Molecules were colliding with each other in periodic boundary resulting the repeated motion. When heat was supplied, the atom will be in vibrational motion and collided with other neighbouring atoms (May & Atoms, 2013). Therefore, raising the temperature was one of the appropriate methods to accelerate the rate of reaction dynamic (Hwang et al., 2015).

4.2.2 Intermolecular Interaction between MEA Solution and CO₂ in Tertiary System

The tertiary system, MEA+H₂O+CO₂, which represented CO₂ absorption process in MEA solution was simulated to study the effect of temperature on intermolecular interaction between these molecules during the absorption process. Intermolecular interaction between MEA and CO₂ was analysed to observe the strength of van der Waals forces between MEA and CO₂ during the absorption process. Table 4.2 shows the RDF result for intermolecular interaction between MEA and CO₂.

O_{mea}: Oxygen atom in MEA
C_{co2}: Carbon atom in CO₂
N_{mea}: Nitrogen atom in MEA

Table 4.2 Summary data of RDF result for intermolecular interaction between MEA and CO₂

	O_{mea}-C_{co2}	N_{mea}-C_{co2}
298K	3.75, 1.0456	4.75, 1.2312
308K	3.75, 1.1360	4.25, 1.4268
313K	3.75, 1.1791	4.25, 1.5724
318K	3.75, 0.9637	3.75, 1.1386

Based on RDF results, intermolecular interaction between O_{mea}-C_{co2} occurred at the distance of 3.75 Å at first neighbouring atom. But N_{mea}-C_{co2} bond showed higher tendency to has interaction with $g(r) = 1.5724$ compared to O_{mea}-C_{co2} bond. This result supports the reaction mechanism proposed by Hwang et al., (2015) when CO₂ is directly binding with N atom of MEA by the zwitterion pathway to absorb CO₂ and form carbamate ion. Subsequently, the carbamate ion was dissolved in water to form bicarbonate species. Higher intermolecular interaction of N_{mea}-C_{co2} compared to O_{mea}-C_{co2} obtained from this study support this reaction mechanism. For example at temperature 318 K, around 18.15% increment of strength intermolecular interaction between temperature N_{mea}-C_{co2} and O_{mea}-C_{co2}. Figure 4.1 shows the single-step for reaction of CO₂, H₂O and amine. Lone-pair electron of nitrogen in amine created reaction with carbon in CO₂. Figure 4.1 shows the electron in a nitrogen was transfer to carbon in

CO₂ to form covalent bond. From RDF result give clear explanation on this mechanism where covalent bond occur by a strong physical intermolecular interaction between nitrogen and carbon.

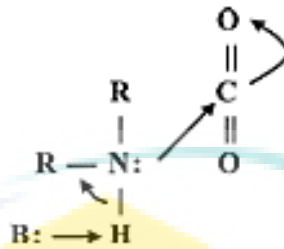


Figure 4.1 Single-step for reaction mechanism between CO₂, H₂O and amine
Source: Crooks & Donnellan, (1989)

The strength of intermolecular interaction for MEA-CO₂ was weaker compared to binary system, which was represented by MEA-water intermolecular interaction. In binary system, the distance of atom with another neighbouring atom was 1.75 Å. While in tertiary system, the distance was 3.75 Å for O_{amine}-C_{co2} and 4.25 Å for N_{amine}-C_{co2}. It shows that hydrogen bonding formed in binary system through molecular interaction of HO_{mea}-O_{water} was stronger than the van der Waals' interaction occurred in tertiary system. Physical absorption which relies on intermolecular interaction alone is not sufficient for CO₂ removal at low concentration of CO₂. Thus, chemical absorption which involves reactions between CO₂ and MEA is preferable technology to increase CO₂ absorption efficiency at low CO₂ concentration.

Based on temperature condition, when the temperature of the system was increased from 298 K to 318 K, the rate of intermolecular interaction between MEA and CO₂ was increased. This finding is in agreement with the study by (Yu, 2012) which reported that more CO₂ was absorbed for the system at the temperature between 313 K and 333 K. The amount of CO₂ absorbed was decreased for the process operating at the temperature higher than 333 K. This resulted in the increasing rate of intermolecular interaction between MEA and CO₂ from 298 K to 318 K that is also supported by Ye et al. (2012) when the diffusivity coefficient of CO₂ and MEA ascended from 1.1×10^{-19} to $2.4 \times 10^{-9} \text{ m}^2\text{s}^{-1}$ and 3.8×10^{-10} to $8.2 \times 10^{-10} \text{ m}^2\text{s}^{-1}$ at 298 K to 338 K, respectively. Many literatures used 313 K as operating temperature for CO₂ absorption process because it is reported that a zwitterion mechanism for reaction of CO₂ with the amine to form

carbamate occurs at this temperature (D'Alessandro, Smit, & Long, 2010). Higher temperature cannot be used in the industries due to the problems of amine loss, degradation, corrosion, and cost of operation (Goff & Rochelle, 2004).

The factor of temperature was important to speed up the reaction but has to limit at certain value because it is related to cost of operation. Absorption process should operate at low temperature. Hydrogen bond has significant influence in CO₂ absorption reaction in aqueous MEA solution (da Silva et al., 2007; Scheiman, 1987). The hydrogen bond between HO_{mea}-O_{water} was formed when a weak base (MEA) was dissolved in H₂O and neutralised by acidic compound. This reaction produced the ionic compound. In primary amine, the carbamate ion was formed (NH₂COO⁻). The carbamate ion formation shows the absorption of CO₂ in MEA solution. The absorption rate was increased with the increase of the system temperature. This was due to the increase of the chemical reaction rate constant (Abharchaei, 2010; Nair & Selvi, 2014).

4.3 Simulation Parameter 2: Effect of Amine Concentration on MEA/H₂O/CO₂ System

4.3.1 Intermolecular Interaction between MEA and Water for Binary (MEA+H₂O) and Tertiary (MEA+H₂O+CO₂) Systems

The effect of amine concentration to the strength intermolecular interaction of CO₂ absorption process will be discussed in this section. Values of amine concentration selected for MEA solvent were 10, 20, 30, and 40 wt.%. In RDF analysis, $r(\text{Å})$ represents the distance of reference point atom to another atom and $g(r)$ represents the probability to find interaction of atoms at that distance. Table 4.3 shows the results of intermolecular interaction between MEA and water for binary and tertiary systems. Binary system consists of amine and water molecules, while tertiary system contains amine, water, and carbon dioxide molecules.

HO_{mea}: Hydrogen atom at oxygen in MEA

O_{water}: Oxygen atom in water

HN_{mea}: Hydrogen atom at nitrogen in MEA

Table 4.3 Summary data of RDF result for binary and tertiary system at 10 wt.%, 20 wt.%, 30 wt.% and 40 wt.% of MEA

	Binary		Tertiary	
	HO _{mea} -O _{water}	HN _{mea} -O _{water}	HO _{mea} -O _{water}	HN _{mea} -O _{water}
10%	1.75, 1.2071	3.25, 1.0023	1.75, 1.3627	3.25, 0.9527
20%	1.75, 1.2877	3.25, 1.0150	1.75, 1.4589	3.25, 0.9694
30%	1.75, 1.4150	3.25, 1.0236	1.75, 1.5970	3.25, 1.0160
40%	1.75, 1.5379	3.25, 1.0435	1.75, 1.7608	3.25, 1.0627

The intermolecular interaction of MEA and water in tertiary system was higher than in binary system around 27.40% for HO_{mea}-O_{water}. In binary system, hydrogen bond for HO_{mea}-O_{water} were (1.75, 1.2071), (1.75, 1.2877), (1.75, 1.4150), and (1.75, 1.5379) at MEA concentration of 10, 20, 30, and 40 wt.%, respectively. For tertiary system, hydrogen bond for HO_{mea}-O_{water} were (1.75, 1.3627), (1.75, 1.4589), (1.75, 1.5970), and (1.75, 1.7608) at MEA concentration of 10, 20, 30, and 40 wt.%, respectively. The addition of CO₂ molecule in the system affected the diffusivity of MEA in water. The higher and closer position of peaks predicted that atom would likely make a bond with other atom. Water molecules play a role in fundamental aspect of amine-CO₂ reaction. Water also acts as bridge for proton transfer from MEA to form MEAH⁺ (protonated MEA). How CO₂ molecules affect the diffusion MEA in water is discussed based on NO₂ analogy (Emmanuelle Masy, 2013). From this analogy, it can be seen that the presence of CO₂ in solution influence the diffusivity to water and MEA. Equation (4.1) shows the analogy of NO₂.

$$(D_{CO_2})_{MEA} = (D_{N_2O})_{MEA} \left(\frac{D_{CO_2}}{D_{N_2O}} \right)_{water} \quad (4.1)$$

Molecular simulation for binary system consists of MEA and H₂O molecules. In tertiary system was shows the addition of CO₂ will cause the rate of interaction between amine and water changed. If CO₂ present, the reactivity of amine with water increased. From Table 4.3, it shows that intermolecular interaction between MEA and water was increased as molar ratio was increased. The reaction of amine with water involved molecular diffusion process. Molecular diffusion is a motion of particle that are temperature, viscosity, and mass of particle dependent. When the amine concentration

was increased, the molecular diffusion was increased as well (Lionel Dubois & Thomas, 2011).

Based on Figure 7 to Figure 10 in Appendix A, the RDF graph was become less structured and low interaction to neighbour atoms was observed when the particle was at large distance around 15 Å. Less structured means the number of RDF peak was reduced when the far distance from the central point. Also, the graph approaches to 1 as the distance was increased due to the lack of long-range interaction. Besides that, sharp peak in graph indicates a strong interaction between atoms in the system.

4.3.2 Intermolecular Interaction between MEA Solution and CO₂ in Tertiary System

Study on the intermolecular interaction for tertiary system involves physical interaction of MEA+CO₂+H₂O solution in an amorphous cell box. As the primary amine, MEA can directly react with CO₂ and intermolecular interaction of MEA and CO₂ represent the CO₂ absorption process. Table 4.4 shows the RDF result for intermolecular interaction of MEA and CO₂ molecules.

O_{mea}: Oxygen in MEA
C_{co2}: Carbon in CO₂
N_{mea}: Nitrogen in MEA

Table 4.4 RDF results for intermolecular interaction between MEA and CO₂

	O_{mea}-C_{carbon dioxide}	N_{mea}-C_{carbon dioxide}
10%	3.75, 0.9793	4.25, 1.2846
20%	3.75, 1.1646	4.25, 1.3013
30%	3.75, 1.1678	4.25, 1.3487
40%	3.75, 1.2013	4.25, 1.4624

As highlighted on RDF results, as MEA concentration was increased, the strength of intermolecular interaction between MEA and CO₂ was also increased. For example at intermolecular interaction of N_{mea}-C_{co2}, the increment was 13.84% from $g(r)$ result. This result is supported by the experimental work done by Dubois and Thomas (2011), where it state that an increase in absorption efficiencies was affected by the increased amine concentration.

Besides, the high concentration of MEA was favourable for CO₂ absorption, in which more MEA reacted with CO₂ at high concentration and made the CO₂ absorption process faster (Ye et al., 2012). Although the intermolecular interaction between amine and CO₂ was increased with the increased of amine concentration, many literatures used 30 wt.% alkanolamine. Kim et. al. (2013) studied about the comparison of CO₂ in aqueous MEA, DEA, TEA, and AMP solution. All alkanolamines analysed were under 30 wt.% (Kim et al., 2013). The high amount of amine concentration will cause corrosive problem (Lunsford & Bullin, 2006).

Another reason for increasing intermolecular interaction at high amine concentration was by using high base strength because the reaction of amine and CO₂ is based on Lewis acid-base equilibrium (Wispelaere, 2014). Therefore, by increasing the concentration of amine, it increases the basicity of the amine. High basicity of amine causes strong attraction to complement bonding to acidic CO₂ to form carbamate ions ([BH]⁺[R₂NCOO]⁻). The interaction of MEA and CO₂ represents a classical donor-acceptor interaction, wherein, CO₂ is the Lewis acid and H₂O is Lewis bases (Hwang et al., 2015).

Results shown in Table 4.4 depict that -NH group of MEA has high probability to have intermolecular interaction with CO₂ compared to oxygen atom. The reaction mechanism for CO₂ and MEA was based on the formation of a zwitterion to form carbamate ion. CO₂ will form a bond to the hydrogen atom at amino group rather than at hydroxyl group (Singh, 2011). Increase the amount of carbamate ion form, it shows the CO₂ absorption capacity increased. The reaction mechanism proposed was supported by molecular dynamic simulation when it shows high intermolecular interaction between nitrogen atoms with CO₂.

The amount of CO₂ loading will increase due to the increased amine concentration. But high amine concentration will cause the solution to be more corrosive because amine acts as an oxidizing agent to dissolve bicarbonate ion (HCO₃⁻) or CO₂, and induce the increase of oxidiser reduction (Nainar & Veawab, 2009). Therefore, blending of more than one amine in a solution was one option to increase the amount CO₂ absorbed and reduce the corrosion rate. The corrosive problem can occur when used too high amine concentration. In addition, an increase in dissolved CO₂ will induce more iron

dissolution. A higher CO₂ loading causes the solution to be more corrosive. Due to these, 30 wt.% of MEA was selected to be optimum amine concentration.

4.4 Simulation Parameter 3: Effect of Different Types Alkanolamines

4.4.1 Intermolecular Interaction between Amine and Water for Binary (Amine+H₂O) and Tertiary (Amine+H₂O+CO₂) Systems

Comparison between intermolecular interactions of amine with water in binary system without CO₂ and tertiary system with CO₂ were performed. The strength of amine-water intermolecular interaction at different types of alkanolamine is discussed in this section. Table 4.5 show the RDF results of the binary and tertiary system for MEA, DEA, MDEA, AMP and PZ solutions.

HO_{amine}: Hydrogen at oxygen in amine

O_{water}: Oxygen in water

N_{amine}: Nitrogen in amine

H_{water}: Hydrogen in water

Table 4.5 Summary data comparison RDF result for amine solution between binary and tertiary system

	Binary		Tertiary	
	HO _{amine} - O _{water}	N _{amine} -H _{water}	HO _{amine} - O _{water}	N _{amine} -H _{water}
MEA	1.75,1.3989	4.75,1.0149	1.75,1.5107	12.75,1.0000
DEA	1.75,1.3867	5.75,1.0164	1.75,1.5994	5.75,1.0131
MDEA	1.75,2.2293	4.75,1.1107	1.75,2.6546	4.75,1.2557
AMP	1.75,2.9029	1.75,1.2976	1.75,1.6362	5.75,1.0364
PZ	-	5.75,1.0255	-	5.75,1.0926

Comparison of binary and tertiary system is discussed based on hydroxyl and amino functional groups. Hydroxyl group in amine was used to increase the solubility in water and amino group leads to reaction with acidic gas (Kohl & Nielsen, 1997).

For hydroxyl group, binary system result order is AMP > MDEA > MEA > DEA and tertiary result order is MDEA > AMP > DEA > MEA. The result is read based on the highest to the lowest intermolecular interaction bonded between two selected atoms. PZ

amine does not have $\text{HO}_{\text{amine}}\text{-O}_{\text{water}}$ interaction because it lack oxygen atom in its molecule structure.

In binary system, AMP (1.75, 2.9029) amine has high tendency to make a bond with water compared to others, the strength percent was 107% (calculated based on $g(r)$ value) compared MEA (1.75, 1.3989). AMP is a primary amine which has steric hindrance. The characteristic of AMP leads to stronger intermolecular interaction with water. AMP is a sterically hindered primary amine but the reaction is similar as tertiary amine (Tobiesen, Svendsen, & Mejdell, 2007). AMP amine is reactive, soluble in water, and easier to regenerate to separate CO_2 gas. It can replace the function of MDEA and be an option to use compared to MEA and DEA. Tertiary amine with the presence of CO_2 also shows high intermolecular interaction with water.

In binary system, hydroxyl group of MDEA (1.75, 2.2293) also shows high tendency to bond with water similar to AMP. Figure 4.2 shows the molecular structure of MDEA. The structure of MDEA can influence the result of RDF. MDEA has two –OH bond which cause it to be more soluble in water compared to MEA and DEA that only has one –OH bond. Besides that, the presence of CO_2 in tertiary system also shows high intermolecular interaction of hydroxyl group in MDEA with water. This is because MDEA cannot directly react with CO_2 to form carbamate ion but has to go through hydrolysis process between CO_2 and water to form bicarbonate ion. The presence of CO_2 and water is essential in order to increase the reactivity of MDEA for CO_2 absorption process.

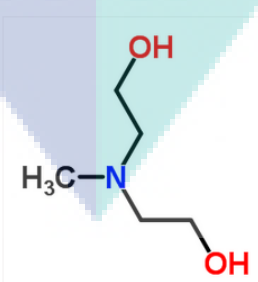


Figure 4.2 Molecular structure of MDEA

Based on binary and tertiary system, the intermolecular interaction of DEA with water is in average level. From this finding, it shows that DEA amine as secondary amine has medium potential to dissolve in water and absorb CO_2 in between primary and tertiary amine. Compared to these four amines, DEA has the weakest intermolecular interaction

with water compared to MEA and AMP. This is because DEA is a secondary amine that is more nucleophilic compared to primary and tertiary amine.

For amino group, binary system result is $AMP > MDEA > MEA > PZ > DEA$ and tertiary result is $MDEA > PZ > AMP > DEA > MEA$. The highest intermolecular interactions with water for amino group for binary and tertiary system are AMP and MDEA, respectively.

But in the presence of CO_2 in AMP amine solution, intermolecular interaction of amino group with water was decreased about 25.20%. Binary and tertiary result for AMP was (1.75, 1.2976) to (5.75, 1.0364). AMP has α -substitute in molecular structure which led to the reduction of the charge of nitrogen atom (Hook, 1997). Thus, the interaction of $N_{amine}-H_{water}$ was weaker and it was expected that the reaction rate with CO_2 was slow. The reaction of AMP with CO_2 produce unstable carbamate ion.

PZ showed weak intermolecular interaction in binary system but had strong interaction in tertiary system. PZ amine alone was less reactive for the absorption process. PZ acts as an activator in solvent to accelerate the reaction especially for tertiary amine, MDEA.

4.4.2 Intermolecular Interaction between Amine Solution and CO_2 in Tertiary System

The aim of this part is to identify amine solvent that has higher tendency to interact with CO_2 . Table 4.6 shows the RDF results of MEA, DEA, MDEA, AMP, and PZ solutions. Same as previous discussion, the intermolecular interaction of amine with CO_2 was determined by comparing which functional group that had more tendencies to interact with CO_2 molecule.

O_{amine} : Oxygen in amine
 C_{co2} : Carbon in CO_2
 N_{amine} : Nitrogen in amine

Table 4.6 Summary data of RDF result for intermolecular interaction of amine solutions with CO₂

	Oamine-Ccarbon dioxide	Namine-Ccarbon dioxide
MEA	3.75, 1.0612	4.25,1.4058
DEA	3.75,1.1399	5.25,1.4259
MDEA	3.75,1.1488	4.75,1.3461
AMP	4.25,1.0416	4.25,1.0063
PZ	-	4.25,1.0705

Based on RDF result, the sequence of the highest intermolecular interaction to the lowest for hydroxyl group with CO₂ (O_{amine}-C_{co2}) are MDEA > DEA > MEA > AMP.

At the same distance of $r = 3.75 \text{ \AA}$, MDEA showed the highest tendency for intermolecular interaction to occur about 8.25% compared to MEA. It is supposed that MDEA has lower intermolecular interaction with CO₂, because it is a tertiary amine. But this intermolecular interaction occurred between hydroxyl groups of MDEA with CO₂. Because MDEA has two –OH bond and other amines only has one –OH bond, molecular structure of MDEA influenced the reaction with CO₂. So this is the reason why RDF results show MDEA was the highest compared others amine.

For amino group (N_{amine}-C_{co2}), the trends of the highest interaction to the lowest are MEA > PZ > AMP > MDEA > DEA.

At same distance of $r = 4.25 \text{ \AA}$, MEA showed the highest tendency for intermolecular interaction to occur about 39.70% compared to AMP. The results obtained have good agreement with the literature study. However, CO₂ absorption efficiencies reported by Dubois and Thomas (2011) was MEA > PZ > PZEA > AMP > MDEA. MEA was supposed to have the strongest intermolecular interaction with CO₂ because it easily absorbed CO₂ compared to secondary and tertiary amine. Based on Zhang et al. (2008), the trend for absorption performance by experimental work were AMP > MEA > DEA > MDEA. Based on this experimental result, MEA and AMP were reactive amine to absorb CO₂. Characteristic of steric hindered amine made AMP to be significant to be used for CO₂ absorption process.

AMP and PZ also showed high value of $g(r)$ same as MEA. AMP has sterically hindered amine properties. The reaction mechanism of AMP was proposed by Sartori and Savage (1983) and explained more by Zhang et al. (2008). The reaction of AMP with water produces low stable carbamate ion. Then, carbamate ion reacts with water again through hydrolysis to produce bicarbonate ion and free amine molecule. This free amine molecule will react with CO_2 , representing the overall absorption process. However, due to the molecular structure of AMP, the reactivity with CO_2 is lower than MEA (Tobiesen et al., 2007). It was reported that when there were more substituents such as methyl and alcohol groups were added, the reactivity of amine towards CO_2 would be decreased. In AMP structure, it has two methyl groups at α -carbon to the nitrogen atom. The presence of substituent methyl group to the amino functional group caused the reaction of AMP with CO_2 to form unstable carbamate ion. Then, the reaction with CO_2 was faster than MDEA (Idris & Eimer, 2014). Moreover, the size of molecule will influence the reactivity of amine itself. The molecular weights of MEA and AMP is 61.08 g/mole and 89.14 g/mole, respectively. It shows that AMP size is much bigger than MEA and consequently the intermolecular interaction strength of AMP with CO_2 is lower than MEA even both of amines are categorised as primary amines. Furthermore, the attraction of base (amine) to positively charge CO_2 for zwitterion reaction became slower when the sterically hindered properties were presence (Bavbek, 1999). PZ contains two nitrogen atom in its molecular structure which will result to double CO_2 absorption compared to one nitrogen at shorter time interaction. Dubois and Thomas (2011) also stated that activator amine showed good efficiencies for CO_2 absorption. AMP and PZ amines are always chosen to blend with MEA and DEA, because these amines are difficult to separate from amine- CO_2 bond in the stripper. Figure 4.3 shows the molecular structure of MEA and AMP.



Figure 4.3 Molecular structure of MEA and AMP

MDEA amine has low tendency to create the intermolecular interaction with CO_2 about 89.47%. This is because MDEA has lack of hydrogen atom attached in amino group

there will be no formation of carbamate ion. MDEA cannot directly absorb CO_2 . Therefore, it is recommended to blend MDEA with activator amine such as AMP and PZ.

DEA amine also shows low tendency to make intermolecular interaction with CO_2 compared to MEA, AMP, and PZ about 80.95%. DEA is a secondary amine and it is recognised as medium amine in CO_2 absorption efficiency. It was proved that DEA was neither the fastest nor the slowest to dissolve in water and to absorb CO_2 . Also DEA poses medium energy requirement for regeneration. In addition, DEA amine gives moderate difficulty to break amine- CO_2 bond.

4.5 Simulation Parameter 4: Comparison of Single and Blended Amines System

Since MDEA has limitation in CO_2 absorption process, blended amine is essential to improve the strength of intermolecular interaction with water and CO_2 . In this research, AMP and PZ were selected to mix with MDEA solution. MDEA, AMP/PZ, MDEA/AMP, and MDEA/PZ solvents were selected to study the effect of single and blended amines toward CO_2 absorption process. Mixtures of MDEA with AMP and PZ were known as activated MDEA.

4.5.1 Intermolecular Interaction for Blended MDEA/AMP

The system consisted of 15 wt.% of AMP, 30 wt.% of MDEA, and 55 wt.% of H_2O for binary MDEA/AMP blended system was simulated. While, a system with 15 wt.% of AMP, 30 wt.% of MDEA, 45 wt.% of H_2O , and 10 wt.% of CO_2 was analysed for tertiary MDEA/AMP blended amine. For single MDEA and AMP, both systems were simulated with an amine concentration of 30 wt.%. The addition of AMP and PZ that act as activator were selected to blend with MDEA in order to enhance the strength of intermolecular interaction between amine- CO_2 - H_2O systems.

4.5.1.1 Comparison Single and Blended MDEA/AMP for Binary and Tertiary System

In this part, comparison of intermolecular interaction between single and blended amine with water are discussed. The comparison also includes the interaction of amine and water for system with and without CO₂. RDF result was also presented in Table 4.7.

HO_{mdea}: Hydrogen at oxygen in MDEA

O_{water}: Oxygen in water

N_{mdea}: Nitrogen in MDEA

H_{water}: Hydrogen in water

HO_{amp}: Hydrogen at oxygen in AMP

N_{amp}: Nitrogen in AMP

Table 4.7 Summary data of RDF result for binary system of MDEA and AMP, and blended MDEA/AMP system

	Binary			
	Homdea-Owater	Nmdea-Hwater	Hoamp-Owater	Namp-Hwater
MDEA	1.75, 2.2293	4.75, 1.1107		
AMP			1.75, 2.9029	1.75, 1.2976
MDEA+AMP	1.75, 1.7541	4.75, 1.2915	1.75, 1.9357	5.75, 1.2270

Based on Table 4.7, hydroxyl groups of MDEA and AMP in single system has high intermolecular interaction with water compared to blended system. As can be seen from Table 4.7, RDF values (r , $g(r)$) for HO_{mdea}-O_{water} and HO_{amp}-O_{water} were (1.75, 2.2293) and (1.75, 2.9029) using single amine, respectively. While, for blended MDEA/AMP, the probability intermolecular interaction were (1.75, 1.7541) and (1.75, 1.9357) corresponding to HO_{mdea}-O_{water} and HO_{amp}-O_{water}, respectively. At a distance of 1.75 Å, almost two times higher probability of finding any atom pair of hydrogen bonding in single MDEA and AMP system was observed.

Single MDEA and AMP were easily attracted to water due to less obstacle to diffuse in water compared to blended system. Solubility was decreased with the increased in the number of carbon atoms. That is the reason why blended MDEA/AMP was slow to dissolve in water compared to single MDEA and AMP. When the length of the carbon chain was increased, the polar -OH group became smaller and the solubility in water was decreased. In blended amines, MDEA, CH₃N(C₂H₄OH)₂, and AMP, C₄H₁₁NO were

mixed. This was the reason for the intermolecular interaction between MDEA and AMP in single system higher than in blended system. The hydroxyl group in amine was to help amine solubility in water (Abharchaei, 2010).

On the contrary, amino group in blended MDEA/AMP has high intermolecular interaction with water than single MDEA about 16.28%. At the same distance of 4.75 Å, the tendency the interactions to happen between nitrogen atoms on MDEA in blended MDEA/AMP was 1.2915 but in single MDEA system the tendency was 1.1107. The lack of –NH bond in the molecular structure of MDEA causes the water molecule to not interact directly with nitrogen atom. But the presence of AMP in blended system was capable to assist the diffusivity of MDEA in water. Whereas, for amino group in single AMP system, higher intermolecular interactions with water was observed compared to blended MDEA/AMP. The first peak of Namp-Hwater in single AMP system occurred at 1.75 Å with a probability value of 1.2976 and for blended MDEA/AMP, the intermolecular interaction was observed at a distance of 5.75 Å with the tendency of 1.2270. This result shows that steric hindrance behaviour in AMP gave advantage to –NH group to dissolve directly in water without the need to blend with other amine. The limitation of MDEA is that it requires to be blended with activator amine like AMP in order to enhance the diffusivity in water.

Meanwhile, for tertiary system, CO₂ molecules were put together in amorphous cell box to study the intermolecular interactions for CO₂ absorption. Table 4.8 shows the RDF results for intermolecular interaction of single MDEA, AMP and blended MDEA/AMP with water with the presence of CO₂. From this analysis, it can be seen that the presence of CO₂ has effect to dissolving amine in water.

HO_{mdea}: Hydrogen atom at oxygen in MDEA

O_{water}: Oxygen atom in water

N_{mdea}: Nitrogen atom in MDEA

H_{water}: Hydrogen atom in water

HO_{amp}: Hydrogen atom at oxygen in amp

Table 4.8 Summary data of RDF result for tertiary system of MDEA and AMP, and blended MDEA/AMP system

	Tertiary			
	Homdea-Owater	Nmdea-Hwater	Hoamp-Owater	Namp-Hwater
MDEA	1.75, 2.6546	4.75, 1.2557	-	-
AMP	-	-	1.75, 1.6362	5.75, 1.0364
MDEA+AMP	1.75, 2.7162	4.75, 1.3460	1.75, 1.9604	5.75, 1.0767

Based on RDF result in Table 4.8, it shows that the intermolecular interaction of single MDEA, AMP, and blended MDEA/AMP was increased in tertiary system compared to binary system. The addition of CO₂ improved the strength of amine interaction with water. For example, RDF values of HO_{mdea}-O_{water} in single MDEA was increased from (1.75, 2.2293) to (1.75, 2.6546) (19.08%) and for N_{mdea}-H_{water}, the RDF values was increased from (4.75, 1.1107) to (4.75, 1.2557) (13.05%), after the addition of CO₂ into the solution.

Both hydroxyl and amino groups of MDEA and AMP in blended system showed higher intermolecular interaction with water than single MDEA and AMP for tertiary system. Comparing the intermolecular interaction rate of blended MDEA/AMP and MDEA with water, it was found that the strength of interaction was increased. The RDF result for HO_{mdea}-O_{water} and HO_{amp}-O_{water} were (1.75, 2.6546) and (1.75, 1.6362), respectively for single MDEA and AMP system. But in MDEA/AMP blended system, the rate of interaction was increased up to (1.75, 2.7162) (2.32%) and (1.75, 1.9604) (19.81%) for HO_{mdea}-O_{water} and HO_{amp}-O_{water}, respectively. Good combination of MDEA and AMP was expected to increase the solubility of amine in water. Theoretically, MDEA and AMP are basic and CO₂ is acidic. The solubility of amine in water was due to the hydrogen bonding between lone electron pair at nitrogen atom in amine and proton at hydrogen in water. The presence of steric hindrance of AMP was identified to increase the energy of the lone pair of electron, thus enriched the basicity of amine. Therefore, the acidic-basic reaction within MDEA/AMP/CO₂/H₂O system had increased the diffusivity of amine in water compared to single MDEA/CO₂/H₂O and AMP/CO₂/H₂O system. Clearly, the presence of CO₂ can enhance the ability of the MDEA and AMP to make intermolecular interaction with water. Other than that, the electrostatic factors also play

a role. In blended MDEA/AMP, there are two nitrogen atoms from MDEA and AMP. The addition of lone electron pair at nitrogen gives high attraction to positive charge at hydrogen in water to form hydrogen bond. The strong intermolecular interaction between $\text{HO}_{\text{mdea}}\text{-O}_{\text{water}}$ and $\text{HO}_{\text{amp}}\text{-O}_{\text{water}}$ was due to strong hydrogen bond. The probability of intermolecular interaction tended towards 1 as the distance increased, signifying the amine solvent was representing the bulk fluid.

4.5.1.2 Comparison Single and Blended MDEA/AMP for Intermolecular Interaction with CO₂ in Tertiary System

The absorption process happened when gas molecules were dissolved in an amine aqueous solution. Therefore, RDF analysis on amine and CO₂ molecules was generated in MD simulation to analyse the intermolecular interaction between these molecules. The strength of intermolecular interaction between single MDEA and AMP, and blended MDEA/AMP with CO₂ was compared. Table 4.9 shows the RDF graphs of intermolecular interaction between amine and CO₂ for MDEA, AMP and MDEA/AMP system.

O_{mdea}: Oxygen atom in MDEA

C_{co2}: Carbon atom in CO₂

N_{mdea}: Nitrogen atom in MDEA

O_{amp}: Oxygen atom in AMP

N_{amp}: Nitrogen atom in AMP

Table 4.9 Summary data of RDF result for intermolecular interaction between amine with CO₂ for MDEA and AMP, and blended MDEA/AMP system

	Tertiary			
	O_{mdea}-C_{co2}	N_{mdea}-C_{co2}	O_{amp}-C_{co2}	N_{amp}-C_{co2}
MDEA	3.75, 1.1488	5.25, 1.5158	-	-
AMP	-	-	4.25, 1.0416	4.25, 1.0063
MDEA+AMP	3.75, 1.5337	5.25, 1.8256	4.25, 1.3185	4.25, 1.1560

Based on Table 4.9, the intermolecular interaction between $\text{O}_{\text{mdea}}\text{-C}_{\text{co2}}$ in single MDEA system was (3.75, 1.1488) and at the same distance (3.75 Å), the RDF result in blended MDEA/AMP was increased to 1.5337 (33.50%). The similar trend was observed on the intermolecular interaction between $\text{N}_{\text{mdea}}\text{-C}_{\text{co2}}$. At a distance of 5.25 Å, the

tendencies for the interaction to happen were 1.5158 and 1.8256 for single MDEA and blended MDEA/AMP, respectively. Moreover, blended MDEA/AMP also showed strong intermolecular interaction with CO₂ compared to single AMP system. At a distance of 4.25 Å, the tendencies for intermolecular interaction to happen on O_{amp}-C_{co2} were 1.0416 and 1.3185, for single AMP and blended MDEA/AMP systems, respectively. For N_{amp}-C_{co2}, the tendencies for intermolecular interaction to happen were 1.0063 and 1.1560 for single AMP and blended MDEA/AMP systems, respectively. RDF results clearly showed that the blended MDEA/AMP gave strong intermolecular interaction with CO₂ compared to single MDEA and AMP.

Figure 4.4 shows the molecular structure of AMP where the addition of two branches chain of alkyl group to carbon atom caused steric hindrance properties with two hydrogen atom attach to nitrogen atom. On the other hand, the molecular structure of MDEA where the nitrogen is connected to three branches of carbon and at least two of them are quite long. Thus, it can be concluded that it is impossible for carbon dioxide to form the first intermolecular interaction around nitrogen within a very short distance at MDEA molecule. That is why the position of the first peak N_{mdea}-C_{co2} was fairly far for single MDEA system (5.25Å, 1.5158) and (5.25 Å, 1.8256) for blended MDEA/AMP system compared to (4.25 Å, 1.0063) for single AMP system and (4.25 Å, 1.1560) for blended MDEA/AMP system. In contrary, such limitation did not exist for CO₂ to surround the oxygen in alcohol group. Oxygen atoms were located at the end of tails of MDEA and AMP. It was quite feasible for CO₂ molecules to approach them. Observing from Table 4.9 the first intermolecular interaction of oxygen with CO₂ was closer at 3.75 Å for MDEA and 4.25 Å for AMP.

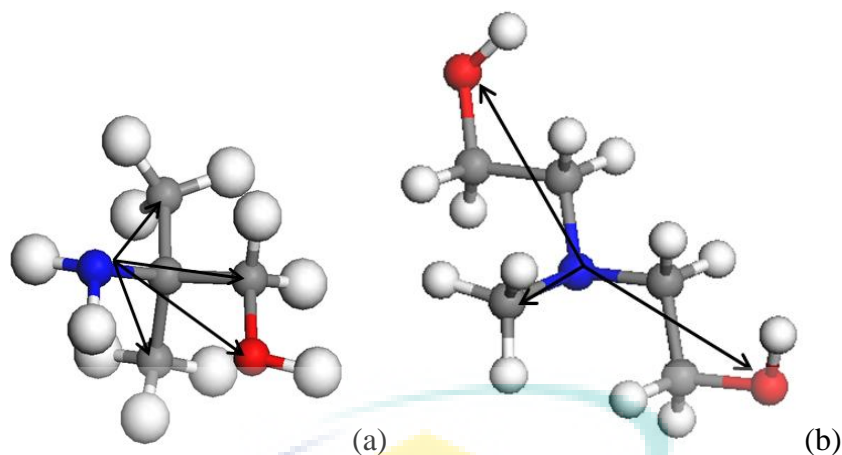


Figure 4.4 N-O and N-C branches in (a) AMP and (b) MDEA molecular structure

Higher intermolecular interaction of nitrogen atom in blended amine with CO_2 than single amine was fit with the expectation. The combination of MDEA and AMP in one system can overcome the limitation on MDEA. The structural property of AMP can cover the limitation of MDEA, which is cannot directly react with CO_2 by forming carbamate and bicarbonate formation. The properties of sterically hindered made blended amine to be more reactive and easily formed carbamate ion when reacted with CO_2 . The reaction of AMP with CO_2 formed less stable carbamate ion. The advantage of using AMP was the solvent exhibited a high boiling point and formed unstable carbamate ion (Gangarapu, Marcelis, & Zuilhof, 2013). Reducing the carbamate stability will affect the electron-withdrawing of the molecule. In addition, AMP will help MDEA to react with CO_2 .

Schubert et al. (2001) reported the mechanism of chemical reaction of CO_2 with a tertiary amine (MDEA). CO_2 molecules interacted and reacted with MDEA solution. Figure 4.5 illustrates the CO_2 absorption process in MDEA solution. The reaction scheme was generated from experimental work from previous research work (Schubert et al., 2001). MDEA cannot directly react with CO_2 . MDEA was dissolved in water to form bicarbonate. The reaction was proceeded to react with CO_2 to form MDEAH^+ and HCO_3^- . The reaction of MDEA with CO_2 was slower compared to MEA and DEA.

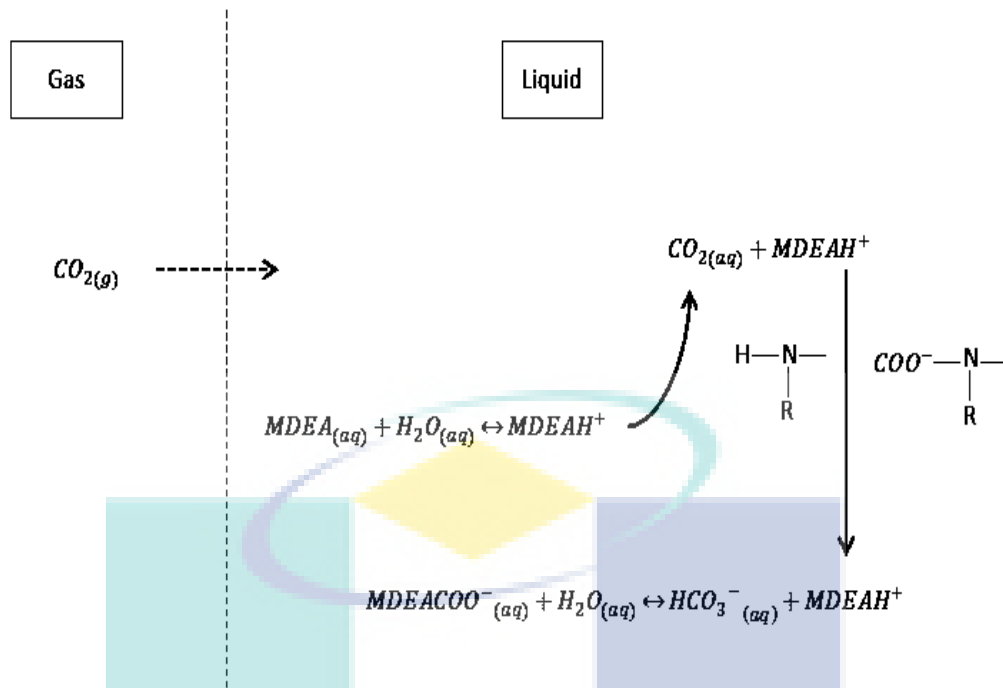
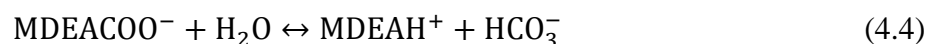


Figure 4.5 Reaction mechanism for CO₂ absorption by MDEA solution
Source: Schubert et al. (2001)

The reaction of CO₂ with AMP formed an unstable carbamate ion due to the structure of AMP induces the steric hindrance character which unfavourable for carbamate formation (Aroua et al., 2002). It was reported that CO₂ loading in 2.0 M AMP solution was higher than 2.0 M MDEA solution due to higher basicity of AMP compared to MDEA. Therefore, blended of MDEA with AMP was essential to improve the CO₂ absorption efficiency and capacity. Sterically hindered amine, AMP will directly react with CO₂ first (to form carbamate ion) and then faster transfer of CO₂ to MDEA. The reaction of MDEA with CO₂ was slow due to the lack of hydrogen atom in amino group. Therefore, the presence of AMP will accelerate the reaction of MDEA with CO₂. This mechanism shows how AMP overcome the limitation of MDEA by performing fast intermolecular interaction with CO₂. The mechanism of the chemical reaction of blended MDEA and AMP amines solution with CO₂ is shown in Equation (4.2) to (4.4) (Lu, Wang, Sun, Li, & Liu, 2005).



In blended amine, the presence of more nitrogen atom can increased CO₂ capture compared to single amine (Adeosun et al., 2013). Nitrogen atom in the molecule influences the attraction of CO₂ towards amine solvent. Intermolecular interaction of amino group with CO₂ reflects the reaction rates with CO₂. Most of the applications prefer to use blended alkanolamine because it gives good absorption performance than single alkanolamine solution (Lu et al., 2005).

4.5.2 Intermolecular Interaction for Blended MDEA/PZ

Another potential activator amine that can be used to improve the efficiency of MDEA in CO₂ absorption process is piperazine (PZ). Binary MDEA/PZ blended system consisted of 10 wt.% of PZ, 30 wt.% of MDEA, and 60 wt.% of H₂O was simulated. Meanwhile, 15 wt.% of PZ, 30 wt.% of MDEA, 50 wt.% of H₂O, and 10 wt.% of CO₂ for tertiary MDEA/PZ blended system was also simulated. For single MDEA and PZ, both amines were simulated at 30 wt.%. PZ as an activator was selected to blend with MDEA in order to enhance the strength of intermolecular interaction between amine-CO₂-H₂O systems.

4.5.2.1 Comparison of Single and Blended MDEA/PZ for Binary and Tertiary System

This part discusses the intermolecular interaction of single MDEA and PZ system and blended MDEA/PZ with water system. The intermolecular interaction with water was compared between binary system (absence of CO₂) and tertiary system (presence of CO₂). MDEA and PZ were tertiary and secondary amines, respectively. PZ is a cyclical amine which does not have hydroxyl group but consists of two nitrogen atoms in its molecular structure. PZ is a special molecule with a symmetrical diamine cyclical. The capabilities of PZ is already proven where many studies were done using PZ in CO₂ absorption process. The intermolecular interaction for CO₂ absorption was compared between activated MDEA and MDEA systems. Table 4.10 shows the RDF result for amine solution in binary system of MDEA, PZ, and MDEA/PZ solution.

HO_{mdea}: Hydrogen atom at oxygen in MDEA
O_{water}: Oxygen atom in water
N_{mdea}: Nitrogen atom in MDEA
H_{water}: Hydrogen atom in water
HO_{pz}: Hydrogen atom at oxygen in PZ
N_{pz}: Nitrogen atom in PZ

Table 4.10 Summary data of RDF result for binary system of MDEA and PZ, and blended MDEA/PZ system

	Binary			
	Homdea-Owater	Nmdea-Hwater	Hopz-Owater	Npz-Hwater
MDEA	1.75, 2.2293	4.75, 1.1107	-	-
PZ	-	-	-	5.75, 1.0255
MDEA+PZ	1.75, 1.6574	4.75, 1.1936	-	5.75, 1.0323

The main reason for performing this simulation was to investigate the distribution of MDEA and PZ in water. Table 4.10 shows the intermolecular interaction between single MDEA and PZ and blended MDEA/PZ with water without the CO₂. It is clearly seen that the intermolecular interaction of HO_{mdea}-O_{water} for single MDEA system was higher than the blended MDEA/PZ. At the same distance of 1.75 Å, the tendency for the interaction to happen for single MDEA and blended MDEA/PZ were $g(r) = 2.2293$ and 1.6574, respectively. It can be concluded that water had stronger intermolecular force of polar bond with HO_{mdea} in single MDEA compared to blended MDEA/PZ (34.51% increment), due to the MDEA structure that had two –OH bonds and it accelerated the intermolecular interaction with water. But in blended MDEA/PZ, the presence of PZ with lack of hydroxyl group affected the tendency of HO_{mdea} interaction with water. No hydrogen atom was directly connected to the nitrogen atom in the molecular structure, thus it cannot generate carbamate ions.

It contrary with amino group, the intermolecular interaction of N_{mdea}-H_{water} and N_{pz}-H_{water} in blended MDEA/PZ was higher compared to single MDEA and PZ. As depicted in Table 4.10, the $g(r)$ value of N_{mdea}-H_{water} for single MDEA system was 1.1107 and for blended MDEA/PZ was 1.1936 (7.46% increment), at the same distance of 4.75 Å. Whereas, $g(r)$ value of N_{pz}-H_{water} for single PZ system was 1.0255 and for blended MDEA/PZ was 1.0323 (0.66% increment), at the same distance of 5.75 Å. The presence of PZ in the solution enhanced the interaction of N_{mdea} with water.

Table 4.11 shows the RDF result for intermolecular interaction between single MDEA and PZ and blended MDEA/PZ in tertiary system with CO₂ in solution.

HO_{mdea}: Hydrogen atom at oxygen in MDEA

O_{water}: Oxygen atom in water

N_{mdea}: Nitrogen atom in MDEA

H_{water}: Hydrogen atom in water

HO_{pz}: Hydrogen atom at oxygen in PZ

N_{pz}: Nitrogen atom in PZ

Table 4.11 Summary data of RDF result for tertiary system of MDEA, PZ, and blended MDEA/PZ system

	Tertiary			
	Homdea-Owater	Nmdea-Hwater	Hopz-Owater	Npz-Hwater
MDEA	1.75, 2.6546	4.75, 1.2557	-	-
PZ	-	-	-	5.75, 1.0926
MDEA+PZ	1.75, 2.7057	4.75, 1.8805	-	5.75, 1.1562

Based on RDF results, in the presence of CO₂, MDEA and PZ solution had strong intermolecular interaction with water compared to MDEA and PZ solution alone (without CO₂ molecules). For example, at same distance of 1.75 Å, the tendency for the intermolecular interaction to occur on binary and tertiary systems of HO_{mdea}-O_{water} for blended MDEA/PZ were 1.6574 and 2.7057 (63.24% increase), respectively. The addition of small PZ was capable to increase the solubility of CO₂ in amine solution (Farmahini, 2010). The similar behaviour was observed for blended MDEA/AMP in previous discussion.

For tertiary system, both hydroxyl and amino groups of blended MDEA/PZ showed strong intermolecular interaction with water compared to single MDEA and PZ. For example, at a distance of 5.75 Å, the intermolecular interaction of amino group of PZ for blended MDEA/PZ and single PZ were 1.1562 and 1.0926 (5.82% increase), respectively. PZ was able to activate the reaction of MDEA with CO₂ (Adeosun et al., 2013). The presence of two nitrogen atoms in PZ increased the uptake of CO₂ to MDEA.

However, the strength of intermolecular interaction for N_{pz}-H_{water} was weaker than hydrogen bonding of HO_{mdea}-O_{water} and N_{mdea}-H_{water} where the result RDF was

1.0926 at a distance of 5.75 Å. PZ as aromatic amine has lone pair electrons which conjugated and shares an electron in the benzene rings. From this, the possibility to form hydrogen bonding was reduced that led to low solubility in water.

Based on the explanation, there was a good significant effect on the diffusion of amine in water with the addition of CO₂. Based on (Lu et al., 2005), blended MDEA/PZ shows good performance for CO₂ absorption compared to single MDEA solution up to 99%. This study also shows that the small quantity of PZ was capable to improve the mass transfer in membrane for CO₂ gas absorption process.

4.5.2.2 Comparison of Single and Blended MDEA/PZ for Intermolecular Interaction with CO₂ in Tertiary System

This sub-chapter explains how PZ molecule in MDEA solution influences the strength of MDEA-CO₂ bonding compared to single MDEA solution. Table 4.12 shows the graphical results for intermolecular interaction between amine and CO₂ for MDEA, PZ, and MDEA/PZ system.

O_{mdea}: Oxygen atom in MDEA
C_{co2}: Carbon atom in CO₂
N_{mdea}: Nitrogen atom in MDEA
O_{pz}: Oxygen atom in PZ
N_{pz}: Nitrogen atom in PZ

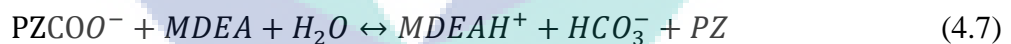
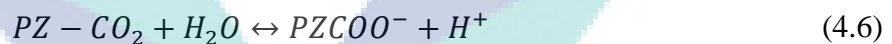
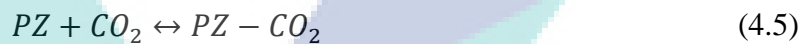
Table 4.12 Summary data of RDF result for reaction between amine with CO₂ on MDEA and PZ, and blended MDEA/PZ system

	Tertiary			
	O_{mdea}-C_{co2}	N_{mdea}-C_{co2}	O_{pz}-C_{co2}	N_{pz}-C_{co2}
MDEA	3.75, 1.1488	5.25, 1.5158	-	-
PZ	-	-	-	4.25, 1.0705
MDEA+PZ	3.75, 1.1883	5.25, 1.8766	-	4.25, 1.4911

The results for the study on tendency of CO₂ towards amine solution were displayed in Table 4.12. From the RDF result, the values of r and $g(r)$ for single MDEA system were (3.75, 1.1488) and (5.25, 1.5158) for O_{mdea}-C_{co2} and N_{mdea}-C_{co2}, respectively. The results show an increment after a small quantity of PZ was added into MDEA, which were (3.75, 1.1883) and (5.25, 1.8766) for O_{mdea}-C_{co2} and N_{mdea}-C_{co2}, respectively. Again,

the addition of PZ in MDEA solution could increase the strength of intermolecular interaction between MDEA and CO₂. The absorption of CO₂ by MDEA solution was more efficient by the additional chemical reaction of PZ (Lu et al., 2005). PZ as an activator was added to MDEA solution in order to accelerate the intermolecular interaction of MDEA with CO₂.

Based on Table 4.12, the distance for intermolecular interaction of N_{pz}-C_{co2} (4.25, 1.4911) was shorter than N_{mdea}-C_{co2} (5.25, 1.8766) because PZ was reacted first with CO₂. MDEA cannot react directly with CO₂ due to the lack of hydrogen atom at amino group. PZ was attracted and combined with CO₂ then transferred to MDEA rapidly (Lu et al., 2005). The reaction of PZ with CO₂ produced carbamate that subsequently reacted with MDEA to form bicarbonate. PZ was acted as a promoter to activate the MDEA to absorb CO₂. The reaction of CO₂ and PZ was in parallel with the reaction of CO₂ with MDEA in the condition of rapid pseudo-first-order reaction (Zhang et al., 2001). The properties of activator caused PZ to coalesce with CO₂ and rapidly transferred to MDEA. Due to rapid transfer of CO₂ to MDEA, the concentration of PZ did not depleted. Equation (4.5) to (4.7) describe the reaction mechanism involved in blended MDEA/PZ system (Lu et al., 2005). The reaction is also known as instantaneous zwitterion mechanism.



Previous studies were carried out to find the CO₂ absorption capacity (Adeosun et al., 2013). The findings show that 30 wt.% of PZ was the highest capacity up to 1.06 mole CO₂/mole amine compared to other amines such as MDEA. The molecular structure of PZ with two nitrogen atoms was expectedly doubled the CO₂ absorption capacity. Another study about membrane gas absorption (MGA) process using hollow fibre contactor, the average overall mass-transfer coefficient of blended MDEA/PZ was 2.25 times higher than single MDEA (Lu et al., 2005). PZ plays an important role for accelerating the absorption process of CO₂ in MDEA solution. Because PZ is a cyclic secondary diamine, its efficiency is attributed to its cyclic diamine structure that may favour rapid formation of carbamate with CO₂. As a mild base, it may serve to catalyse proton extractions in the reaction mechanism. Also, the molecule can theoretically absorb

2 moles of CO₂ for every 1 mole of amine (Cullinane & Rochelle, 2004). Moreover, Svensson et al. (2013) also stated that blended MDE/PZ required low the heat of absorption at regeneration phase. Due to this, interest in using hybrid solvents has increased to date.

4.6 Simulation Parameter 5: Comparison of Different Types of Carbamate Amine (Stripping Process)

The stripping process is the most costly section in the absorption process due to high temperature required to break a bond between amine-CO₂. The stripping process is also known as regeneration process. Regeneration is a process of removal of acid gases from the rich solvent phase after absorption process. The simulation was run based on intermolecular interactions between MEACOO⁻, AMPCOO⁻, and PZCOO⁻ with water to observe the tendency of CO₂ to react with water to form bicarbonate ions which represent the attraction force. Intramolecular interactions between N_{carbamate} and C_{carbamate} in MEA, AMP, and PZ which represent repulsion force was also studied. RDF analysis shows how inter/intramolecular interaction happen between atoms or molecules.

4.6.1 Intermolecular Interaction between Carbamate Ion with Water

In this part, the comparison between carbamate ion of conventional amine, MEA and activator amine, AMP and PZ was simulated to identify which amine solvent has strong intermolecular interaction with water where at this interaction bicarbonate ion form. The simulation results are presented in Table 4.13.

C_{carbamate}: Carbon atom in carbamate molecule

N_{carbamate}: Nitrogen atom in carbamate molecule

O_{water}: Oxygen atom in water

H_{water}: Hydrogen atom in water

Table 4.13 Intermolecular interaction between carbamate ion and water

	MEACOO	AMPCOO	PZCOO
C_{carbamate}-O_{water}	3.75, 1.1398	3.75, 1.3833	3.75, 1.1309
N_{carbamate}-H_{water}	3.75, 1.0068	5.75, 1.1036	5.25, 1.0593

Table 4.13 shows the RDF results for the intermolecular interaction between MEA, AMP, and PZ carbamate ions with water. As shown in Table 4.13, $C_{\text{carbamate-O}_{\text{water}}}$ has high peak attractive interaction compared to $N_{\text{carbamate-H}_{\text{water}}}$. For example, MEACOO has the first peak at 3.75 Å with a value of 1.1398 implying that it was almost 13.21% tendency to find pair of atoms to make interaction for $C_{\text{carbamate-O}_{\text{water}}}$ compared to 1.0068 for $N_{\text{carbamate-H}_{\text{water}}}$. An AMP molecule, $C_{\text{carbamate-O}_{\text{water}}}$ has short distance to make first peak interaction within 3.75 Å, while $N_{\text{carbamate-H}_{\text{water}}}$ has interaction at a distance of 5.75 Å. The intermolecular interaction between $C_{\text{carbamate-O}_{\text{water}}}$ was also higher because ionic carbamate tended to react with water to form bicarbonate and recycled amine. This interaction is also known as ion dipole bonding. Besides that, the interaction between $N_{\text{carbamate-H}_{\text{water}}}$ was lower because it only formed hydrogen bonding. It is in agreement with the fact that the ion dipole bonding is stronger than hydrogen bonding. According to Hunt et al. (2015), the hydrogen bonding only involves the partial charges of the molecules while the ion dipole bonding involves a full charged ion and partial charge of the dipole molecule. In the hydrogen bond, there are ionic and covalent bonds. The movement of charge from ion dipole bonding will form a hydrogen bond. On the other hand, the water molecule is not linear and the centre of the positive charges does not coincide with the centre of the negative charges. Hence, it is a polar molecule (a dipole) that makes the carbamate ion tend to form ion dipole bonding with water.

Figure 4.6 illustrates the mechanism for intermolecular interaction between carbamate ions and water in MEA solvent to separate the CO_2 molecules from amine compound.

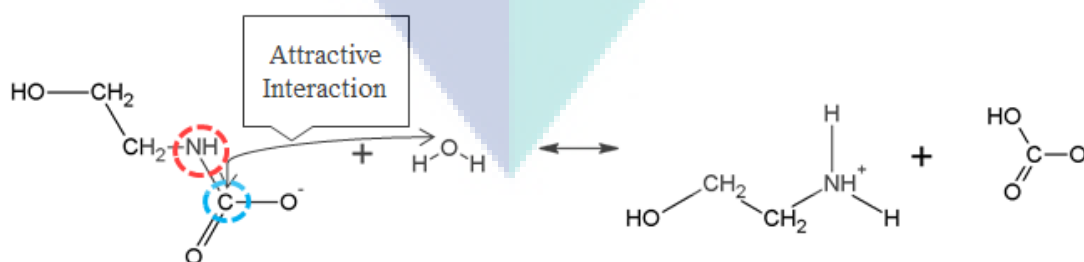


Figure 4.6 Example mechanism for interaction between carbamate ions with water in MEA solvent. $N_{\text{carbamate}}$ and $C_{\text{carbamate}}$ are red circle and blue circle, respectively.

Comparison between MEA, AMP, and PZ for $C_{\text{carbamate-O}_{\text{water}}}$ shows that AMP has the highest intermolecular interaction with water. At a distance of 3.75 Å, the chances

of finding pair of atoms were 1.3833, 1.1398, and 1.1309 for AMP, MEA, and PZ, respectively. It shows that about 22.32% chances to interaction happen on AMP compared PZ. It is expected due to the steric hindrance properties of AMP that affect the carbamate stability of AMP.

On the contrary, comparison between MEA, AMP, and PZ for $N_{\text{carbamate}}-O_{\text{water}}$ shows that MEA has the highest intermolecular interaction with water. Within short distance ($r = 3.75 \text{ \AA}$), there is a peak of interaction compared to others at 5 \AA and above. The values of r and $g(r)$ for MEACOO, AMPCOO, and PZCOO were (3.75, 1.0068), (5.75, 1.1036), and (5.25, 1.0593), respectively. Based on RDF results, water had more tendency to interact intermolecular with MEA. But the main interaction to focus is the intramolecular interaction of $N_{\text{carbamate}}-C_{\text{carbamate}}$ due to the high energy requirement to break bond at carbamate ions during the stripping process.

4.6.2 Intramolecular Interaction between C-Carbamate and N-Carbamate

The strength of the intramolecular interaction between $C_{\text{carbamate}}$ and $N_{\text{carbamate}}$ is discussed in this subsection. Table 4.14 shows graphical for intramolecular interaction between carbamate ions and CO_2 .

$N_{\text{carbamate}}$: Nitrogen atom in carbamate molecule

$C_{\text{carbamate}}$: Carbon atom in carbamate molecule

Table 4.14 Intramolecular interaction between carbamate ions and COO

	$N_{\text{carbamate}}-C_{\text{carbamate}}$
MEA	1.25, 20.0273
AMP	1.25, 36.5978
PZ	1.25, 42.6252

Table 4.14 shows the intramolecular interaction between three amines and COO . PZ has the strongest repulsive interaction compared to MEA and AMP. It shows that 212.84% strength of repulsive interaction from PZ compared to MEA. This is because PZ forms bicarbonate ions. Thus breaking C–O bonds requires less energy in bicarbonate and carbonate breakdown than that required for breaking C–N bonds in carbamate breakdown (Kim et al., 2011). The application of PZ and AMP in amine-based absorption

process is a good choice because the tendency to interact with water to form protonated amine and breaking bond within covalent bond of N-C were higher compared to primary amine, MEA. When there was high tendency for intramolecular interaction, it required a minimum heat to break the bond. It is in agreement with the fact that the application of AMP and PZ can lower down the heat duty for amine solvent regeneration in CO₂ capture process (Zhang et al., 2016).

With reference to the repulsive interaction in MEA, carbamate ions of high stability were produced that caused difficulty in breaking the bond. It is reported that MEA was good in absorption but showed limitation in the stripping process (Damartzis et al., 2015). According to Damartzis et al. (2015), MEA have advantage with high reactivity with CO₂ while the disadvantage is required high heat demand for regeneration process. The heat duty of solvent regeneration is controlled mainly from the reactions as described in Eqs. (2), (3), and (4) because these reactions are highly endothermic, which according to (Caplow, 1968). Hydrogen ion was used to catalyze the decarboxylation of carbamate. In a rapid equilibrium, proton transfer happen from water. The extend study has been studied by (Shi et al., 2014), where there are an endothermic proton transfer to proton acceptor (HCO₃⁻, H₂O) from a proton donor (MEA^{H+}). The reactions mechanism proposed for the primary amine can be explained as follows:

Zwitterion formation for MEA:



Carbamate formation from MEA zwitterion:



Dissociation of protonated amine:



Based on Table 4.14, less efficiency of MEA in stripping process shows that it has to be blended with activator amine in order to reduce the stability of carbamate bond and minimise the energy consumption. AMP and PZ produce bicarbonate ions in an amine solution during CO₂ absorption, resulting in an easy bicarbonate breakdown and low energy requirement to release CO₂ compared to MEA.

The peak shown by the repulsive interaction was different from the attractive interaction. Repulsive interaction has only one peak and no peak is observed in the rest of the process. This is because the repulsive interaction occurs in a short time. The factor influences the repulsive interaction is the strength of N-C bond. If the stability of N-C bond is as high as carbamate ion, it requires high heat to force the repulsive interaction to happen. The intramolecular interaction (strong bonding) involves the covalent bond, metallic bond, and ionic bond. The intermolecular interaction (weak bonding) involves the van der Waals' forces, hydrogen bond, and non-covalent bond. Intramolecular interaction requires more energy for the repulsion force to happen compared to the intermolecular interaction (Kirchner et. al., 2012).

Figure 4.7 shows the repulsive interaction between carbamate ions in MEA solvent. Bond between -NH and C needs to be broken to allow CO₂ to react with water to form bicarbonate ion.

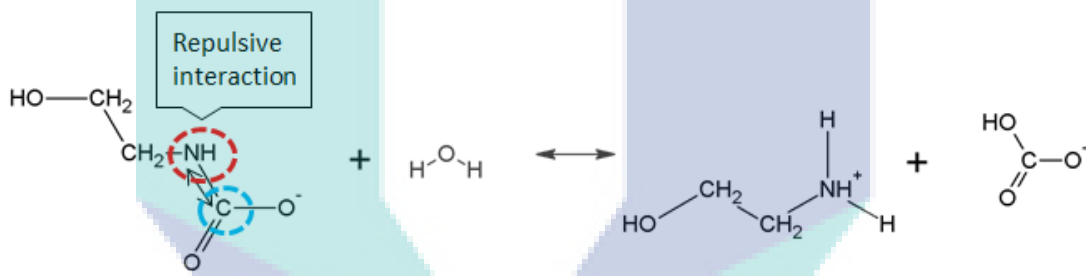


Figure 4.7 Mechanism for intramolecular interaction between carbamate ions in MEA solvent

CHAPTER 5

CONCLUSIONS AND RECOMMENDATIONS

5.1 Conclusions

The study on molecular interaction establishment of CO₂ capture by amine-based absorption using molecular dynamic simulation can be concluded as:

- (a) RDF analysis was done to analyse the effect of temperature on intermolecular interaction of monoethanolamine absorption process for CO₂ removal using molecular dynamic simulation. Strong intermolecular interaction of MEA-H₂O and MEA-CO₂ were observed as the temperature of the system was increased. A temperature of 313 K was used in the simulation case studies because it is reported that a zwitterion mechanism for reaction of CO₂ with the amine to form carbamate occurs at this temperature (D'Alessandro et al., 2010). Nmea-Cco₂ bond showed higher tendency to make intermolecular interaction compared to Omea-Cco₂ for tertiary system. This results support the reaction mechanism proposed by Hwang (2014). CO₂ was directly bound with N atom of MEA via zwitterion pathway to absorb CO₂ and formed carbamate ions (Hwang et al., 2015).
- (b) Intermolecular interaction of MEA-H₂O and MEA-CO₂ was increased with the increased of amine concentration. Higher amine concentration caused a strong base to react with CO₂ to generate carbamate amine ($[BH]^+[R_2NCOO]^-$). Amine concentration of 30 wt.% was selected for the simulation work due to the possibility of corrosion problem at higher amine concentration (Lunsford & Bullin, 2006).

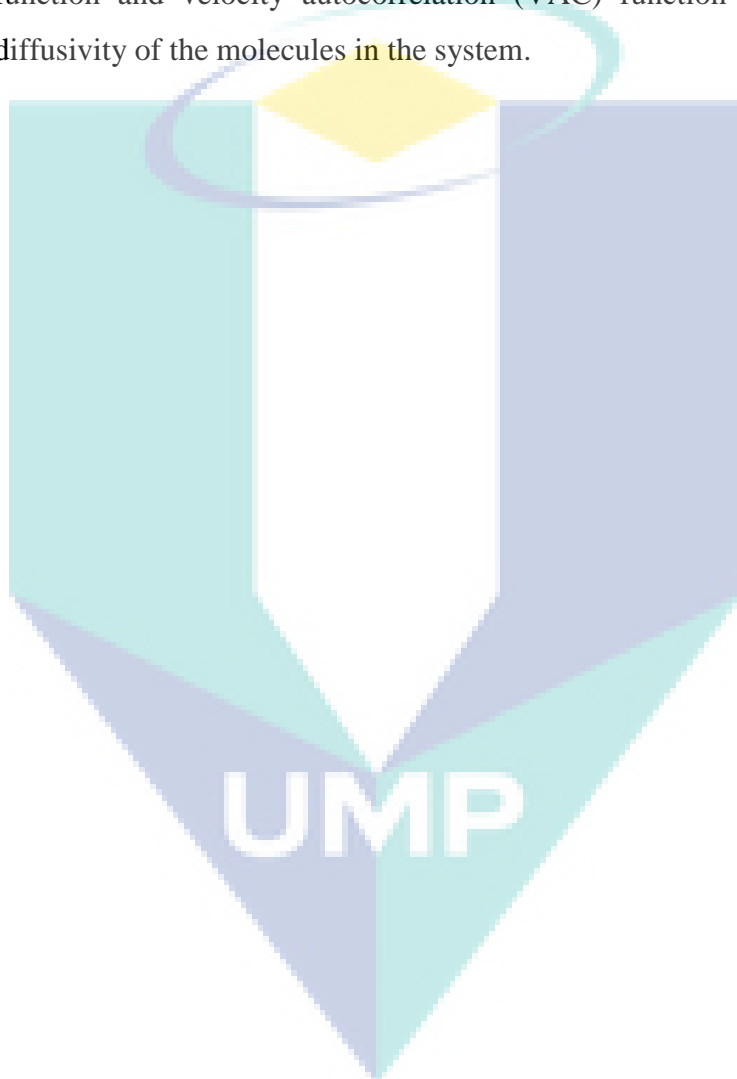
- (c) Five amines were compared, i.e., MEA, DEA, MDEA, AMP, and PZ. MEA showed the strongest intermolecular interaction with CO₂. Due to this, MEA easily absorb CO₂ compared to secondary and tertiary amines. It was also observed that MDEA had low tendency to create the intermolecular interaction with CO₂. Moreover, the good interaction of steric hinder amine, AMP, and cyclic amine, PZ, with CO₂, was expected to activate the reactivity of MDEA absorption process.
- (d) Blended MDEA/AMP and MDEA/PZ showed strong intermolecular interactions with CO₂ compared to pure MDEA system. The presence of activator amine, AMP and PZ, improved the intermolecular interaction of MDEA with CO₂.
- (e) For stripping process, AMP and PZ carbamate amines showed strong inter and intramolecular interaction compared to MEA carbamate. AMP and PZ were capable to break a bond in carbamate molecule and easily removed CO₂ compared to MEA carbamate. It was also proven that MEA was good in absorption but has limitation in stripping process because the repulsive interaction in MEA carbamate was low.

5.2 Recommendations

It is clear that molecular dynamic simulation was useful to identify the process operating conditions such as temperature, concentration, and types of amine molecular that affected the intermolecular interaction and hence influence the CO₂ absorption process. Based on the study conducted, some recommendations are given for future work:

- (a) Study must be conducted in a longer time to get better results (above 1 ns). The simulation can calculate the intermolecular interaction between molecules and behaviour of molecules with more accurate, efficient and comprehensive with in the longer time. This work used Material Studio version of 7.0. Due to the limited time and computer resources, there were limitation to simulate in longer time. The used of latest version Material Studio software is recommended for future work.

- (b) It is also recommend to study the chemistry of the desorption process, i.e., the breaking bond between carbamate amine formed to remove CO₂. It helps to improve the efficiency of desorption process and hence to reduce cost of energy in the industries.
- (c) Other types of analysis also can be run to valid the computational work with experimental work in literature such as mean square displacement (MSD) function and velocity autocorrelation (VAC) function that calculate the diffusivity of the molecules in the system.



REFERENCES

- Aaron, D., & Tsouris, C. (2005). Separation of CO₂ from Flue Gas: A Review. *Separation Science and Technology*, 40(1–3), 321–348.
- Abdul Halim, H. N., M. Shariff, A., Tan, L. S., & Bustam, M. a. (2015). Mass Transfer Performance of CO₂ Absorption from Natural Gas using Monoethanolamine (MEA) in High Pressure Operations. *Industrial & Engineering Chemistry Research*, 54(5), 1675–1680.
- Abharchaei, P. R. (2010). Kinetic study of carbon dioxide absorption by aqueous solutions of 2 (methyl)-aminoethanol in stirred tank reactor. Chalmers University of Technology.
- Accelrys. (2014). Accelrys materials studio. San Diego, California: Accelrys Inc.
- Adams, R., Williams, H., & Rory Adams, H. W. (2011). Intermolecular Forces. Retrieved from http://cnx.org/contents/da66d6a7-9cf7-46a7-ac14db65fe0126b4@2/Intermolecular_Forces
- Adcock, S. a, & McCammon, J. A. (2006). Molecular Dynamics: Survey of Methods for Simulating the Activity of Proteins. *Chemical Reviews*, 106(5), 1589–1615.
- Adeosun, A., Hadri, N. El, Goetheer, E., & Abu-, M. R. M. (2013). Absorption of CO₂ by Amine Blends Solution : An Experimental Evaluation. *International Journal Of Engineering And Science*, 3(9), 12–23.
- Allen, M. P. (2004). Introduction to Molecular Dynamics Simulation. *Computational Soft Matter: From Synthetic Polymers to Proteins*, 23, 1–28.
- AMP Properties. (2000). Retrieved from <http://www.dow.com/scripts/litorder.asp?filepath=angus/pdfs/noreg/319-00016.pdf>
- Arapatsakos, C., Karkanis, A., Strofylla, S. M., Engineering, M., & Street, V. S. (2012). The effect of temperature on gas emissions. *International Journal of Recent Research and Applied Studies*, 11(April), 89–100.
- Aroonwilas, A., & Veawab, A. (2004). Characterization and Comparison of the CO₂ Absorption Performance into Single and Blended Alkanolamines in a Packed Column. *Industrial & Engineering Chemistry Research*, 43(9), 2228–2237.

- Aroua, M. K., Ramasamy, K., Haji-Sulaiman, M. Z., & Ramasamy, K. (2002). Modelling of carbon dioxide absorption in aqueous solutions of AMP and MDEA and their blends using Aspenplus. *Separation and Purification Technology*, 29, 153–162.
- Babu, P., Kumar, R., & Linga, P. (2013). Pre-combustion capture of carbon dioxide in a fixed bed reactor using the clathrate hydrate process. *Energy*, 50(1), 364–373.
- Bajer, C. (2002). Time integration methods, 1(Theoretical Foundations of Civil Engineering), 45–54.
- Baker, R. W. (2002). Future Directions of Membrane Gas Separation Technology. *Industrial & Engineering Chemistry Research*, 41(6), 1393–1411.
- Bansal, M., & M., B. (2011). Elementary introduction to Molecular Mechanics and Dynamics. Retrieved from https://www.google.com/url?sa=t&rct=j&q=&esrc=s&source=web&cd=1&cad=rja&uact=8&ved=0ahUKEwiW343Yk7_NAhUBQI8KHR2uDQ8QFgghMAA&url=http://www.tau.ac.il/~ephraim/MM+MD.doc&usg=AFQjCNEWMb11Xpeh_xBH2enDZFlcLwTtMg&sig2=EX9h6YvCptjMQztM4kCIqQ&bvm=bv.125221236,d.c
- Barker, T. (2007). *Climate Change 2007 : Synthesis Report*. Valencia, Spain.
- Barzagli, F., Mani, F., & Peruzzini, M. (2010). Continuous cycles of CO₂ absorption and amine regeneration with aqueous alkanolamines: a comparison of the efficiency between pure and blended DEA, MDEA and AMP solutions by ¹³C NMR spectroscopy. *Energy & Environmental Science*, 3(6), 772.
- Bavbek, O. (1999). Reaction Mechanism and Kinetics of Aqueous Solutions of Primary and Secondary Alkanolamines. *Turkish Journal of Chemistry*, 23(3), 293–300.
- Berendsen, H.J.C., van Gunsteren, W.F., Egberts, E. & de Vlieg, J. (1987). Supercomputer Research in Chemistry and Chemical Engineering, Chapter 7: dynamic simulation of complex molecular system. (K. F. Jensen & D. G. Truhlar, Eds.) (Vol. 353). Washington, D.C.: American Chemical Society.
- Bishnoi, S., & Rochelle, G. T. (2000). Absorption of carbon dioxide into aqueous piperazine: reaction kinetics, mass transfer and solubility. *Chemical Engineering Science*, 55(22), 5531–5543.
- Bougie, F., & Iliuta, M. C. (2012). Sterically Hindered Amine-Based Absorbents for the Removal of CO₂ from Gas Streams. *Journal of Chemical & Engineering Data*, 57(3), 635–669.

- Brennen, G., Deutsch, I., & Jessen, P. (2000). Entangling dipole-dipole interactions for quantum logic with neutral atoms. *Physical Review A*, 61(6), 61–71.
- Brian Fisher, N. N. (2007). Issues related to mitigation in the long-term context. (M. B. (Kuwait) John Weyant (USA), Ed.). Geneva 2, Switzerland: Intergovernmental Panel on Climate Change (IPCC).
- Brittain, C. G., & G., B. C. (2007). *One Page Lesson : Intermolecular Attractive Forces*.
- Brown, T. L., & Lemay, H. E. (2001). Intermolecular Forces , Liquids , and Solids States of Matter. *Chemistry, The Central Science, Chapter 11*(10th edition), 1–107.
- C. David Sherrill, Sherrill, C. D., C. David Sherrill, & Sherrill, C. D. (2001). *Molecular Mechanics*. Georgia Institute of Technology.
- Caplow, M. (1968). Kinetics of carbamate formation and breakdown. *Journal of the American Chemical Society*, 90(24), 6795–6803.
- Charless E. Ophardt. (2003). *Intermolecular forces*. Elmhurst College.
- Charpentier, J. (2002). The triplet “molecular processes–product–process” engineering: the future of chemical engineering? *Chemical Engineering Science*, 57(22–23), 4667–4690.
- Chemspider. (2016). ChemSpider Database. Retrieved November 22, 2016, from <http://www.chemspider.com/>
- Chen, L., Yong, S. Z., & Ghoniem, A. F. (2012). Oxy-fuel combustion of pulverized coal: Characterization, fundamentals, stabilization and CFD modeling. *Progress in Energy and Combustion Science*, 38(2), 156–214.
- Choi, W. J., Seo, J. B., Jang, S. Y., Jung, J. H., & Oh, K. J. (2009). Removal characteristics of CO₂ using aqueous MEA/AMP solutions in the absorption and regeneration process. *Journal of Environmental Sciences*, 21(7), 907–913.
- Chung, J., & Hulbert, G. M. (1994). A family of single-step Houbolt time integration algorithms for structural dynamics. *Computer Methods in Applied Mechanics and Engineering*, 118(1–2), 1–11.

- Conway, W., Bruggink, S., Beyad, Y., Luo, W., Melián-Cabrera, I., Puxty, G., & Feron, P. (2015). CO₂ absorption into aqueous amine blended solutions containing monoethanolamine (MEA), N,N-dimethylethanolamine (DMEA), N,N-diethylethanolamine (DEEA) and 2-amino-2-methyl-1-propanol (AMP) for post-combustion capture processes. *Chemical Engineering Science*, 126, 446–454.
- Crooks, J. E., & Donnellan, J. P. (1989). Kinetics and mechanism of the reaction between carbon dioxide and amines in aqueous solution. *Journal of the Chemical Society, Perkin Transactions 2*, 2(4), 331.
- Cullinane, J. T., & Rochelle, G. T. (2004). Carbon dioxide absorption with aqueous potassium carbonate promoted by piperazine. *Chemical Engineering Science*, 59(17), 3619–3630.
- D'Alessandro, D. M., Smit, B., & Long, J. R. (2010). Carbon dioxide capture: Prospects for new materials. *Angewandte Chemie-International Edition*, 49(35), 6058–6082.
- da Silva, E. F., Kuznetsova, T., Kvamme, B., & Merz, K. M. (2007). Molecular dynamics study of ethanolamine as a pure liquid and in aqueous solution. *The Journal of Physical Chemistry. B*, 111(14), 3695–703.
- Damartzis, T., Papadopoulos, A. I., & Seferlis, P. (2015). Process flowsheet design optimization for various amine-based solvents in post-combustion CO₂ capture plants. *Journal of Cleaner Production*, 111, 204–216.
- Danckwerts, P. V. (1979). The reaction of CO₂ with ethanolamines. *Chemical Engineering Science*, 34(4), 443–446.
- Davis, J. D. (2009). *Thermal Degradation of Aqueous Amines Used for Carbon Dioxide Capture*. The University of Texas at Austin.
- Derks, P. W. J., & Versteeg, G. F. (2009). Kinetics of absorption of carbon dioxide in aqueous ammonia solutions. *Energy Procedia*, 1(1), 1139–1146.
- Desideri, U., & Paolucci, A. (1999). Performance modelling of a carbon dioxide removal system for power plants. *Energy Conversion and Management*, 40(18), 1899–1915.
- Dinca, C. (2015). Critical parametric study of circulating fluidized bed combustion with CO₂ chemical absorption process using different aqueous alkanolamines. *Journal of Cleaner Production*, 2, 1–14.
- Donaldson, T. L., & Nguyen, Y. N. (1980). Carbon Dioxide Reaction Kinetics and

- Transport in Aqueous Amine Membranes. *Industrial & Engineering Chemistry Fundamentals*, 19(3), 260–266.
- Dubois, L., Kahasha Mbasha, P., & Thomas, D. (2010). CO₂ Absorption into Aqueous Solutions of a Polyamine (PZEA), a Sterically Hindered Amine (AMP), and their Blends. *Chemical Engineering & Technology*, 33(3), 461–467.
- Dubois, L., & Thomas, D. (2011). Carbon dioxide absorption into aqueous amine based solvents: Modeling and absorption tests. *Energy Procedia*, 4, 1353–1360.
- Dubois, L., & Thomas, D. (2012). Screening of Aqueous Amine-Based Solvents for Postcombustion CO₂ Capture by Chemical Absorption. *Chemical Engineering and Technology*, 35(3), 513–524.
- Dugas, R., & Rochelle, G. (2009). Absorption and desorption rates of carbon dioxide with monoethanolamine and piperazine. *Energy Procedia*, 1(1), 1163–1169.
- Ebner, A. D., & Ritter, J. a. (2009). State-of-the-art Adsorption and Membrane Separation Processes for Carbon Dioxide Production from Carbon Dioxide Emitting Industries. *Separation Science and Technology* (Vol. 44).
- Edali, M., Idem, R., & Aboudheir, A. (2010). 1D and 2D absorption-rate/kinetic modeling and simulation of carbon dioxide absorption into mixed aqueous solutions of MDEA and PZ in a laminar jet apparatus. *International Journal of Greenhouse Gas Control*, 4(2), 143–151.
- Emmanuelle Masy. (2013). Predicting the Diffusivity of CO₂ in Substituted Amines. Delft University of Technology.
- Energy, T. S. (2013). Annual Report 2013. Gansu Province, China. Retrieved from http://www.trinasolar.com/HtmlData/downloads/us/TrinaSolar_Annual_Report.pdf
- Essmann, U., Perera, L., Berkowitz, M. L., Darden, T., Lee, H., & Pedersen, L. G. (1995). A smooth particle mesh Ewald method. *The Journal of Chemical Physics*, 103(19), 8577.
- Eswaran, S., Adhikari, A. V., Chowdhury, I. H., Pal, N. K., & Thomas, K. D. (2010). New quinoline derivatives: synthesis and investigation of antibacterial and antituberculosis properties. *European Journal of Medicinal Chemistry*, 45(8), 3374–83.

- Farmahini, A. H. (2010). Molecular Dynamics Simulation Studies of Piperazine Activated MDEA Absorption Solution with Methane and Carbon Dioxide. University of Bergen Norway.
- Farmahini, A. H., Kvamme, B., & Kuznetsova, T. (2011). Molecular dynamics simulation studies of absorption in piperazine activated MDEA solution. *Physical Chemistry Chemical Physics : PCCP*, 13, 13070–13081.
- Fauth, D. J., Frommell, E. a., Hoffman, J. S., Reasbeck, R. P., & Pennline, H. W. (2005). Eutectic salt promoted lithium zirconate: Novel high temperature sorbent for CO₂ capture. *Fuel Processing Technology*, 86(14–15), 1503–1521.
- Folger, P. (2013). Carbon Capture : A Technology Assessment. Congressional Research Service. United States of America.
- Fryda, L., Sobrino, C., Cieplik, M., & Van De Kamp, W. L. (2010). Study on ash deposition under oxyfuel combustion of coal/biomass blends. *Fuel*, 89(8), 1889–1902.
- Gangarapu, S., Marcelis, A. T. M., & Zuilhof, H. (2013). Carbamate Stabilities of Sterically Hindered Amines from Quantum Chemical Methods: Relevance for CO₂ Capture. *ChemPhysChem*, 14(17), 3936–3943.
- García-Abuín, A., Gómez-Díaz, D., Navaza, J. M., & Vidal-Tato, I. (2011). Kinetics of carbon dioxide chemical absorption into cyclic amines solutions. *AIChE Journal*, 57(8), 2244–2250.
- Glarborg, P., & Bentzen, L. (2007). Chemical effects of a high CO₂ concentration in oxy-fuel combustion of methane. *Energy & Fuels*, (20), 291–296.
- Goff, G. S., & Rochelle, G. T. (2004). Monoethanolamine Degradation: O₂ Mass Transfer Effects under CO₂ Capture Conditions. *Industrial & Engineering Chemistry Research*, 43, 6400–6408.
- González, M. A. (2011). Force fields and molecular dynamics simulations. *Collection SFN*, 12, 169–200.
- Griebel, M., & Hamaekers, J. (2005). Molecular Dynamics Simulations of the Mechanical Properties of Polyethylene-Carbon Nanotube Composites. Germany.
- Gutowski, K. E., & Maginn, E. J. (2008). Amine-functionalized task-specific ionic liquids: A mechanistic explanation for the dramatic increase in viscosity upon

- complexation with CO₂ from molecular simulation. *Journal of the American Chemical Society*, 130(44), 14690–14704.
- Harun, N., Nittaya, T., Douglas, P. L., Croiset, E., & Ricardez-Sandoval, L. a. (2012). Dynamic simulation of MEA absorption process for CO₂ capture from power plants. *International Journal of Greenhouse Gas Control*, 10, 295–309.
- Hehre, W. J. (2003). *A Guide to Molecular Mechanics and Quantum Chemical Calculations*. United States of America.
- Herzog, H. (1999). An Introduction to CO₂ Separation and Capture Technologies. *Second Dixy Lee Ray Memorial Symposium*, 1–8.
- Hilber, H. M., Hughes, T. J. R., & Taylor, R. L. (1977). Improved numerical dissipation for time integration algorithms in structural dynamics. *Earthquake Engineering & Structural Dynamics*, 5(3), 283–292.
- Hook, R. J. (1997). An Investigation of Some Sterically Hindered Amines as Potential Carbon Dioxide Scrubbing Compounds. *Industrial & Engineering Chemistry Research*, 36(5), 1779–1790.
- Hunt, P. A., Ashworth, C. R., & Matthews, R. P. (2015). Hydrogen bonding in ionic liquids. *Chem. Soc. Rev.*, 44(5), 1257–1288.
- Hwang, G. S., Stowe, H. M., Paek, E., & Manogaran, D. (2015). Reaction mechanisms of aqueous monoethanolamine with carbon dioxide: a combined quantum chemical and molecular dynamics study. *Phys. Chem. Chem. Phys.*, 17(2), 831–839.
- Idem, R., Edali, M., & Aboudheir, A. (2009). Kinetics, modeling, and simulation of the experimental kinetics data of carbon dioxide absorption into mixed aqueous solutions of MDEA and PZ using laminar jet apparatus with a numerically solved absorption-rate/kinetic model. *Energy Procedia*, 1(1), 1343–1350.
- Idris, Z., & Eimer, D. a. (2014). Representation of CO₂ Absorption in Sterically Hindered Amines. *Energy Procedia*, 51(1876), 247–252.
- IEA. (2015). CO₂ emissions from fuel combustion: highlights. International Energy Agency. France.
- International Transport Forum. (2010). Reducing transport greenhouse gas emissions. Leipzig, Germany.

- Istadi. (2007). Intermolecular Forces : Polarity of Molecules Types of Intermolecular Forces.
- J. Israelachvili, & J., I. (1992). Chemical Bonds and Intermolecular Interactions. *Intermolecular and Surface Forces*, 1–19.
- James T. Yeh and Henry W. Pennline. (2004). Aqua ammonia process for simultaneous removal of CO₂ , SO₂ and NO. *International Journal Environmental Technology and Management*, 4(1/2), 89–104.
- Jean M. (2015). Practical Aspects of Molecular Dynamics Simulations. *Chemistry*, (2), 1–4.
- Jim Clark. (2012). Metallic bonding.
- Jos G. J. Olivier, Greet Janssens-Maenhout, Marilena Muntean, J. A. H. W. P. (2013). Trends in global CO₂ emissions 2013 report. The Netherlands: PBL Netherlands Environmental Assessment Agency, Joint Research Centre.
- Kachko, A., van der Ham, L. V., Bakker, D. E., van de Runstraat, A., Nienoord, M., Vlugt, T. J. H., & Goetheer, E. L. V. (2016). In-Line Monitoring of the CO₂ , MDEA, and PZ Concentrations in the Liquid Phase during High Pressure CO₂ Absorption. *Industrial & Engineering Chemistry Research*, 55(13), 3804–3812.
- Kallevik, O. B. (2010). Cost estimation of CO₂ removal in HYSYS. Telemark University College.
- Kanniche, M., Gros-Bonnivard, R., Jaud, P., Valle-Marcos, J., Amann, J. M., & Bouallou, C. (2010). Pre-combustion, post-combustion and oxy-combustion in thermal power plant for CO₂ capture. *Applied Thermal Engineering*, 30(1), 53–62.
- Keskes, E., Adjiman, C., Galindo, A., & Jackson, G. (2006). A Physical Absorption Process for the Capture of CO₂ from CO₂-Rich Natural Gas Streams. *Chemical Engineering Department, Imperial College London*. Retrieved from <http://www.geos.ed.ac.uk/ccs/Publications/Keskes.pdf>
- Kim, D. Y., Lee, H. M., Min, S. K., Cho, Y., Hwang, I.-C., Han, K., Kim, K. S. (2011). CO₂ Capturing Mechanism in Aqueous Ammonia: NH₃-Driven Decomposition–Recombination Pathway. *The Journal of Physical Chemistry Letters*, 2(7), 689–694.
- Kim, S. M., Lee, J. D., Lee, H. J., Lee, E. K., & Kim, Y. (2011). Gas hydrate formation

- method to capture the carbon dioxide for pre-combustion process in IGCC plant. *International Journal of Hydrogen Energy*, 36(1), 1115–1121.
- Kim, W. K., Woo, K. K., & Kim, W. K. (2009). Accelerated Molecular Dynamics Simulations of Atomic Force Microscope Experiments. University of Michigan.
- Kim, Y. E., Lim, J. A., Jeong, S. K., Yoon, Y. Il, Bae, S. T., & Nam, S. C. (2013). Comparison of Carbon Dioxide Absorption in Aqueous MEA, DEA, TEA, and AMP Solutions. *Bulletin of the Korean Chemical Society*, 34(3), 783–787.
- Kirchner, B., Vrabec, J., & Abrol, R. (2012). Multiscale molecular methods in applied chemistry (Topics in current chemistry, 307). *Top. Curr. Chem.* (Vol. 307).
- Kohl, A. L., & Nielsen, R. B. (1997). *Gas Purification* (Firth Edit). Houston, Texas: Gulf Publishing Company, Houston, Texas.
- Kothandaraman, A. (2010). Carbon Dioxide Capture by Chemical Absorption : A Solvent Comparison Study. Carbon. Massachusetts Institute of Technology. Retrieved from http://sequestration.mit.edu/pdf/Anusha_Kothandaraman_thesis_June2010.pdf
- Lawal, M. W. A., Stephenson, P., Sidders, J., Ramshaw, C., & Yeung, H. (2011). Post-combustion CO₂ Capture with Chemical Absorption : A State-of-the-art Review. *Chemical Engineering Research and Design*, 89(9), 1609–1624.
- Lee, A. S., Eslick, J. C., Miller, D. C., & Kitchin, J. R. (2013). Comparisons of amine solvents for post-combustion CO₂ capture: A multi-objective analysis approach. *International Journal of Greenhouse Gas Control*, 18, 68–74.
- Lee, H. J., Lee, J. D., Linga, P., Englezos, P., Kim, Y. S., Lee, M. S., & Kim, Y. Do. (2010). Gas hydrate formation process for pre-combustion capture of carbon dioxide. *Energy*, 35(6), 2729–2733.
- Lee, L.-H. (1991). Fundamentals of Adhesion. (L.-H. Lee, Ed.), *Igarss 2014*. Boston, MA: Springer US.
- Lewars, E. G. (2010). *Computational Chemistry: Introduction to the Theory and Applications of Molecular and Quantum Mechanics (Second)*. United States of America: Springer Science & Business Media.

- Li, B., Sheng, X., Xing, W., Dong, G., Liu, Y., Zhang, C., Qin, Z. (2010). Molecular Dynamic Simulation on the Absorbing Process of Isolating and Coating of α -olefin Drag Reducing Polymer. *Chinese Journal of Chemical Physics*, 23(6), 630–636.
- Li, J.-R., Ma, Y., McCarthy, M. C., Sculley, J., Yu, J., Jeong, H.-K., Zhou, H.-C. (2011). Carbon dioxide capture-related gas adsorption and separation in metal-organic frameworks. *Coordination Chemistry Reviews*, 255(15–16), 1791–1823.
- Liang, Y. (2003). Carbon Dioxide Capture From Flue Gas Using Regenerable Sodium-Based Sorbents. Tsinghua University.
- López, a. B., La Rubia, M. D., Navaza, J. M., Pacheco, R., & Gómez-Díaz, D. (2015). Characterization of MIPA and DIPA aqueous solutions in relation to absorption, speciation and degradation. *Journal of Industrial and Engineering Chemistry*, 21, 428–435.
- Lu, J., Wang, L., Sun, X., Li, J., & Liu, X. (2005). Absorption of CO₂ into aqueous solutions of methyldiethanolamine and activated methyldiethanolamine from a gas mixture in a hollow fiber contactor. *Industrial and Engineering Chemistry Research*, 44(24), 9230–9238.
- Lucas, T. R., Bauer, B. a, & Patel, S. (2012). Charge equilibration force fields for molecular dynamics simulations of lipids, bilayers, and integral membrane protein systems. *Biochimica et Biophysica Acta*, 1818(2), 318–29.
- Lunsford, K. M., & Bullin, J. A. (2006). Optimization of Amine Sweetening Units. In *Bryan Research & Engineering, Inc*, 1996 (pp. 1–14). New York, American: AIChE Spring National Meeting.
- M. P. Allen and D. J. Tildesley. (1991). *Computer Simulation of Liquids* (Reprint ed). United States of America: Oxford University Press.
- M.R. Roussel. (2012). Intermolecular forces, (Chemistry 1000 Lecture 15), 1–19.
- MacDowell, N., Florin, N., Buchard, A., Hallett, J., Galindo, A., Jackson, G., Fennell, P. (2010). An overview of CO₂ capture technologies. *Energy & Environmental Science*, 3(11), 1645.
- Machado, S. P. (2012). Structural and Mechanical Properties of Metallic Nanowires: In The Border Between Crystallinity and Weird Configurations. University of Autonoma Madrid.

- Maginn, E. J., & Elliott, J. R. (2010). Historical Perspective and Current Outlook for Molecular Dynamics As a Chemical Engineering Tool. *Industrial & Engineering Chemistry Research*, 49(7), 3059–3078.
- Maiti, A., Bourcier, W. L., & Aines, R. D. (2010). CO₂ capture in primary and tertiary amines - insights from atomistic modeling. United States of America.
- Mandal, B. P., & Bandyopadhyay, S. S. (2005). Simultaneous absorption of carbon dioxide and hydrogen sulfide into aqueous blends of 2-amino-2-methyl-1-propanol and diethanolamine. *Chemical Engineering Science*, 60(22), 6438–6451.
- Mandal, B. P., & Bandyopadhyay, S. S. (2006). Absorption of carbon dioxide into aqueous blends of 2-amino-2-methyl-1-propanol and monoethanolamine. *Chemical Engineering Science*, 61(16), 5440–5447.
- Mandal, B. P., Biswas, a. K., & Bandyopadhyay, S. S. (2003). Absorption of carbon dioxide into aqueous blends of 2-amino-2-methyl-1-propanol and diethanolamine. *Chemical Engineering Science*, 58(18), 4137–4144.
- Mandal, B. P., Guha, M., Biswas, a. K., & Bandyopadhyay, S. S. (2001). Removal of carbon dioxide by absorption in mixed amines: Modelling of absorption in aqueous MDEA/MEA and AMP/MEA solutions. *Chemical Engineering Science*, 56(21–22), 6217–6224.
- Martini, A. (2009). Short Course on Molecular Dynamics Simulation: Integration Algorithms. Retrieved from https://nanohub.org/resources/7575/download/Martini_L3_IntegrationAlgorithms.pdf
- Matsuzaki, Y., Yamada, H., Chowdhury, F. a., Higashii, T., Kazama, S., & Onoda, M. (2013). Ab Initio Study of CO₂ Capture Mechanisms in Monoethanolamine Aqueous Solution: Reaction Pathways from Carbamate to Bicarbonate. *Energy Procedia*, 37, 400–406.
- Matthew F. Schlecht. (1997). *Molecular Modeling on the PC* (1st editio). Wiley-VCH.
- May, J. M. S., & Atoms, T. A. (2013). *Molecular Dynamics Simulations of Phase Transitions*. United States of America.
- Merkel, T. C., Lin, H., Wei, X., & Baker, R. (2010). Power plant post-combustion carbon dioxide capture: An opportunity for membranes. *Journal of Membrane Science*, 359(1–2), 126–139.

- Mizukami, K., Takaba, H., Kobayashi, Y., Oumi, Y., Belosludov, R. V, Takami, S., ... Miyamoto, A. (2001). Molecular dynamics calculations of CO₂/N₂ mixture through the NaY type zeolite membrane. *Journal of Membrane Science*, 188(1), 21–28.
- Mores, P., Scenna, N., & Mussati, S. (2011). Post-combustion CO₂ capture process: Equilibrium stage mathematical model of the chemical absorption of CO₂ into monoethanolamine (MEA) aqueous solution. *Chemical Engineering Research and Design*, 89(9), 1587–1599.
- Muñoz, D. M., Portugal, A. F., Lozano, A. E., de la Campa, J. G., & de Abajo, J. (2009). New liquid absorbents for the removal of CO₂ from gas mixtures. *Energy & Environmental Science*, 2(8), 883.
- Nainar, M., & Veawab, A. (2009). Corrosion in CO₂ Capture Process Using Blended Monoethanolamine and Piperazine. *Industrial & Engineering Chemistry Research*, 48(20), 9299–9306.
- Nair, P. S., & Selvi, P. P. (2014). Absorption of Carbon dioxide in Packed Column. *International Journal of Scientific and Research Publication*, 4(4), 1–11.
- Newman, S. A. (1985). *Acid and Sour Gas Treating Processes* (1st editio). Gulf Publishing Company, Houston, Texas.
- Nor Kamarudin, Khairul Sozana, Mat, H. (2009). Synthesis And Modification Of Micro And Mesoporous Materials As CO₂ Adsorbent . Skudai, Johor.
- Olajire, A. a. (2010). CO₂ capture and separation technologies for end-of-pipe applications-A review. *Energy*, 35(6), 2610–2628.
- Pinto, A. M., Rodríguez, H., Arce, A., & Soto, A. (2014). Combined physical and chemical absorption of carbon dioxide in a mixture of ionic liquids. *The Journal of Chemical Thermodynamics*, 77, 197–205.
- Powell, C. E., & Qiao, G. G. (2006). Polymeric CO₂/N₂ gas separation membranes for the capture of carbon dioxide from power plant flue gases. *Journal of Membrane Science*, 279(1–2), 1–49.
- Prakash, P., & Venkatnathan, A. (2016). Molecular mechanism of CO₂ absorption in phosphonium amino acid ionic liquid. *RSC Adv.*, 6(60), 55438–55443.
- Price, D. J., & Brooks, C. L. (2002). Modern protein force fields behave comparably in molecular dynamics simulations. *Journal of Computational Chemistry*, 23(11),

1045–57.

- Puxty, G., & Rowland, R. (2011). Modeling CO₂ Mass Transfer in Amine Mixtures: PZ-AMP and PZ-MDEA. *Environmental Science & Technology*, 45(6), 2398–2405.
- Rahman, I. a., Saad, B., Shaidan, S., & Sya Rizal, E. S. (2005). Adsorption characteristics of malachite green on activated carbon derived from rice husks produced by chemical-thermal process. *Bioresource Technology*, 96(14), 1578–1583.
- Rao, A. B., & Rubin, E. S. (2002). A Technical, Economic, and Environmental Assessment of Amine-Based CO₂ Capture Technology for Power Plant Greenhouse Gas Control. *Environmental Science & Technology*, 36(20), 4467–4475.
- Rayer, A. V., Sumon, K. Z., Henni, A., & Tontiwachwuthikul, P. (2011). Kinetics of the reaction of carbon dioxide (CO₂) with cyclic amines using the stopped-flow technique. *Energy Procedia*, 4(September 2015), 140–147.
- Rayer, A. V., & Henni, A. (2014). Heats of Absorption of CO₂ in Aqueous Solutions of Tertiary Amines: N -Methyldiethanolamine, 3-Dimethylamino-1-propanol, and 1-Dimethylamino-2-propanol. *Industrial & Engineering Chemistry Research*, 53(12), 4953–4965.
- Roberto Lopez-Rendon, J. A. (2008). Molecular Dynamics Simulations of the Solubility of H₂S and CO₂ in Water. *Journal of The Mexican Chemical Society*, 52(1), 88–92.
- Robinson, K., McCluskey, A., & Attalla, M. (2011). The effect molecular structural variations has on the CO₂ absorption characteristics of heterocyclic amines. *Energy Procedia*, 4, 224–231.
- Rochelle, G., Chen, E., Freeman, S., Van Wagener, D., Xu, Q., & Voice, A. (2011). Aqueous piperazine as the new standard for CO₂ capture technology. *Chemical Engineering Journal*, 171(3), 725–733.
- Sartori, G., & Savage, D. W. (1983). Sterically hindered amines for carbon dioxide removal from gases. *Industrial & Engineering Chemistry Fundamentals*, 22(2), 239–249.
- Scheiman, M. A. (1987). A Review of Monoethanolamine Chemistry. Washington: Defense Technical Information Center.
- Schubert, S., Grünewald, M., & Agar, D. W. (2001). Enhancement of carbon dioxide absorption into aqueous methyldiethanolamine using immobilised activators.

- Shakhashiri. (2011). Water. Retrieved from <http://scifun.chem.wisc.edu/chemweek/PDF/COW-Water-Jan2011.pdf>
- Shao, R., & Stangeland, A. (2009). Amines Used in CO₂ Capture - Health and Environmental Impacts. Oslo, Norway.
- Shi, H., Naami, A., Idem, R., & Tontiwachwuthikul, P. (2014). Catalytic and non catalytic solvent regeneration during absorption-based CO₂ capture with single and blended reactive amine solvents. *International Journal of Greenhouse Gas Control*, 26, 39–50.
- Singh, P. (2011, June). Amine based solvent for CO₂ absorption: from molecular structure to process. University of Twente, Enschede, The Netherlands.
- Singh, P., Niederer, J. P. M., & Versteeg, G. F. (2007). Structure and activity relationships for amine based CO₂ absorbents I. *International Journal of Greenhouse Gas Control*, 1(1), 5–10.
- Singh, P., Niederer, J. P. M., & Versteeg, G. F. (2009). Structure and activity relationships for amine-based CO₂ absorbents-II. *Chemical Engineering Research and Design*, 87(2), 135–144.
- Strazisar, B. R., Anderson, R. R., & White, C. M. (2001). Degradation of Monoethanolamine Used in Carbon Dioxide Capture from Flue Gas of a Coal-fired Electric Power Generating Station. *Journal of Energy & Environmental Research*, 1(1), 33–39. Retrieved from http://www.netl.doe.gov/publications/proceedings/01/carbon_seq/4b3.pdf
- Sumon, K. Z., Henni, A., & East, A. L. L. (2014). Molecular dynamics simulations of proposed intermediates in the CO₂ + aqueous amine reaction. *Journal of Physical Chemistry Letters*, 5(7), 1151–1156.
- Svensson, H., Hulteberg, C., & Karlsson, H. T. (2013). Heat of absorption of CO₂ in aqueous solutions of N-methyldiethanolamine and piperazine. *International Journal of Greenhouse Gas Control*, 17, 89–98.
- Tan, C.-S., & Chen, J.-E. (2006). Absorption of carbon dioxide with piperazine and its mixtures in a rotating packed bed. *Separation and Purification Technology*, 49(2), 174–180.

- Tangallapally, R. P., Yendapally, R., Lee, R. E., Lenaerts, A. J. M., & Lee, R. E. (2005). Synthesis and evaluation of cyclic secondary amine substituted phenyl and benzyl nitrofuranyl amides as novel antituberculosis agents. *Journal of Medicinal Chemistry*, 48(26), 8261–8269.
- Tobiesen, F. A., Svendsen, H. F., & Mejdell, T. (2007). Modeling of Blast Furnace CO₂ Capture Using Amine Absorbents. *Industrial & Engineering Chemistry Research*, 46(23), 7811–7819.
- Toftegaard, M. B., Brix, J., Jensen, P. a., Glarborg, P., & Jensen, A. D. (2010). Oxy-fuel combustion of solid fuels. *Progress in Energy and Combustion Science*, 36(5), 581–625.
- Toon, T. Y. (2003). *Physical Chemistry for STPM*. (D. Day, Ed.) (4th ed.). Malaysia: Penerbit Fajar Bakti.
- Tran, Q. H., Nguyen, V. Q., & Le, A.-T. (2013). Silver nanoparticles: synthesis, properties, toxicology, applications and perspectives. *Advances in Natural Sciences: Nanoscience and Nanotechnology*, 4(3), 1–20.
- Tu, Y. (2011). *Molecular Dynamics Simulations*. Royal Institute of Technology (KTH).
- U.S. Environmental Protection Agency. (2014). *Inventory of U . S . Greenhouse Gas Emissions and Sinks : 1990-2012*. Washington.
- Vaidya, P. D., & Kenig, E. Y. (2007). CO₂-Alkanolamine Reaction Kinetics: A Review of Recent Studies. *Chemical Engineering & Technology*, 30(11), 1467–1474.
- Wang, Z., & Giammar, D. E. (2013). Mass Action Expressions for Bidentate Adsorption in Surface Complexation Modeling: Theory and Practice. *Environmental Science & Technology*, 47(9), 3982–3996.
- White, C. M., Strazisar, B. R., Granite, E. J., Hoffman, J. S., Pennline, W., & Pennline, H. W. (2003). Separation and Capture of CO₂ from Large Stationary Sources and Sequestration in Geological Formations Coalbeds and Deep Saline Aquifers *Journal of the Air & Waste Management Association*, 53(6), 645–715.
- Wispelaere, I. M. de. (2014). *The interaction of CO₂ with amines as molecular control factor in catalytic processes*. RWTH Aachen University.
- Wongsinlatam, W., & Remsungnen, T. (2013). Molecular Dynamics Simulations of CO₂ Molecules in ZIF-11 Using Refined AMBER Force Field. *Journal of Chemistry*,

2013, 1–10.

- Xing, H., Zhao, X., Yang, Q., Su, B., Bao, Z., Yang, Y., & Ren, Q. (2013). Molecular Dynamics Simulation Study on the Absorption of Ethylene and Acetylene in Ionic Liquids. *Industrial & Engineering Chemistry Research*, 52(26), 9308–9316.
- Yamada, H., Matsuzaki, Y., Chowdhury, F., & Higashii, T. (2013). Computational investigation of carbon dioxide absorption in alkanolamine solutions. *Journal of Molecular Modeling*, 19(10), 4147–4153.
- Ye, C., Chen, G., & Yuan, Q. (2012). Process characteristics of CO₂ absorption by aqueous monoethanolamine in a microchannel reactor. *Chinese Journal of Chemical Engineering*, 20(1), 111–119.
- Yeh, J. T., Resnik, K. P., Rygle, K., & Pennline, H. W. (2005). Semi-batch absorption and regeneration studies for CO₂ capture by aqueous ammonia. *Fuel Processing Technology*, 86(14–15), 1533–1546.
- Young, P. (2014). The Leapfrog Method and Other “Symplectic” Algorithms for Integrating Newton’s Laws of Motion. Retrieved from <http://young.physics.ucsc.edu/115/leapfrog.pdf>
- Yu, C.-H. (2012). A Review of CO₂ Capture by Absorption and Adsorption. *Aerosol and Air Quality Research*, 12, 745–769.
- Zhang, P., Shi, Y., Wei, J., Zhao, W., & Ye, Q. (2008). Regeneration of 2-amino-2-methyl-1-propanol used for carbon dioxide absorption. *Journal of Environmental Sciences*, 20(1), 39–44.
- Zhang, R., Liang, Z., Liu, H., Rongwong, W., Luo, X., Iden, R., & Yang, Q. (2016). Study of Formation of Bicarbonate Ions in CO₂-Loaded Aqueous Single 1DMA2P and MDEA Tertiary Amines and Blended MEA–1DMA2P and MEA–MDEA Amines for Low Heat of Regeneration. *Industrial & Engineering Chemistry Research*, 55(12), 3710–3717.
- Zhang, X., Zhang, C.-F., Qin, S.-J., & Zheng, Z.-S. (2001). A Kinetics Study on the Absorption of Carbon Dioxide into a Mixed Aqueous Solution of Methyl-diethanolamine and Piperazine. *Industrial & Engineering Chemistry Research*, 40(17), 3785–3791.

APPENDIX A
RADIAL DISTRIBUTION FUNCTION (RDF) GRAPH

4.2 Simulation Parameter 1: Effect of Temperature on MEA/H₂O/CO₂ System

4.2.1 Intermolecular Interaction between MEA and Water for Binary (MEA+H₂O) and Tertiary (MEA+H₂O+CO₂) Systems

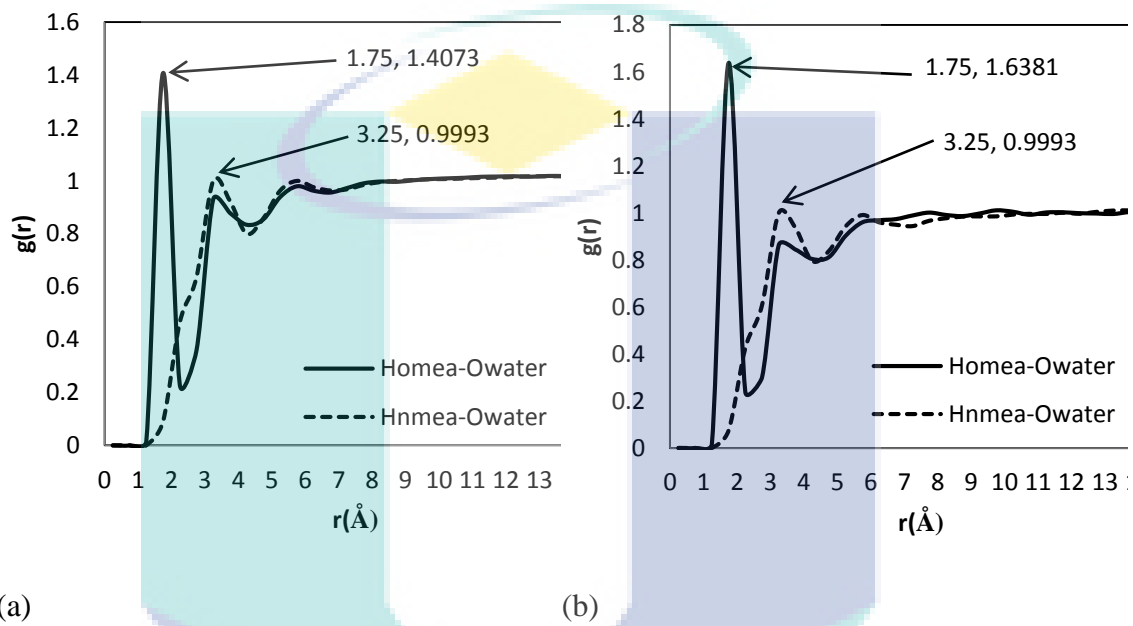


Figure 1: RDF molecular attractive interaction of (a) binary and (b) tertiary MEA+H₂O at 298 K

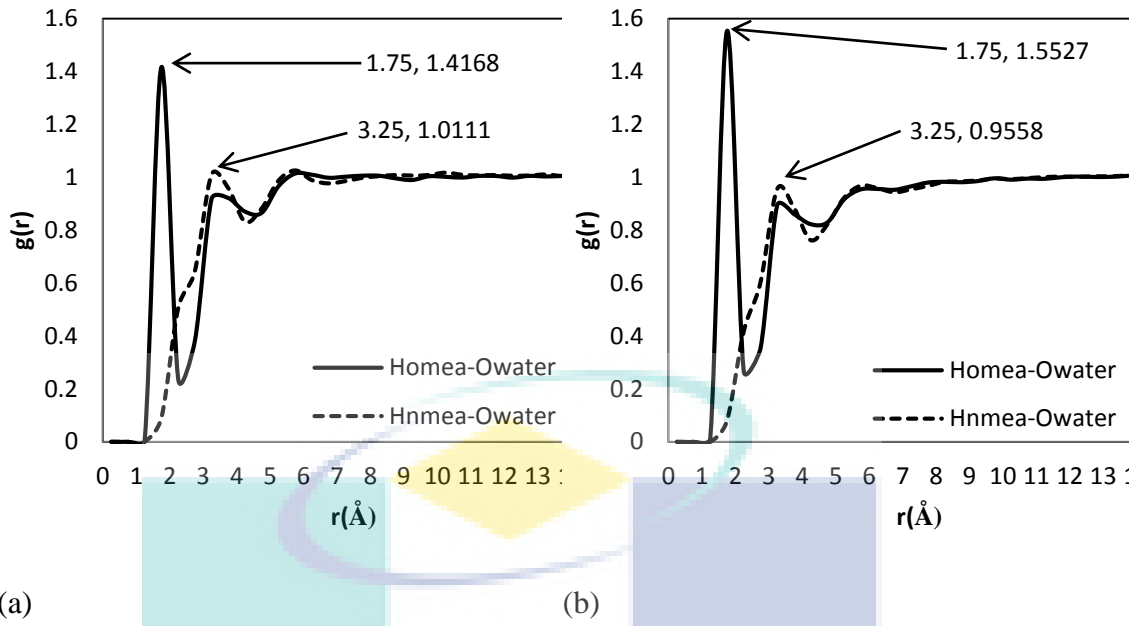


Figure 2: RDF molecular attractive interaction of (a) binary and (b) tertiary MEA+H₂O at 308 K

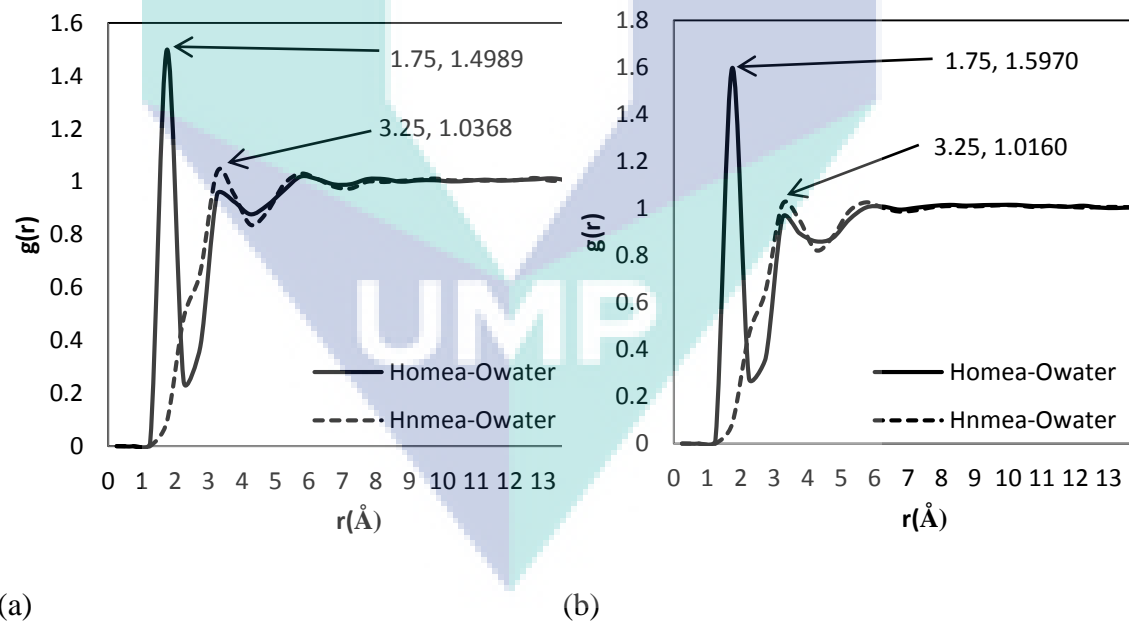


Figure 3: RDF molecular attractive interaction of (a) binary and (b) tertiary MEA+H₂O at 313 K

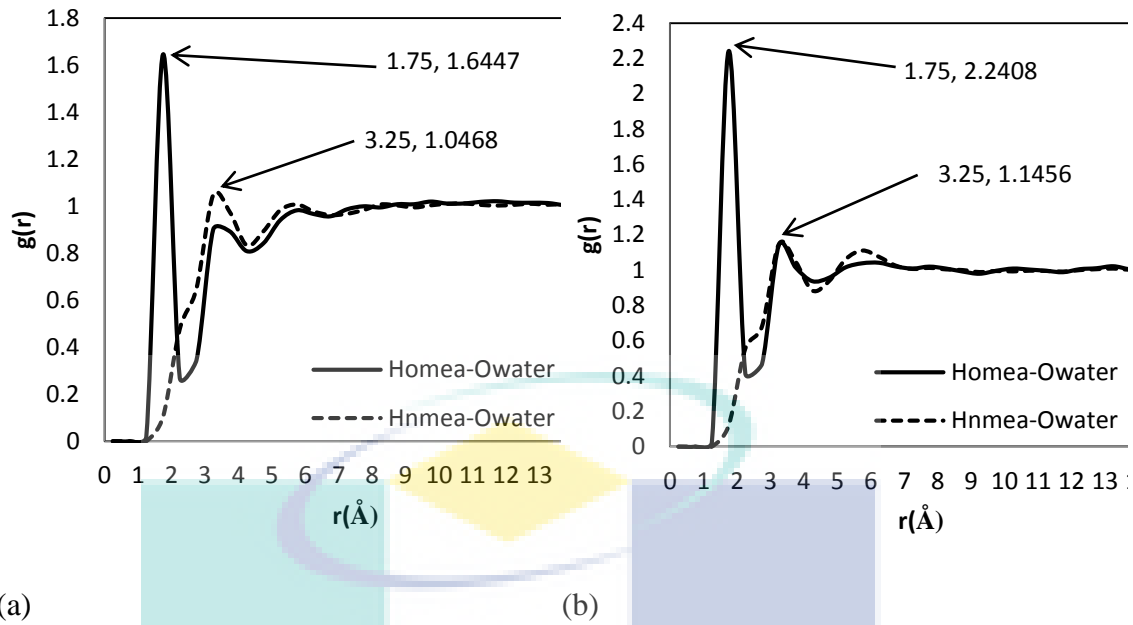


Figure 4: RDF molecular attractive interaction of (a) binary and (b) tertiary MEA+H₂O at 318 K

4.2.2 Intermolecular Interaction between MEA Solution and CO₂ in Tertiary System

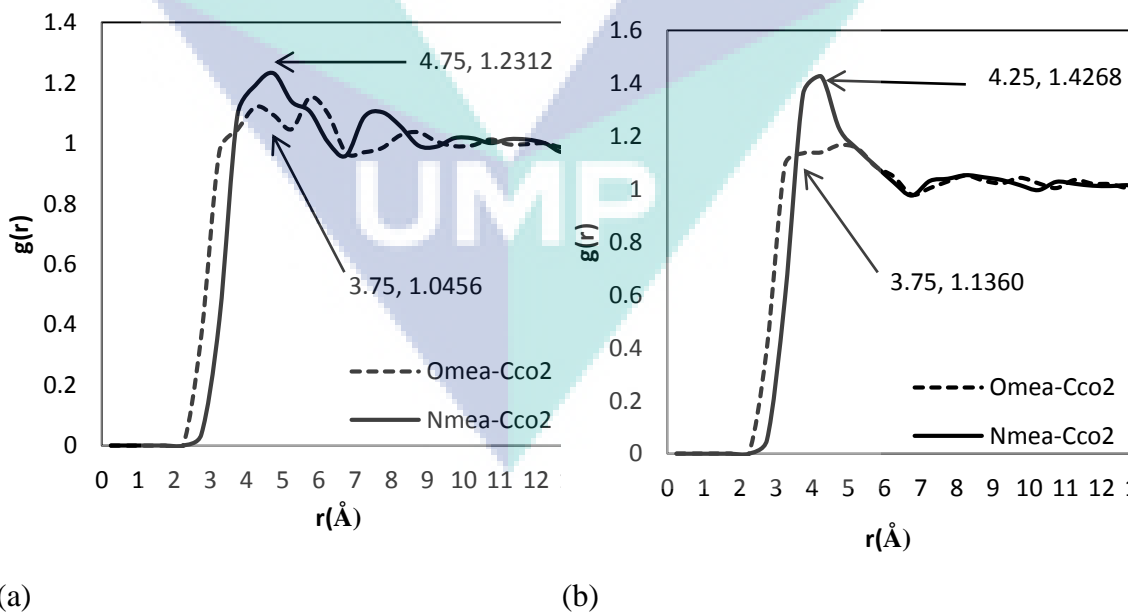


Figure 5: RDF molecular interaction of MEA and CO₂ in tertiary MEA+H₂O+CO₂ at (a) 298 K and (b) 308 K

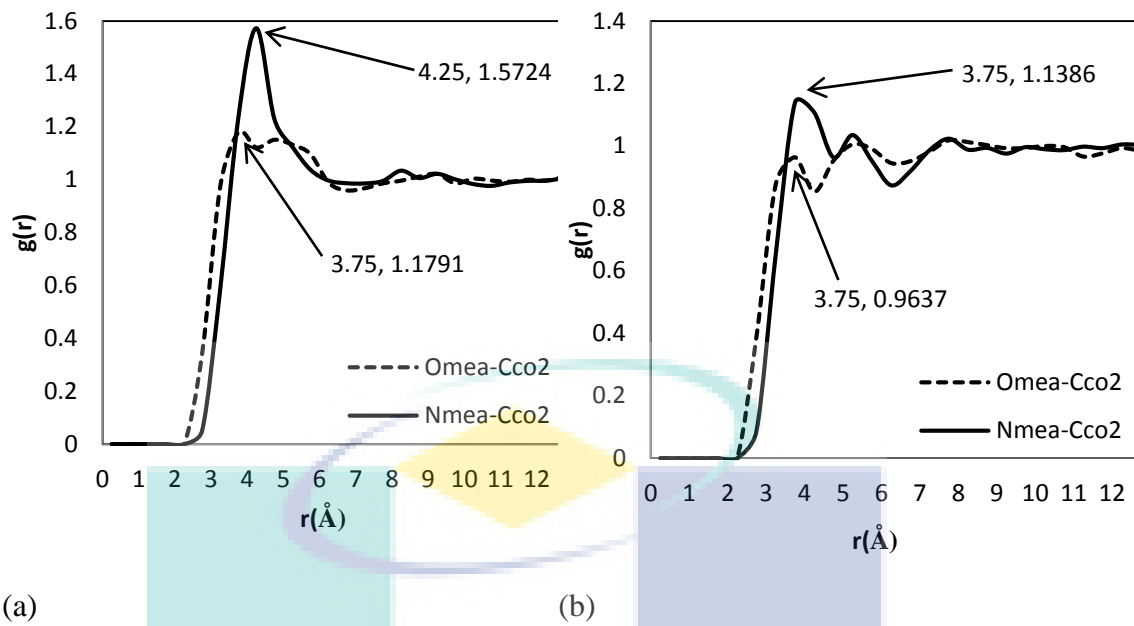


Figure 6: RDF molecular interaction of MEA and CO₂ in tertiary MEA+H₂O+CO₂ at (a) 313K and (b) 318K

4.3 Simulation Parameter 2: Effect of Amine Concentration on MEA/H₂O/CO₂ System

4.3.1 Intermolecular Interaction between MEA and Water for Binary (MEA+H₂O) and Tertiary (MEA+H₂O+CO₂) System

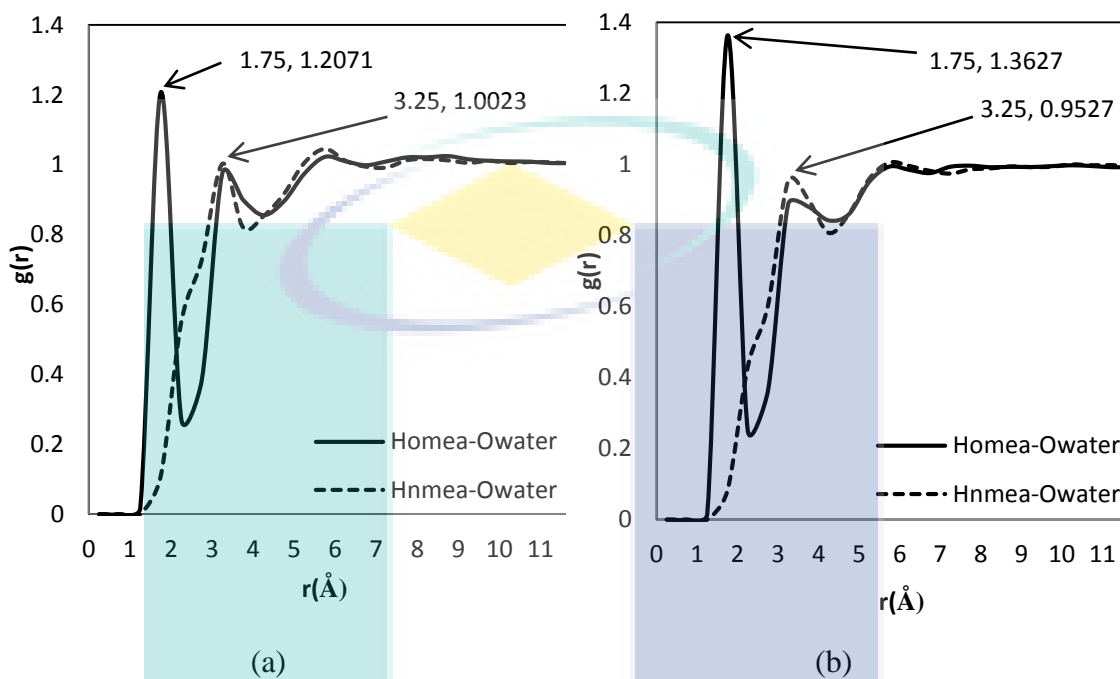


Figure 7: (a) Binary and (b) Tertiary system for 10 wt.% MEA

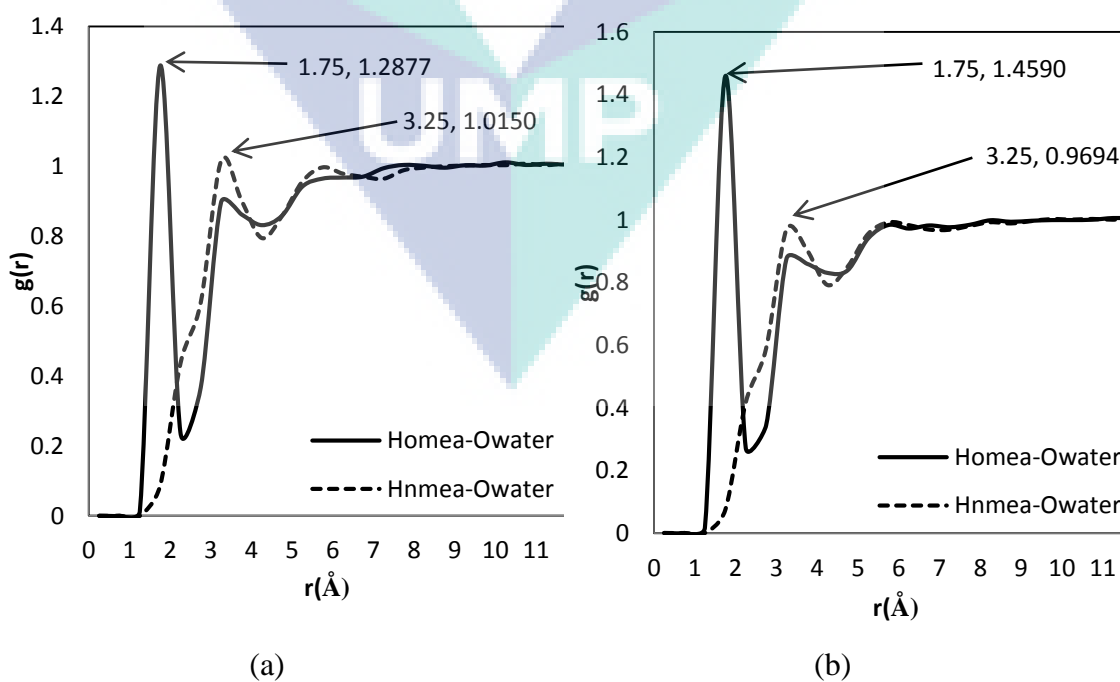


Figure 8: (a) Binary and (b) Tertiary system for 20 wt.% MEA

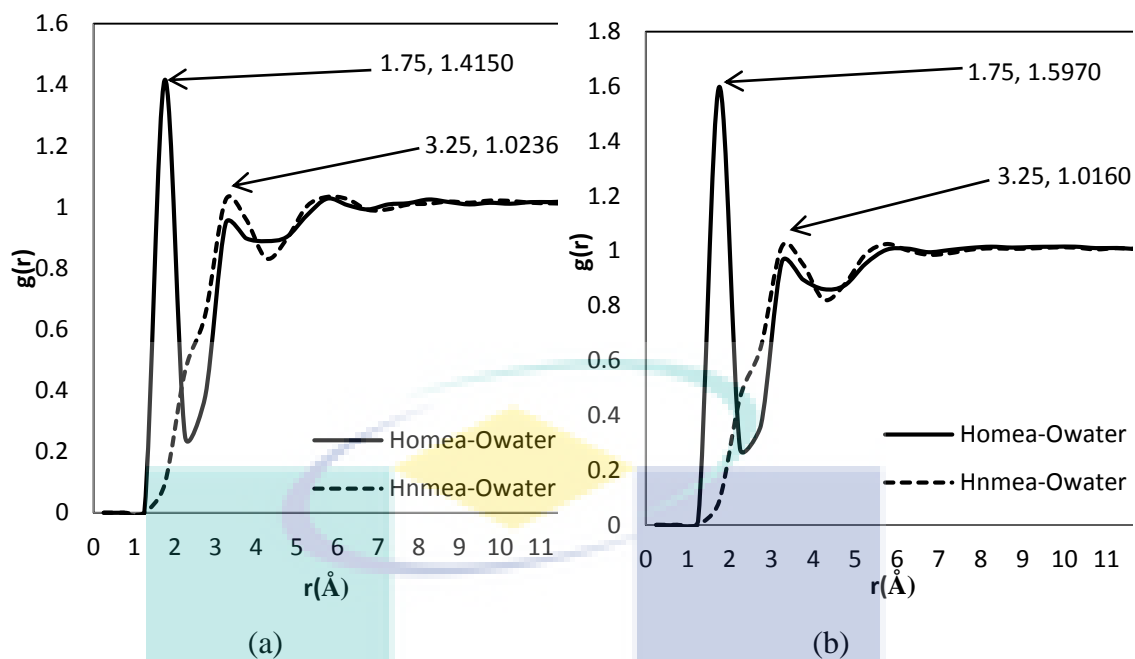


Figure 9: (a) Binary and (b) Tertiary system for 30 wt.% MEA

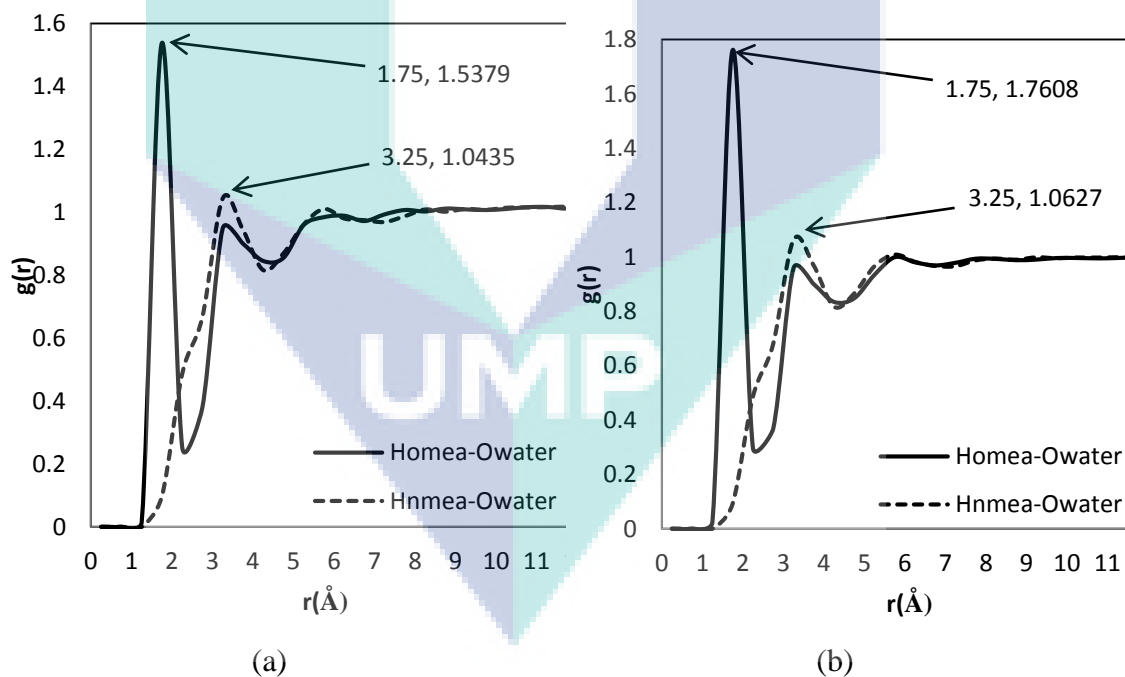


Figure 10: (a) Binary and (b) Tertiary system for 40 wt.% MEA

4.3.2 Intermolecular Interaction between MEA Solution and CO₂ in Tertiary System

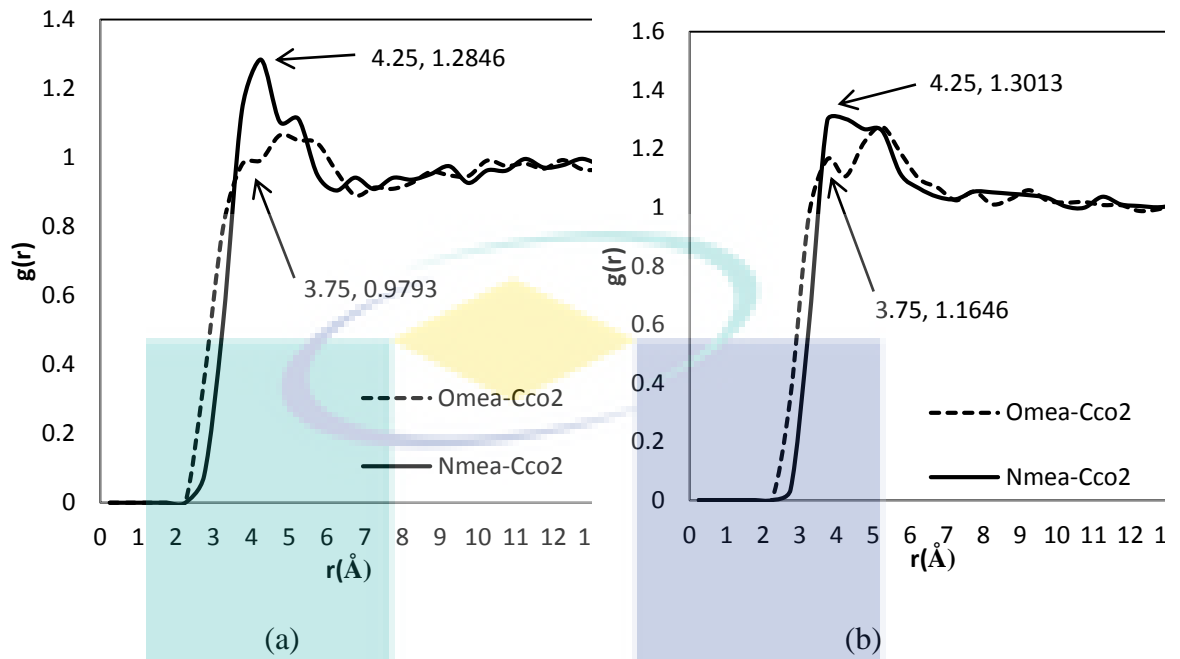


Figure 11: Intermolecular interaction of (a) 10 wt.% and (b) 20 wt.% MEA with CO₂

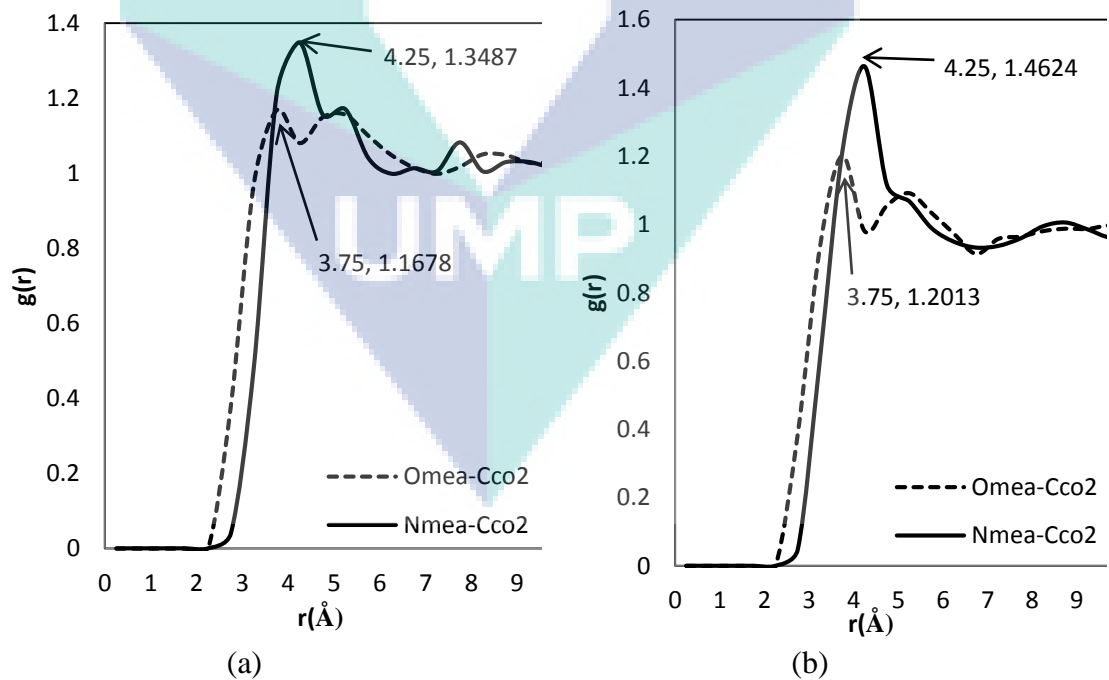


Figure 12: Intermolecular interaction of 30 wt.% MEA with CO₂

4.4 Simulation Parameter 3: Effect of Different Types Alkanolamines

4.4.1 Intermolecular Interaction between Amine and Water for Binary (Amine+H₂O) and Tertiary (Amine+H₂O+CO₂) Systems

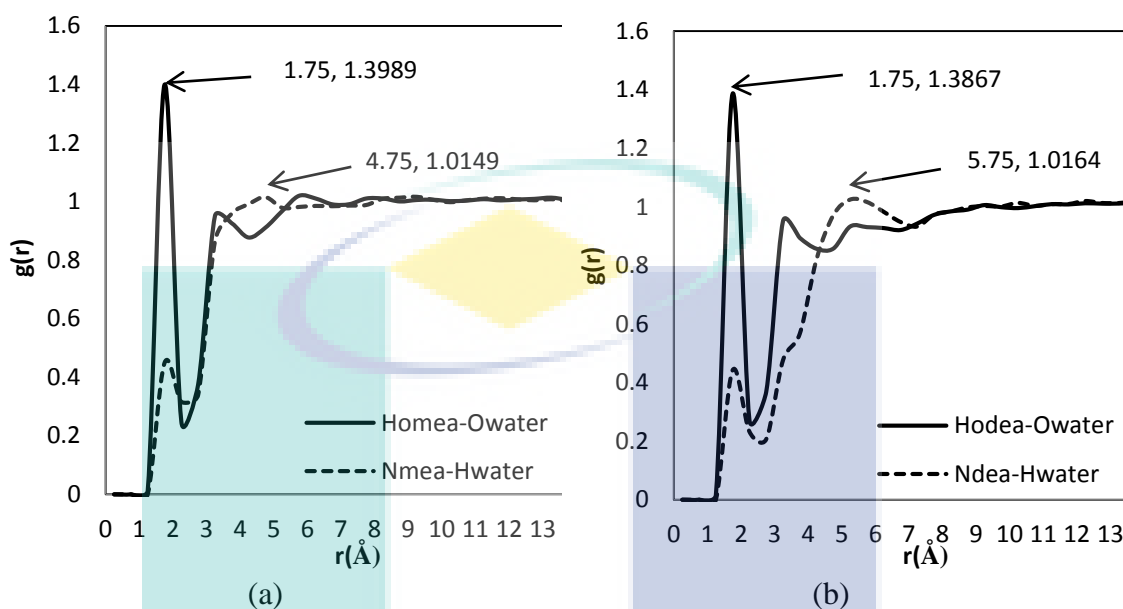


Figure 13: Binary system (a) MEA and (b) DEA solution

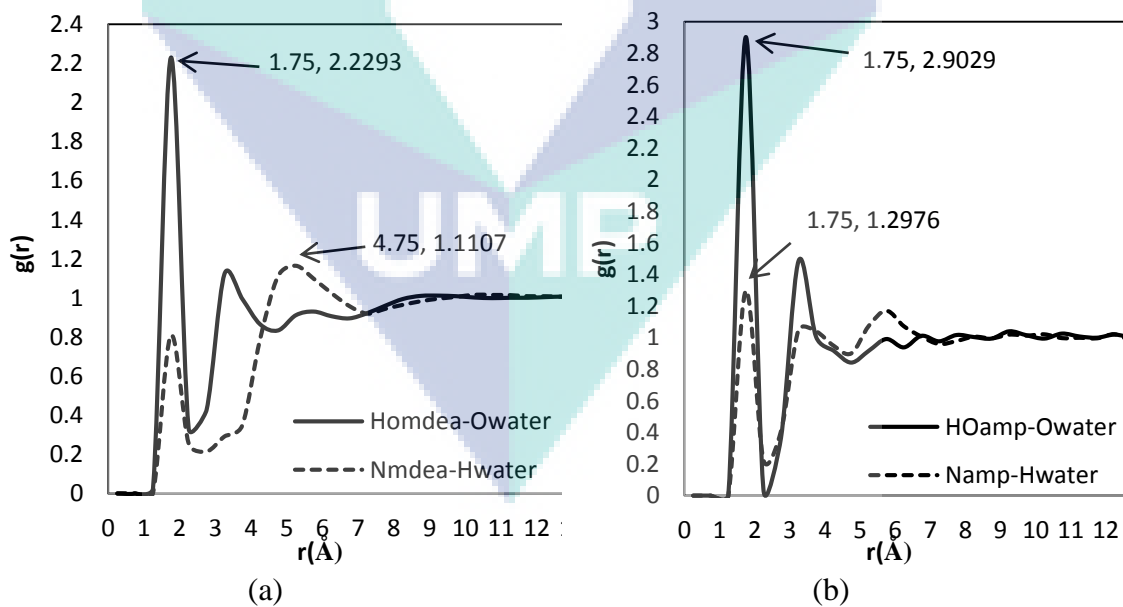


Figure 14: Binary system (a) MDEA (b) AMP solution

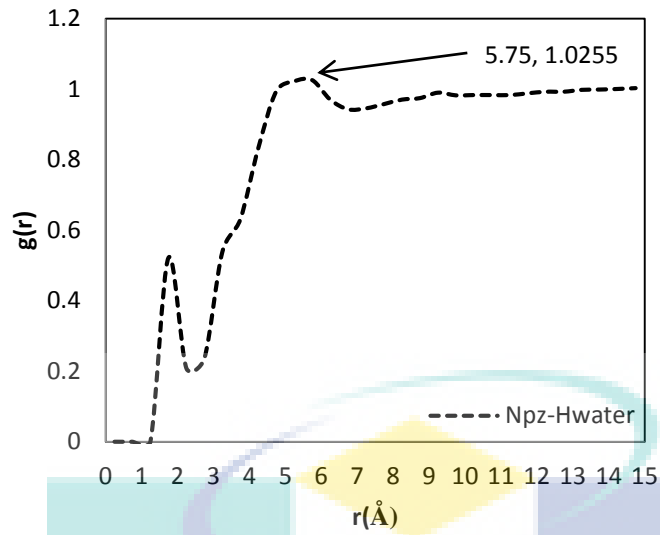


Figure 15: Binary system PZ solution

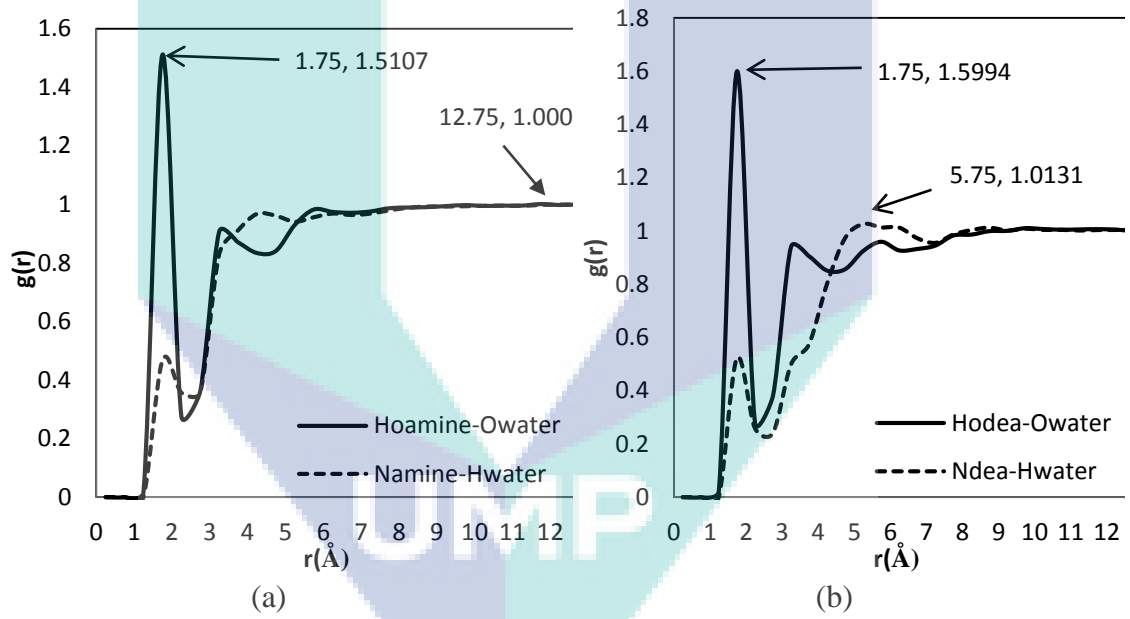


Figure 16: Tertiary system (a) MEA (b) DEA solution

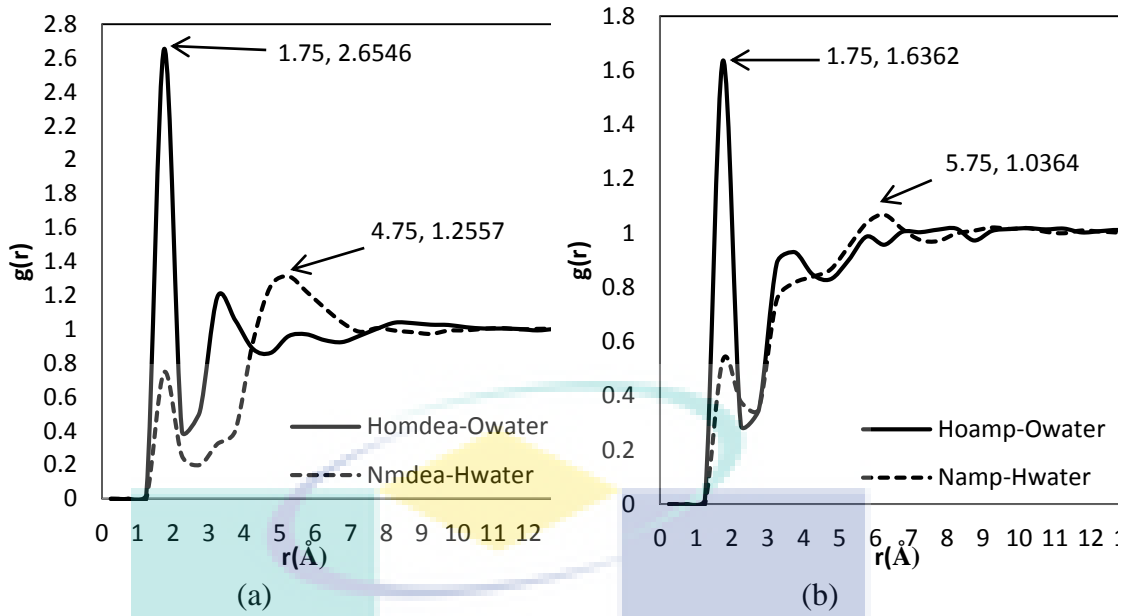


Figure 17: Tertiary system (a) MDEA and (b) AMP solution

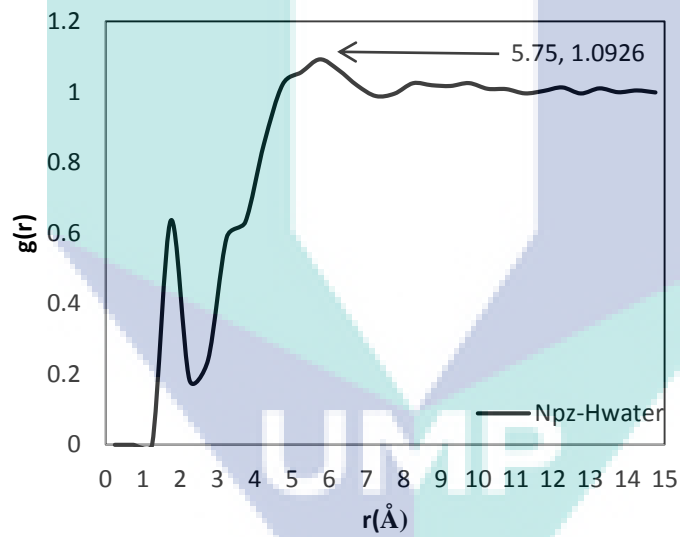


Figure 18: Tertiary system PZ solution

4.4.2 Intermolecular Interaction between Amine Solution and CO₂ in Tertiary System

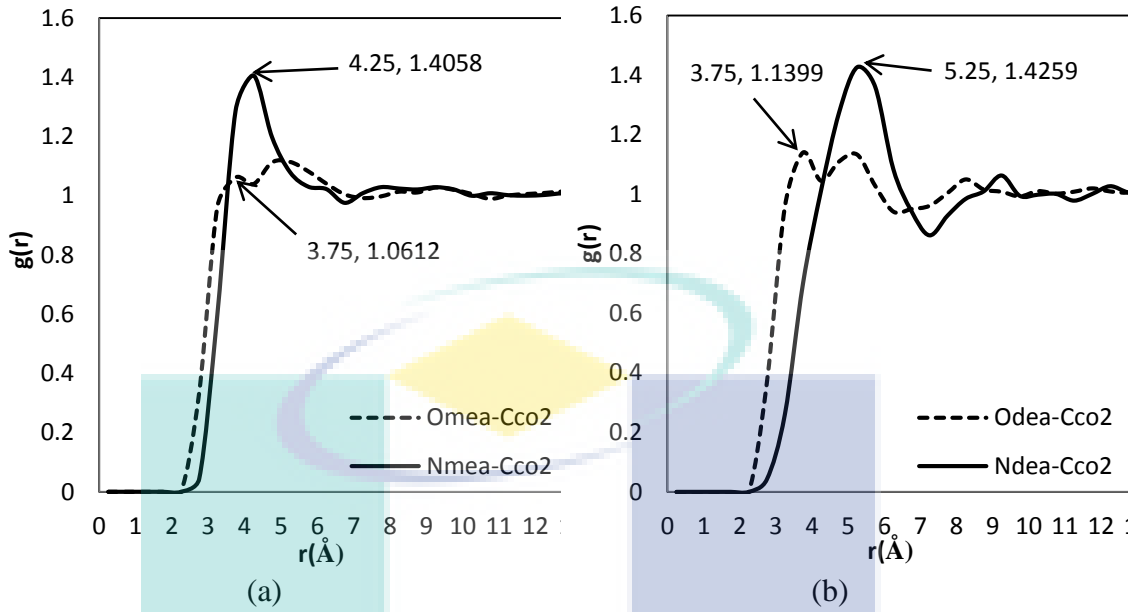


Figure 19: Intermolecular interaction of (a) MEA and (b) DEA solutions with CO₂

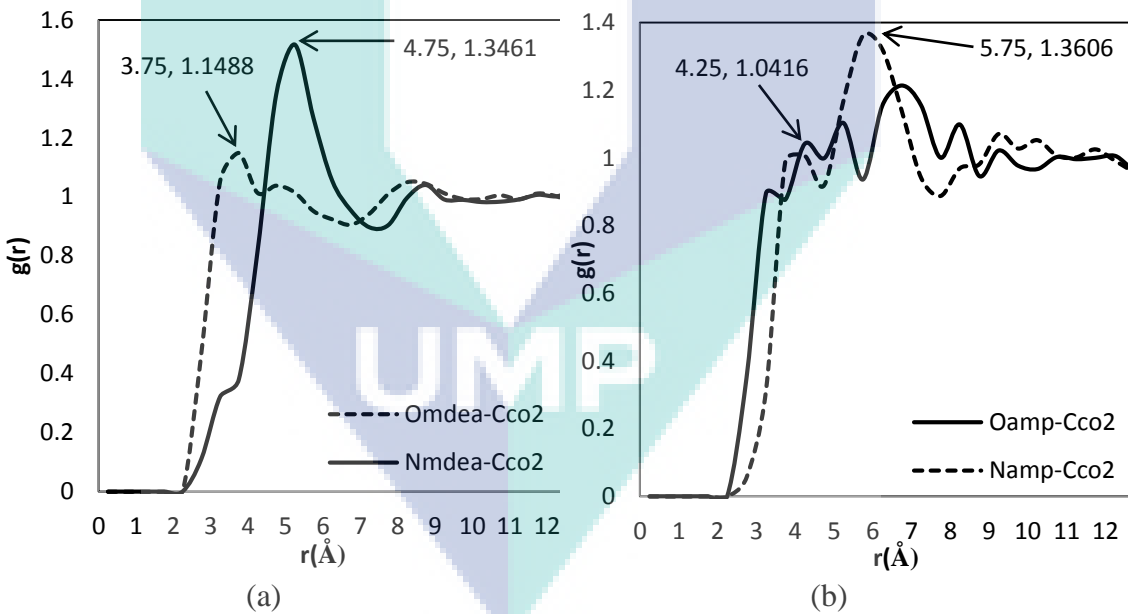


Figure 20: Intermolecular interaction of (a) MDEA (b) AMP solutions with CO₂

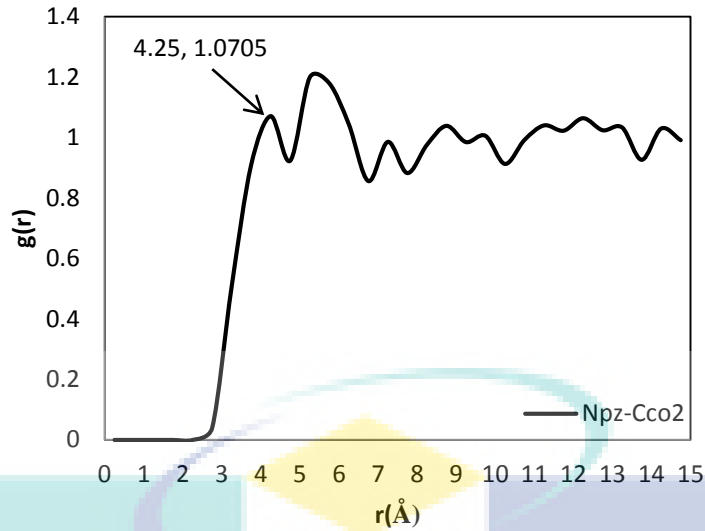


Figure 21: Intermolecular interaction of PZ solutions with CO₂

4.5 Simulation Parameter 4: Comparison of Single and Blended Amines System

4.5.1 Intermolecular Interaction for Blended MDEA/AMP

4.5.1.1 Comparison Single and Blended MDEA/AMP for Binary and Tertiary System

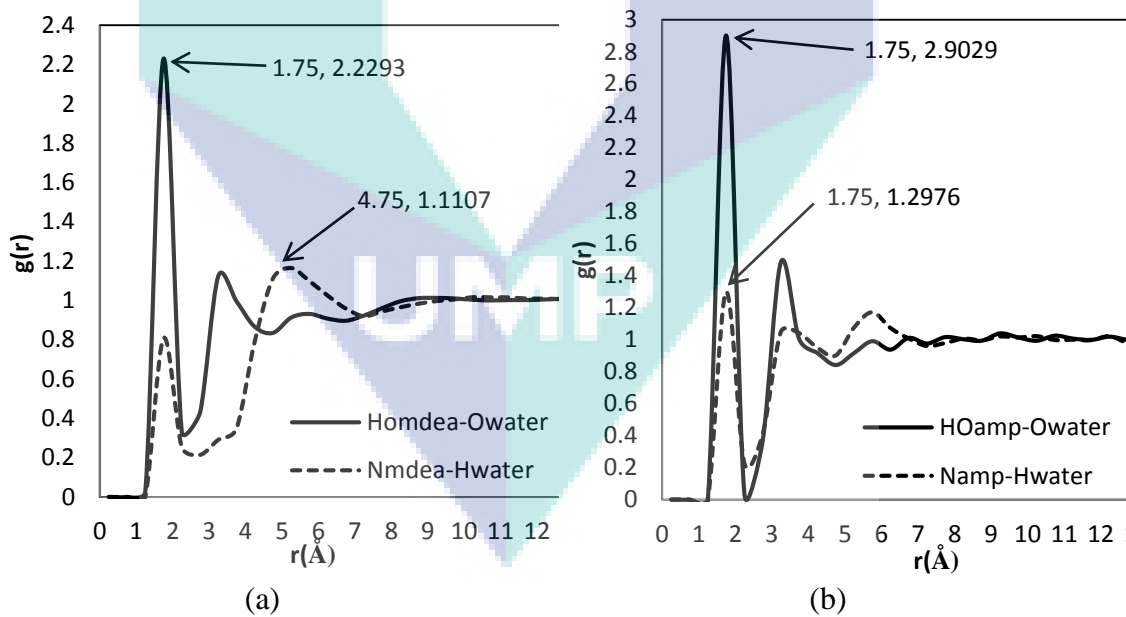


Figure 22: Intermolecular interaction of amine and water in binary system using (a) MDEA and (b) AMP solution

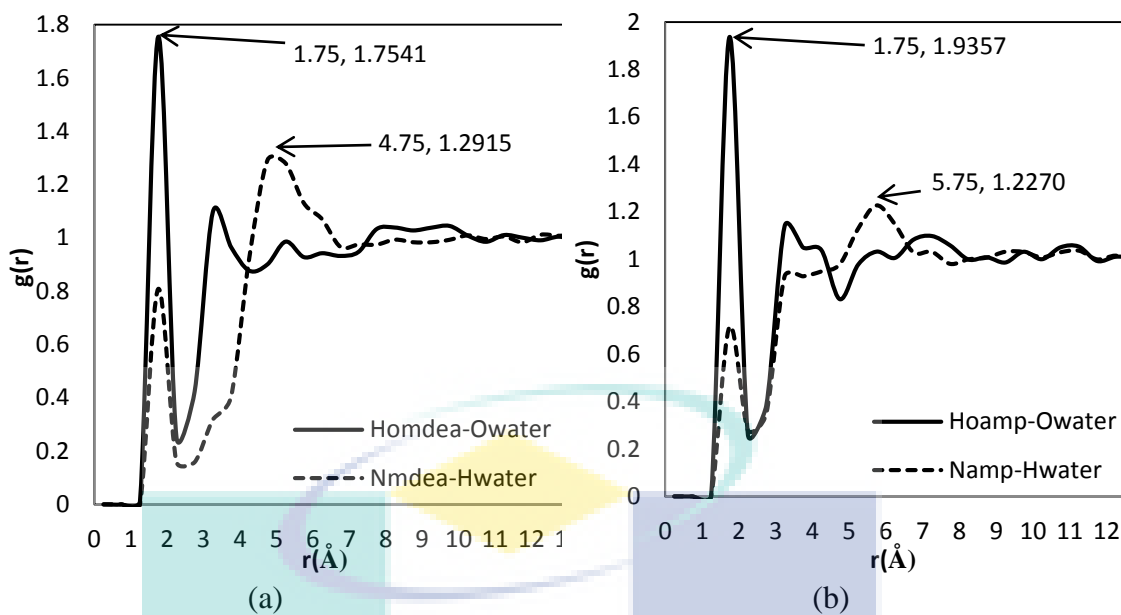


Figure 23: Intermolecular interaction of (a) MDEA and water and (b) AMP and water for binary system of blended MDEA/AMP

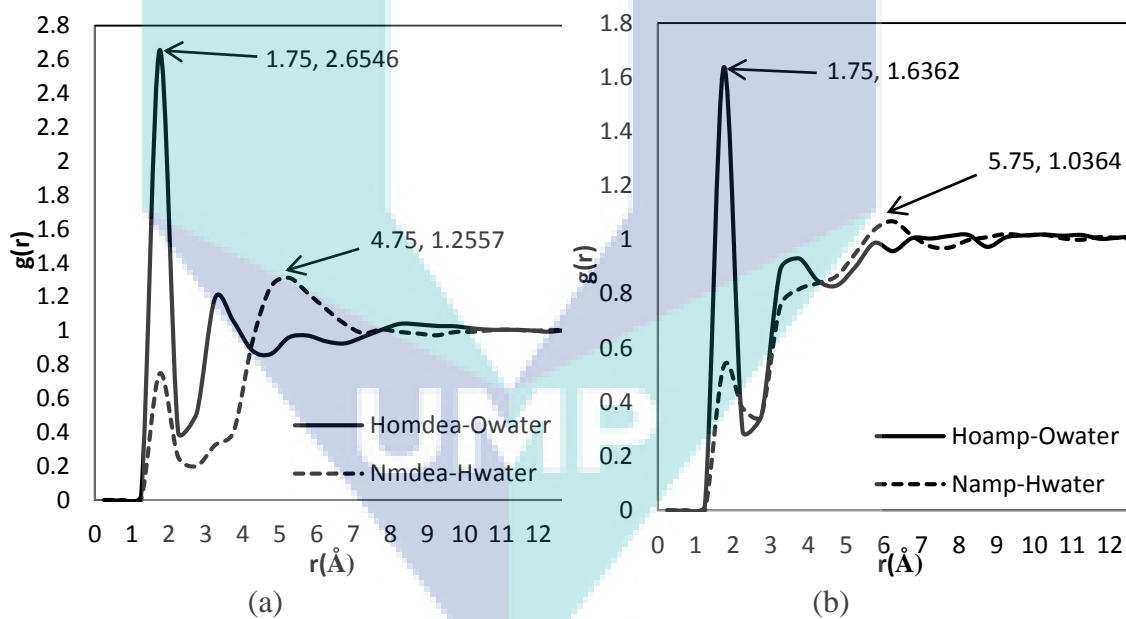


Figure 24: Intermolecular interaction of amine and water in tertiary system using (a) MDEA (b) AMP solution

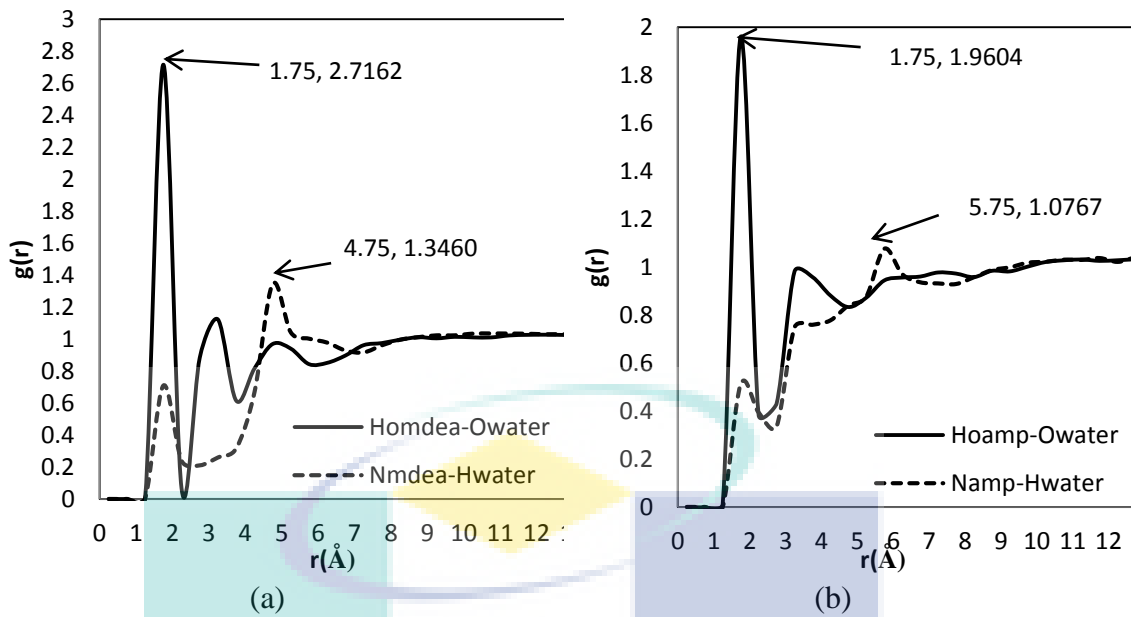


Figure 25: Intermolecular interaction of (a) MDEA and water and (b) AMP and water for tertiary system of blended MDEA/AMP

4.5.1.2 Comparison Single and Blended MDEA/AMP for Intermolecular Interaction with CO₂ in Tertiary System

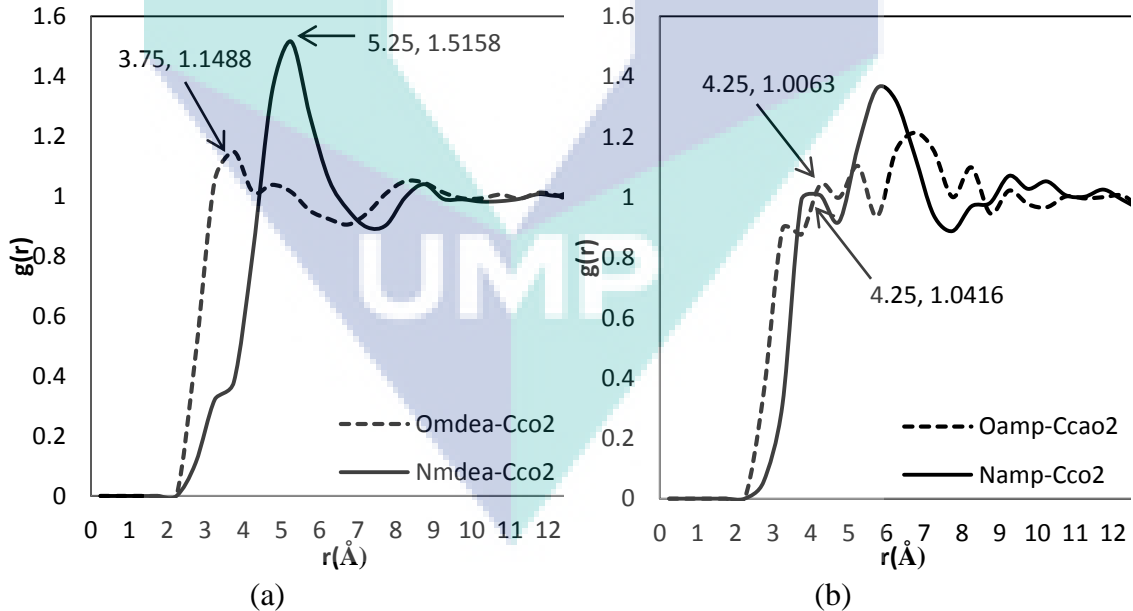


Figure 26: Intermolecular interaction of amine and CO₂ in tertiary system using (a) MDEA and (b) AMP solution

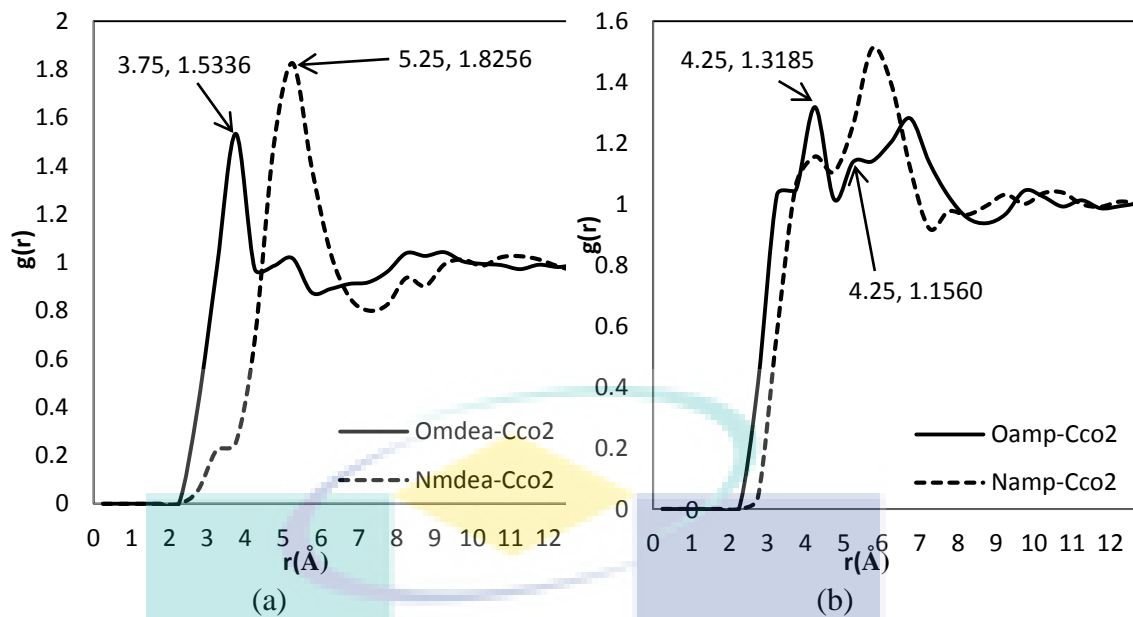


Figure 27: Intermolecular interaction of (a) MDEA and CO₂ and (b) AMP and CO₂ for tertiary system of blended MDEA/AMP

4.5.2 Intermolecular Interaction for Blended MDEA/PZ

4.5.2.1 Comparison of Single and Blended MDEA/PZ for Binary and Tertiary System

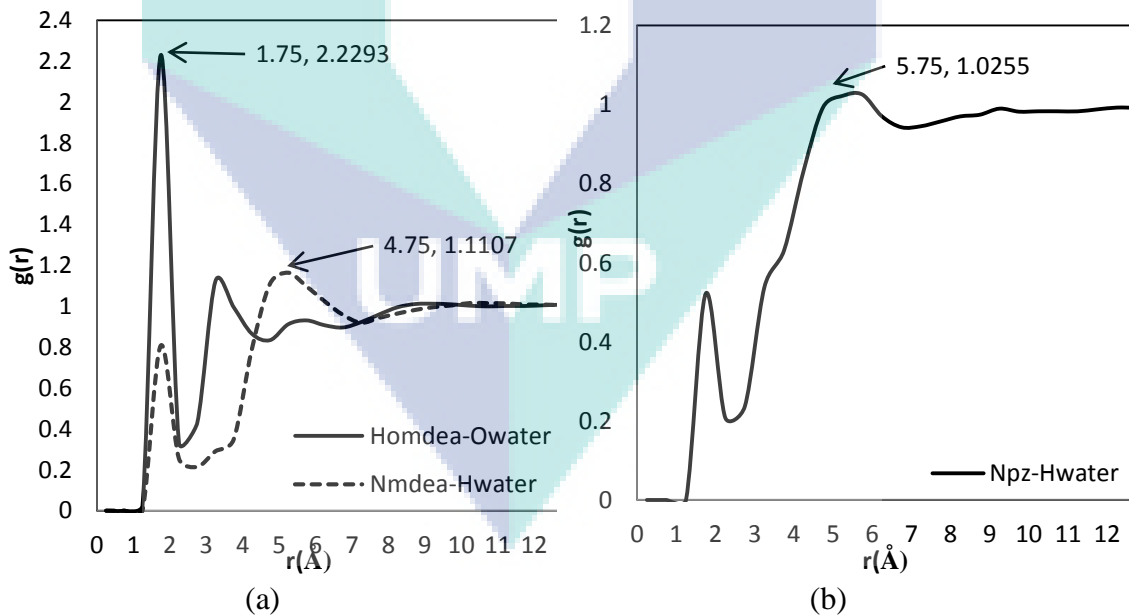


Figure 28: Intermolecular interaction of amine and water in binary system using (a) MDEA and (b) PZ solution

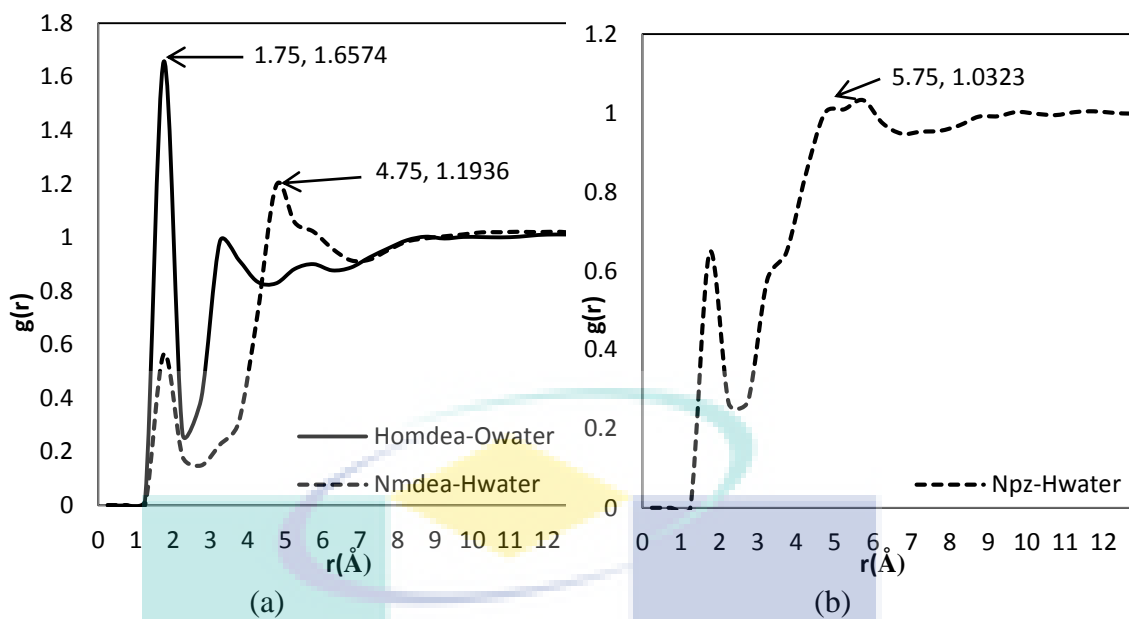


Figure 29: Intermolecular interaction of (a) MDEA and water and (b) PZ and water for binary system of blended MDEA/PZ

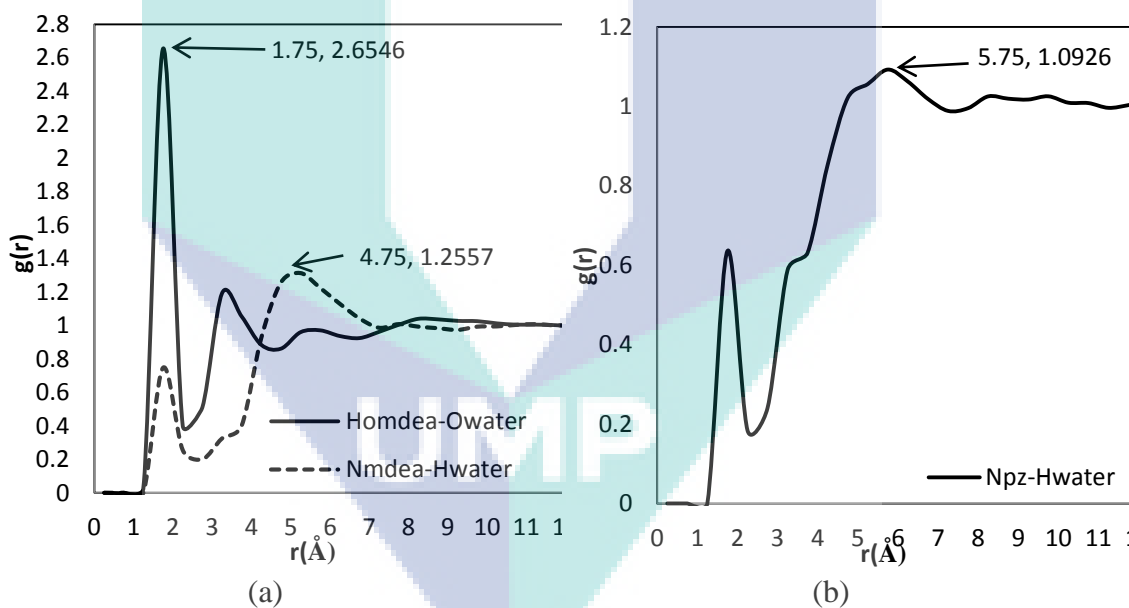


Figure 30: Intermolecular interaction of amine and water in tertiary system using (a) MDEA and (b) PZ solution

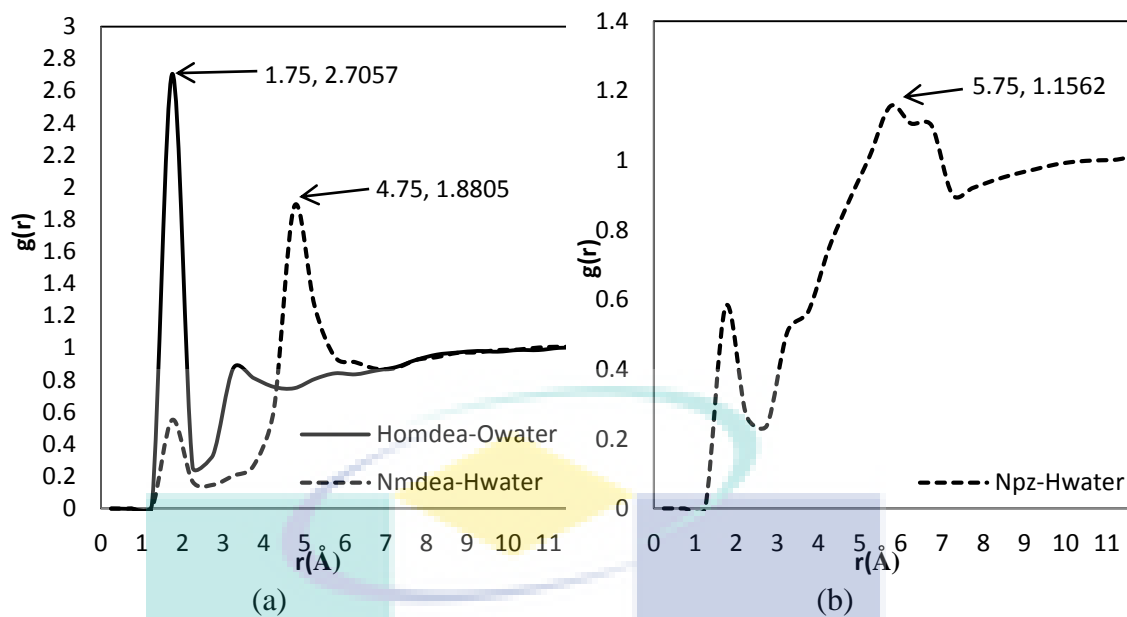


Figure 31: Intermolecular interaction of (a) MDEA and water (b) PZ and water for tertiary system of blended MDEA/PZ

4.5.2.2 Comparison of Single and Blended MDEA/PZ for Intermolecular Interaction with CO₂ in Tertiary System

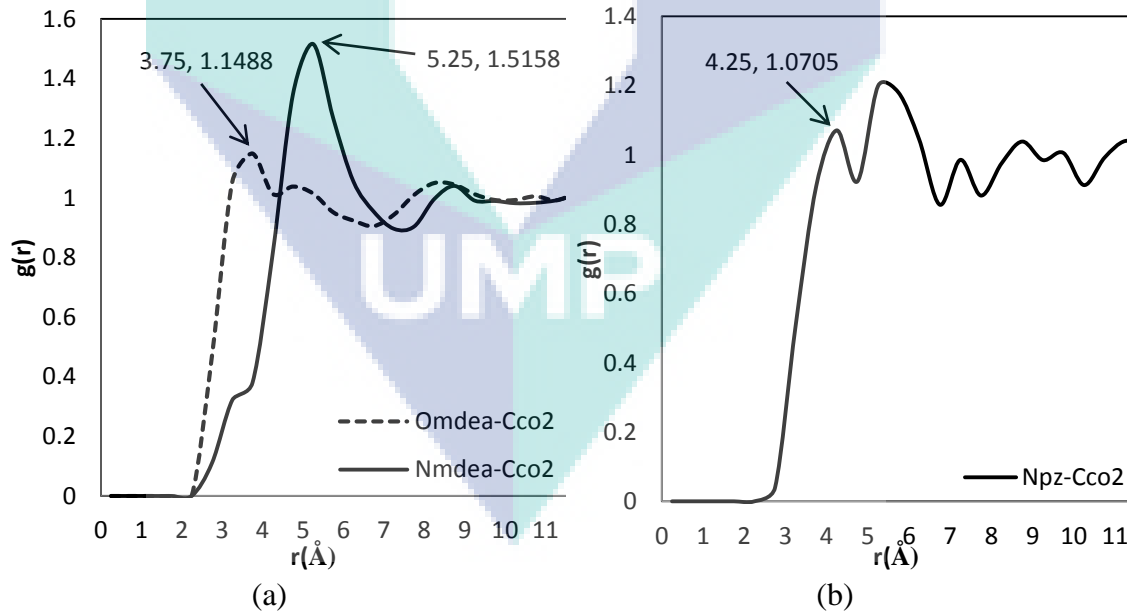


Figure 32: Intermolecular interaction of amine and CO₂ in tertiary system using (a) MDEA and (b) PZ solution

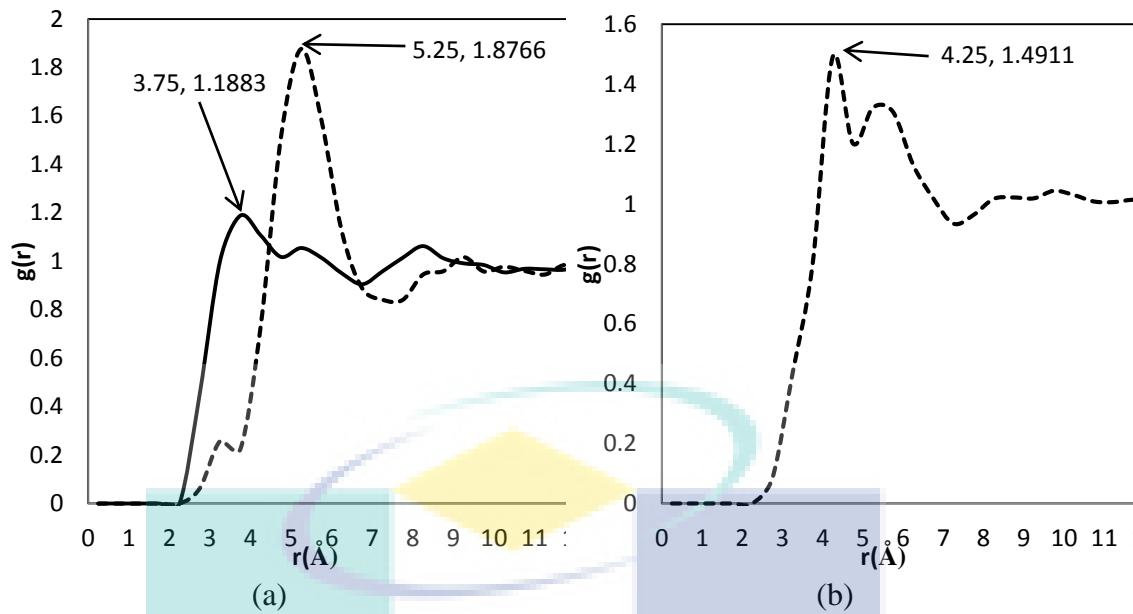


Figure 33: Intermolecular interaction of (a) MDEA and CO₂ and (b) PZ and CO₂ for tertiary system of blended MDEA/PZ

4.6 Simulation Parameter 5: Comparison of Different Types of Carbamate Amine (Stripping Process)

4.6.1 Intermolecular Interaction between Carbamate Ion with Water

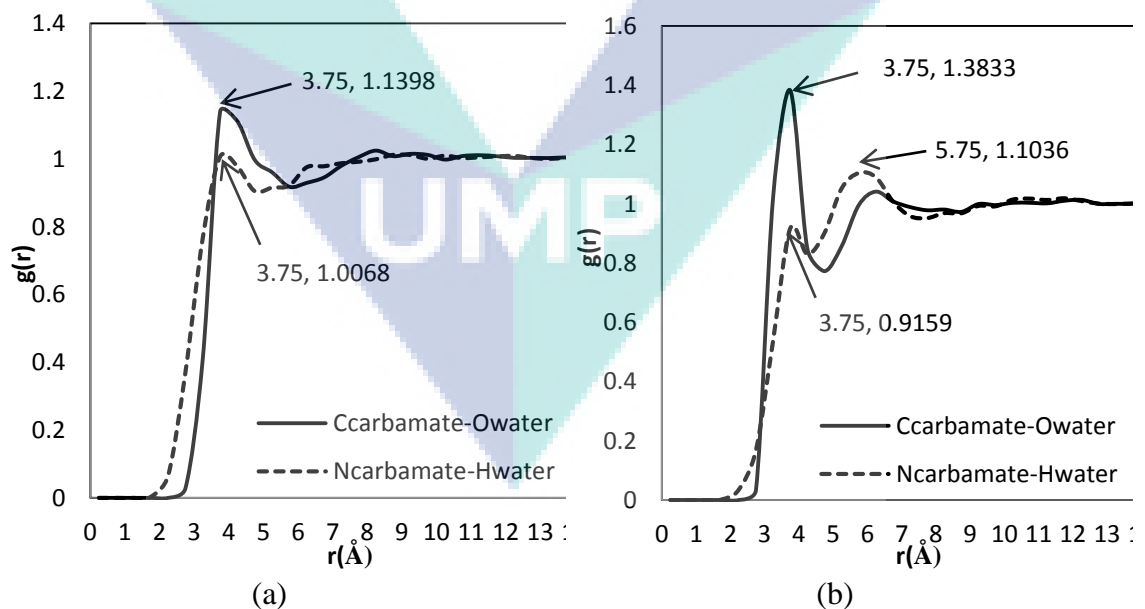


Figure 34: Intermolecular interaction between (a) MEA carbamate ions and (b) AMP carbamate ions with water

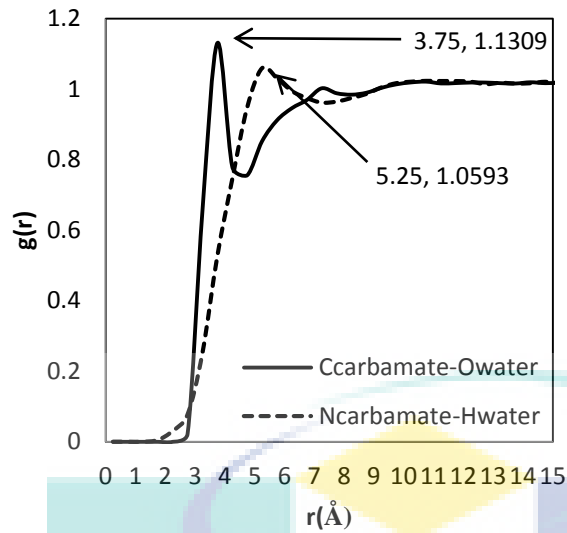


Figure 35: Intermolecular interaction between PZ carbamate ions with water

4.6.2 Intramolecular Interaction between C-Carbamate and N-Carbamate

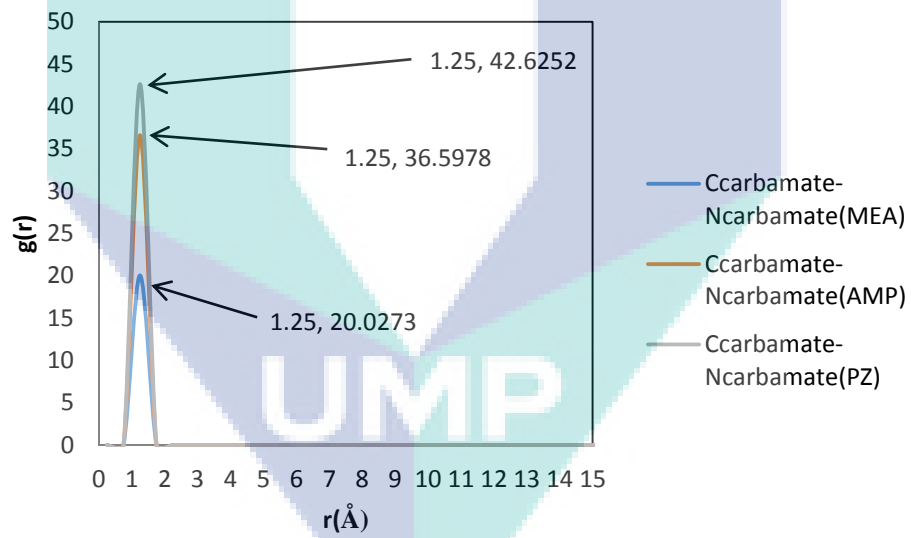
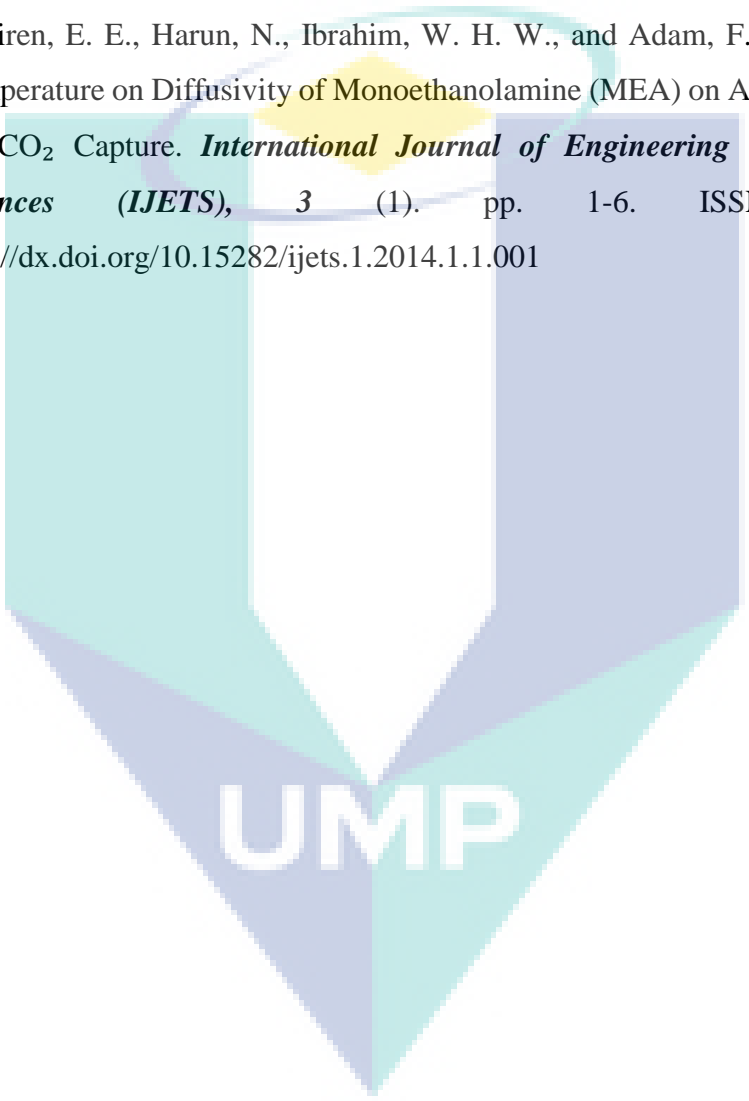


Figure 36: Intramolecular interaction between $C_{\text{carbamate}}$ and $N_{\text{carbamate}}$ for MEA, AMP and PZ

APPENDIX B
LIST OF PUBLICATIONS

1. Masiren, E. E., Harun, N., Ibrahim, W. H. W., and Adam, F. 2014. The Effect of Temperature on Intermolecular Interaction of Monoethanolamine Absorption Process for CO₂ Removal. *International Journal of Chemical and Environment Engineering*, 5(5): 297-300 (Chapter 4.2)
2. Masiren, E. E., Harun, N., Ibrahim, W. H. W., and Adam, F. (2015) Effect of Temperature on Diffusivity of Monoethanolamine (MEA) on Absorption Process for CO₂ Capture. *International Journal of Engineering Technology And Sciences (IJETS)*, 3 (1). pp. 1-6. ISSN 2289-697X
<http://dx.doi.org/10.15282/ijets.1.2014.1.1.001>

The logo of UMP (Universitas Muhammadiyah Palembang) is a large, stylized shield shape. It is composed of several overlapping geometric shapes in shades of teal, light blue, and white. The letters 'UMP' are prominently displayed in white, bold, sans-serif font across the center of the shield.

UMP

LIST OF CONFERENCE PRESENT

1. Masiren, E. E., Harun, N., Ibrahim, W. H. W., and Adam, F. 2014. The effect of temperature on intermolecular interaction of monoethanolamine absorption process for CO₂ removal. Oral Presentation at 5th International Journal of Chemical and Environment Engineering Conference (ICEEC'14), Kuala Lumpur, November 2014.
2. Masiren, E. E., Harun, N., Ibrahim, W. H. W., and Adam, F. 2015. Effect of temperature on diffusivity of monoethanolamine on absorption process for CO₂ capture. Poster Presentation at National Conference for Postgraduate Research (NCON'15), Universiti Malaysia Pahang, January 2015.
3. Masiren, E. E., Harun, N., Ibrahim, W. H. W., and Adam, F. 2015. Study on intermolecular interaction of MEA and MDEA absorption process to capture CO₂ using molecular dynamic simulation. Oral Presentation at Fluid Chemical Engineering Conference (FluidsChe'15), Langkawi, November 2015.
4. Masiren, E. E., Harun, N., Ibrahim, W. H. W., and Adam, F. 2016. Amine absorption for CO₂ capture using molecular dynamic simulation approach. Poster Presentation at 1st Global Conference on Process System & Safety Engineering (PSSE'16), Kuala Lumpur, January 2016.
5. Masiren, E. E., Harun, N., Ibrahim, W. H. W., and Adam, F. 2016. Intermolecular Interaction of Monoethanolamine, Diethanolamine, Methyl diethanolamine, 2-Amino-2-methyl-1-propanol and Piperazine Amines in Absorption Process to Capture CO₂ using Molecular Dynamic Simulation Approach. Oral Presentation at National Conference for Postgraduate Research (NCON'16), Universiti Malaysia Pahang, September 2016.
6. Masiren, E. E., Harun, N. Comparison of Different Types of Carbamate Amine for Stripping Process. Oral Presentation at International Conference on Low Carbon Asia (Iclca'16), Universiti Teknologi Malaysia, Kuala Lumpur.
7. Harun, N., Masiren, E. E. Molecular Dynamic Simulation of CO₂ Absorption Into Mixed Aqueous Solutions MDEA/PZ. Oral Presentation at International Conference of Chemical Engineering and Industrial Biotechnology 3rd ICCEIB Conference, Melaka, November 2016.

8. Harun, N., Masiren, E. Molecular Dynamic Simulation of Amine-CO₂ Absorption Process. Oral Presentation at Fluid Chemical Engineering Conference (FluidsChe'15), Langkawi, April 2017.

